

Russian Academy of Sciences

PGI -13-01-129

PHYSICS OF AURORAL PHENOMENA

36th Annual Seminar

26 February – 1 March 2013

Abstracts



"Северное сияние" Я. Штанакова, 13 лет, г. Горно-Алтайск

Apatity
2013

Russian Academy of Sciences
KOLA SCIENCE CENTER
Polar Geophysical Institute

PGI -13-01-129

PHYSICS OF AURORAL PHENOMENA

36th Annual Seminar Abstracts

26 February – 1 March 2013

Apatity

2013

The organizing committee:

Alexander Yahnin (chair)
Anatoly Pashin
Yuri Katkalov
Nadezhda Semenova
Alexey Mochalov
Irina Despirak

Addresses:

Apatity department
Akademgorodok, 26a
Apatity, 184209
Murmansk region
Russia

Murmansk department
Khalturina str., 15
Murmansk, 183010
Russia

The editorial board:

A.G. Yahnin
N.V. Semenova

E-mail: seminar@pgia.ru
<http://pgia.ru/seminar>

CONTENTS

SESSION 1. GEOMAGNETIC STORMS AND SUBSTORMS

I.A. Chernyaev, V.A. Sergeev, M.V. Kubyshkina, V. Angelopoulos	Using adaptive model to investigate the dipolarization events	13
I.V. Despirak, A.A. Lubchich, R. Koleva	Magnetic reconnection site in the magnetotail during different solar wind streams	13
N.P. Dmitrieva, M.M. Beloshkurskaya, T.A. Kornilova, I.A. Kornilov	The relation of equatorward-moving auroral traces with energetic particle injections at the geostationary orbit	13
Y.I. Feldstein, V.G. Vorobjev	Scheme of space-time distribution of auroral luminescence in the dayside sector	14
E. Gordeev, M. Amosova, V. Sergeev	The role of IMF Bx component in the global magnetotail dynamics	14
I.B. Ievenko, S.G. Parnikov, V.N. Alexeyev	Ground and satellite observations of the SAR arc in the dusk-bulge region of plasmasphere	15
Ju. Katkalov, M. Wik, A. Viljanen	Visualisation tool for geomagnetically induced currents	15
T.A. Kornilova, I.A. Kornilov	THEMIS observations of three similar dipolarization events	15
I.A. Kornilov, F. Sigernes, T.A. Kornilova,	Ground based, THEMIS and DMSP observations of 24.01.2012 CME event	16
T.V. Kozelova, B.V. Kozelov	Behavior of ions near the substorm onset from THEMIS observations	16
A.E. Levitin, L.I. Gromova, S.V. Gromov, L.A. Dremukhina	Extremely quiet 2009 state of geomagnetic field as a reference level amplitude of the local geomagnetic disturbances	16
V.V. Mishin, V.M. Mishin, Yu.A. Karavaev, S.B. Lunyushkin	On significant additional contribution of "old" tail lobes to substorm power	17
V.M. Mishin, V.V. Mishin, S.B. Lunyushkin	The 27 Aug 2001 magnetospheric substorm: Field-aligned currents and mesoscale plasma vortices in the polar ionosphere	17
A.V. Nikolaev, V.A. Sergeev, N.A. Tsyganenko, H. Singer, V. Angelopoulos	The Magnetospheric Magnetic field deformation: Effects of double-loop Substorm Current Wedge	17
V.C. Roldugin, A.V. Roldugin, S.V. Pilgaev	Proton precipitation in the auroral zone during interplanetary shock on 24 January 2012	18
Ya. Sakharov, Ju. Katkalov, A. Viljanen, R. Pirjola, P. Wintoft	Modeling of GIC in the regional power system for strong geomagnetic storm	18
I.I. Shagimuratov, Iu. Cherniak, I. Ephishov, I. Zakharenkova	The structure of irregularities in disturbed high latitude ionosphere observed by GPS/GLONASS TEC measurements	18
S.A. Timofeeva, V.A. Sergeev	Analysis of the energetic particle observations during satellite passes over the auroral bulge	19

O.I. Yagodkina, I.V. Despirak	Dynamics of the auroral precipitation zones during recurrent stream on 19- 22 February, 2006	19
A.Е. Левитин, Л.И. Громова, С.В. Громов, Л.А. Дремухина	Как нам реорганизовать расчет геомагнитной активности	20
Ю.А. Копытенко, В.С. Исмагилов, А.Л. Котиков, М.С. Петрищев, П.Е. Терещенко, А.В. Петленко, Д.Б. Зайцев, Д.Ю. Сарычев	Исследование динамики положения плазмопаузы во время сильной магнитной суббури по данным меридиональной цепочки станций	20

SESSION 2. FIELDS, CURRENTS, PARTICLES IN THE MAGNETOSPHERE

I.B. Ievenko	SAR arc formation due to the interplanetary shock and substorm on December 14, 2006	23
I.A. Kornilov, F. Sigernes, T.A. Kornilova	Dayside aurora	23
K.Yu. Slivka, V.S. Semenov, N.P. Dmitrieva	The study of magnetic barrier parameters dependence on the direction and intensity of the interplanetary magnetic field	23
M.A. Volkov	The model calculations of the Poynting flux over the auroral arc	24
A.G. Yahnin, T.A Yahnina	Long –lived proton auroras equatorward of the auroral oval on the dayside	24
В.С. Исмагилов, Ю.А. Копытенко, Г.М. Попов	Аномальные возмущения в вековых вариациях магнитного поля Земли перед катастрофическим землетрясением в Японии 11.03.2011	24
Б.В. Козелов	Анизотропия пространственного скейлинга в полярных сияниях по наземным наблюдениям в Апатитах	25
С.Е. Ревунов, Д.В. Шадруков, Н.В. Косолапова	Отождествление долгопериодных МГД пульсаций в магнитосфере методами вейвлет-скелетонного анализа как предвестников протонных солнечных вспышек	25
Т.А. Яхнина, А.Г. Яхнин, Т.А. Попова	Новый тип высыпаний энергичных протонов к экватору от изотропной границы	26

SESSION 3. WAVES, WAVE-PARTICLE INTERACTION

V.B. Belakhovsky, V.A. Pilipenko, S.N. Samsonov, D.Yu. Klimushkin	Pg wave detected by array of satellites	29
V.B. Belakhovsky, V.A. Pilipenko	The investigation of the spatial distribution of auroral Pc5 pulsations and its connection with simultaneous Pc5 pulsations in geomagnetic field and CNA	29
T.V. Bondareva, N.A. Smirnova	Comparative analysis of the ULF emissions fractal characteristics in quiet and disturbed conditions	29
A.G. Demekhov	Cyclotron acceleration of radiation belt electrons by whistler-mode chorus waves	30

I.V. Golovchanskaya	Interplay of Alfvénic and electrostatic ion-cyclotron processes in the magnetosphere-ionosphere coupling on small scales	30
V.A. Lubchich	Application of extremely low frequency electromagnetic waves for subsurface - surface communication in mines.	30
J. Manninen, N.G. Kleimenova, O.V. Kozyreva	Spectacular quasi-periodic VLF emissions in the auroral latitudes	30
J. Manninen, E.E. Titova, A.G. Demekhov, A.E. Kozlovsky, D.L. Pasmanik	Quasi-periodic VLF emissions: An analysis of the periods on different time scales.	31
V.A. Pilipenko, V.B. Belakhovsky, D. Murr, M. Terramoto	Modulation of the total electron content by geomagnetic Pc5 pulsations	31
E.E. Titova, A.G. Demekhov, A.A. Mochalov, A.B. Pashin, M.M. Mogilevskiy	ELF electromagnetic disturbances in the outer ionosphere produced by the HAARP heating facility	32
A.G. Yahnin, T.A. Yahnina, E.N. Ermakova, A.G. Demekhov, F. Soraas	Unusual proton aurora correlated with unusual “Pc1”	32
Б.В. Козелов, Е.Е. Титова	Характеристики потоков высывающихся частиц в пульсирующих полярных сияниях по триангуляционным наблюдениям в Апатитах	32
Ю.А. Копытенко, В.С. Исмагилов, А.Л. Котиков, М.С. Петрищев, П.Е. Терещенко, А.В. Петленко, Д.Б. Зайцев, Д.Ю. Сарычев, А.Г. Коробейников, Г.М. Попов	Использование фазовых скоростей УНЧ геомагнитных вариаций для исследования геоэлектрической структуры земной коры	33
А.А. Любич	Генерация колебаний убывающего периода облаком дрейфующих протонов	33

SESSION 4. THE SUN, SOLAR WIND, COSMIC RAYS

Yu.V. Balabin	Anomalous barometric coefficient of microsecond intervals into NM	37
Yu.V. Balabin, E.V. Vashenyuk, A.V. Germanenko, B.B. Gvozdevsky	New middle latitude station with multiplicity recording	37
Yu.V. Balabin, E.V. Vashenyuk, B.B. Gvozdevsky, A.V. Germanenko	All GLEs in one package	38
Yu.V. Balabin, E.V. Vashenyuk, B.B. Gvozdevsky, A.V. Germanenko	The first GLE of new 24th solar cycle	38
O.V. Kozyreva, N.G. Kleimenova	Fluctuations in the solar wind density and IMF and their ground effects	38
E.A. Maurchev, A.V. Germanenko, Yu.V. Balabin, E.V. Vashenyuk, B.B. Gvozdevsky	Simulation of the lead-free neutron monitor response function	39

A.I. Podgorny, I.M. Podgorny	The search of positions of X-ray emission sources in the magnetic field obtained by solar flare MHD simulation in a real active region	39
I.M. Podgorny, A.I. Podgorny, N.S. Meshalkina	The magnetic field dynamics of large active regions in the pre-flare state and during solar flares	40
N.V. Zolotova, D.I. Ponyavin	Role of tilt orientation of BMRs and meridional circulation in the polar magnetic field reversal on the Sun	40
Н.А. Бархатов, А.Е. Левитин, Е.А. Ревунова	Конфигурация магнитных облаков и сезонная зависимость геомагнитной активности	40
А.А. Любич	Взаимодействие малых магнитогидродинамических возмущений с вращательным разрывом в плазме низкого давления	41
С.Е. Ревунов, Д.В. Шадруков, Н.В. Косолапова	Отражение динамики солнечных плазменных потоков в вейвлет-скелетонных картинах параметров околоземного космического пространства	41

SESSION 5. IONOSPHERE AND UPPER ATMOSPHERE

F.S. Bessarab, Yu.N. Koren'kov, M.V. Klimenko, V.V. Klimenko	Spatial distribution of NO _x components during geomagnetic storms	45
M.G. Botova, A.A. Namgaladze, B.E. Prokhorov	Investigation of the polar cap soft electrons fluxes' influence on the latitudinal variations of the ionosphere total electron content and peak F2-layer electron density	45
S.A. Chernouss, I.I. Shagimuratov, I.I. Efishev	Auroral ovals and the irregularity ovals on the base of optical and GPS measurements	45
S. Chernouss, M. Shvec, M. Filatov, O. Antonenko	Case study of disturbed polar ionosphere impact on navigation systems by auroral and GPS data	46
M. Filatov, S. Chernouss, M. Shkrabalyuk, A. Nikitenko, A. Larchenko, S. Pilgaev, Yu. Fedorenko	VLF direction finder in Lovozero	46
D.A. Kargapolov, L.N. Makarova, A.V. Shirochkov	Auroral ionosphere dynamics during the two types of geomagnetic storms (CIR and CME)	47
M.I. Karpov, A.A. Namgaladze	Modeling of the TEC disturbances generated by seismogenic electric currents for different seasons	47
V.V. Klimenko, A.T. Karpachev, M.V. Klimenko, K.G. Ratovsky	Yakutsk Anomaly (YA) according to the satellite and ionosonde network observation data and its representation using the GSM TIP model	47
V.V. Klimenko, M.V. Klimenko, F.S. Bessarab, Yu.N. Koren'kov	Geomagnetic activity influence on the global changes in the ionospheric parameters during 2009 Sudden Stratospheric Warming	48
D.S. Kotova, M.V. Klimenko, V.V. Klimenko, V.E. Zakharov	Ionospheric response on May 2, 2010 geomagnetic storm and its influence on HF radio wave propagation at high-latitudes	48

B.V. Kozelov, B.U.E. Brandstrom, F. Sigernes, A.V. Roldugin, S.A. Chernouss	Practice of CCD cameras' calibration by LED low-light source	48
A.V. Larchenko, O.M. Lebed, Yu.V. Fedorenko	The measuring of induction magnetometer transfer function	49
O. Lebed, A. Larchenko, S. Pilgaev, O. Akhmetov, Yu. Fedorenko	Field structure of natural electromagnetic signals in ELF range in March 2012	49
O. Lebed, A. Larchenko, S. Pilgaev, Yu. Fedorenko	Vertical electric field measurements in ELF range	49
G.I. Mingaleva, V.S. Mingalev	A model study of the influence of artificial heating of the nighttime high-latitude ionosphere on the spatial distributions of the ionospheric parameters	49
I.V. Mingalev, G.I. Mingaleva, V.S. Mingalev	Numerical modeling the influence of magnetic activity on the global circulation of the middle atmosphere for January conditions	50
V.D. Nikolaeva, A.L. Kotikov, A.V. Shirochkov, L.N. Makarova, T. Raita	Dynamics of the precipitation spectral characteristics during sawtooth substorms	50
A.B. Pashin, A.A. Mochalov	Estimation of artificially enhanced electron temperature in lower ionosphere with absorption of the HF electromagnetic wave.	51
G.F. Remenets, A.M. Astafjev	Southern boundary of the ultra relativistic electron precipitation on May 13, 1987	51
V.C. Roldugin, M.E. Shkarbalyuk, A.V. Roldugin, S.V. Pilgaev	Auroral riometer absorption may be caused by auroral protons	52
N.V. Semenova, A.G. Yahnin	Horizontal scale of the Ionospheric Alfvén Resonator inferred from simultaneous auroral and magnetic observations	52
O.S. Ugolnikov, I.A. Maslov	Mesosphere temperature profile retrieval based on the wide-angle polarization measurements of scattering radiation during the twilight period	53
V.G. Vorobjev, V.K. Roldugin, O.I. Yagodkina	Optical characteristics of aurorae during undulation events on December 12, 2010	53
О.И. Ахметов, И.В. Мингалев, О.В. Мингалев, Ю.В. Федоренко, В.С. Мингалев, О.М. Лебедь	Модель распространения ультра и сверх низкочастотных сигналов в волноводе Земля — ионосфера, основанная на численном решении уравнений Максвелла с учетом реалистичной тензорной проводимости ионосферы	53
О.М. Бархатова, Н.В. Косолапова, Р.И. Серебрякова	Обнаружение магнитогравитационных волн по данным о вариациях концентрации ионосферного слоя F2 и магнитным наблюдениям в периоды высокоэнергичных геофизических событий	54
Е.Н. Ермакова, Д.С. Котик, А.В. Рябов, А.А. Панютин	Исследование вклада локальных грозовых очагов в формирование РСС и вариаций поляризации фонового магнитного шума	55
В.Л. Зверев, В.Г. Воробьев, Я.И. Фельдштейн	Околополуденное авроральное свечение на высоких широтах	55

А.П. Киреев, А.М. Крымский	Особенности распространения радиоволн в периоды высыпания частиц в мини-магнитосферах Марса	56
А.Л. Котиков, А.В. Франк-Каменецкий, А.А. Круглов, Н.Г. Клейменова, О.В. Козырева, М. Кубицки, А. Оджимек	Влияние возмущений в полярной ионосфере на вариации атмосферного электрического поля	56
В.Д. Терещенко	Влияние гравитации на распространение магнитозвуковых волн в нижней ионосфере Земли	57
Е.Е. Тимофеев, С.Л. Шалимов, О.Г. Чхетиани, М.К. Валлинкоски, Й. Кангас	Двухпараметрический характер термо-аномалии запылённого ночного аврорального динамо слоя	57
В.А. Ульев, О.А. Данилова, О.И. Шумилов	Связь некоторых характеристик ППШ с температурой верхней мезосфера	58
О.И. Ягодкина, В.Г. Воробьев	Электронные и ионные высыпания в утреннем и вечернем секторах в зависимости от уровня магнитной активности	58

SESSION 6. LOW ATMOSPHERE, OZONE

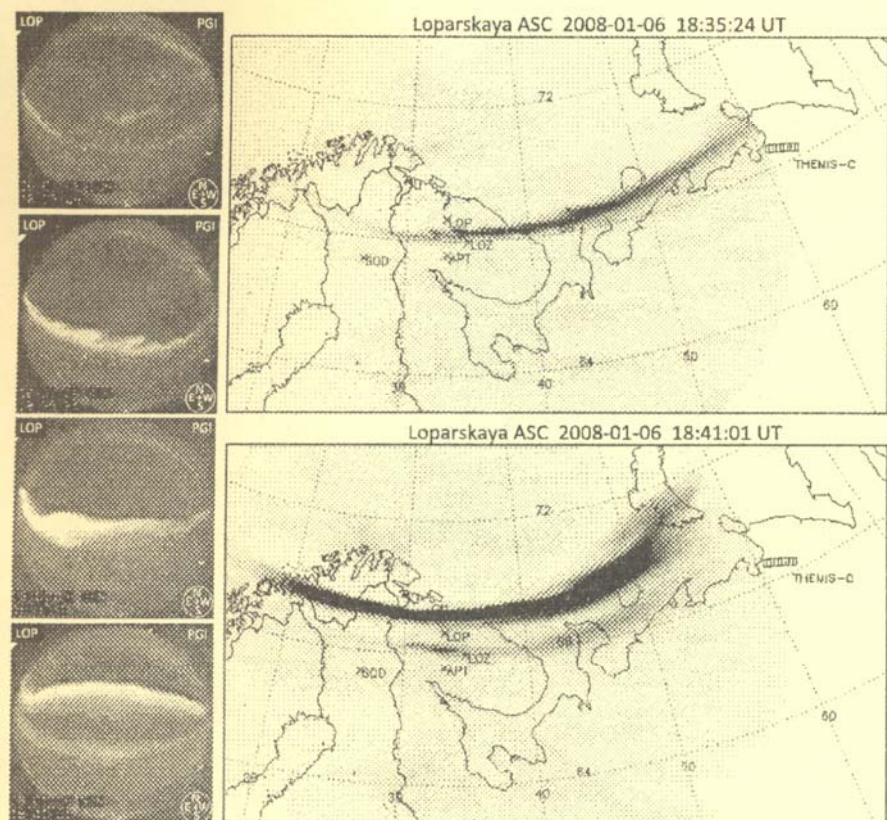
I.V. Artamonova, S.V. Veretenenko	Variations of sea level pressure in the Northern and Southern hemispheres in association with Forbush decreases of galactic cosmic rays	61
K.E. Beloushko	Modeling of the lower and upper atmosphere interconnection	61
V.I. Demin	Sensitivity of the tropospheric circulation to the GLE	61
V.I. Demin, P.A. Chernous, V.N. Moroz	Long-term changes in the vertical air temperature profile in the Khibiny Mountains	61
V.I. Kirillov, V.V. Pchelkin, M.I. Beloglazov, A.A. Galakhov	Seasonal changes of diurnal variation of atmospherics ELF-VLF range on observations at the Kola Peninsula	62
Y.Y. Kulikov, V.L. Frolov	Influence is artificial the indignant ionosphere on mesospheric ozone	62
I.V. Mingalev, N.M. Astafieva, K.G. Orlov, V.S. Mingalev, O.V. Mingalev, V.M. Chechetkin	Numerical simulation of the initial stage of the formation of large-scale cyclonic vortices in the vicinity of the intratropical convergence zone	63
I.V. Mingalev, K.G. Orlov, V.S. Mingalev	Simulation study of the mechanism of the formation of polar cyclones at high latitudes of the northern hemisphere	63
V.V. Pchelkin	On one kind of anomalies in angular distributions of the natural electromagnetic emissions in the ELF range from measurements in Lovozero observatory	64
O.S. Ugolnikov, A.F. Punanova, V.V. Krushinsky	Investigations of Antarctic stratosphere gas composition based on the high-resolution spectroscopy of the Moon during the lunar eclipse	64
A.M. Zvyagintsev, I.N. Kuznetsova	Comparison of air quality in Moscow and London megacities	64
Ю.В. Балабин, А.В. Германенко	Сезонные вариации в различных компонентах вторичных космических лучей	65

Ю.В. Балабин, А.В. Германенко, Э.В. Вашенюк, Б.Б. Гвоздевский	Баланс энергии и происхождение возрастаний приземного гамма-фона	65
А.В. Германенко, Ю.В. Балабин, Э.В. Вашенюк, Б.Б. Гвоздевский	Возрастания гамма-фона и состояние атмосферы в приземном слое	66
И.В. Мингалев, Е.А. Федотова	Метод расчета радиационных потоков в атмосферах Земли и других планет, удобный для применения параллельных вычислений	66

SESSION 7. HELIOBIOSPHERE

N.K. Belisheva, E.A. Maurchev, E.V. Vashenyuk	Biological effects, neutron fluxes and ambient equivalent doses near the Earth surface during GLE events in October 1989	69
E.S. Gorshkov, V.V. Ivanov	About interrelation of biochemical and physiological indicators with the cosmophysical factors, the system of data processing of Deep Data Diver revealed with use	70
V.V. Ivanov, E.S. Gorshkov	Cosmophysical conditionality of fluctuations of a ratio of pulse rates and breath in the conditions of Antarctic	70
A.A. Martynova, N.K. Belisheva, S.V. Pryanichnikov, V.V. Pozharskaya	The interrelationship of the physiological parameters and effects of heliogeophysical agents	71
R.E. Mikhailov, H.K. Belisheva, R.G. Novoseltsev, S.D. Chernej	Frequency distribution of deaths in psychoneurological boarding by phases of the solar cycle and the relationship of mortality with variations of geophysical agents	72
D.A. Petrashova, N.K. Belisheva, N.A. Melnik	Evaluation of the natural ionizing radiation genotoxicity on the meristematic cells of the <i>Vigna radiata</i>	72
S.V. Pryanichnikov, N.K. Belisheva, A.A. Martynova, V.V. Pozharskaya	Psychophysiological effects of heliogeophysical agent	73
O.I. Shumilov, E.A. Kasatkina, A.G. Kanatjev	Impact of solar and volcanic activity on the growth of pine trees at Kola Peninsula over the last 560 years.	74
O.I. Shumilov, E.A. Kasatkina, T.B. Novikova, A.V. Chramov	Space weather and injury rates among people living and working behind the Polar Circle.	74
T.S. Zavadskaya, N.K. Belisheva, I.V. Kalashnikova	Influence heliogeophysical agent on the functional state of human peripheral blood conditions of the Arctic	75
Author index		76

Geomagnetic Storms and Substorms



Using adaptive model to investigate the dipolarization events

I.A. Chernyaev¹, V.A. Sergeev¹, M.V. Kubyshkina¹, V. Angelopoulos²

¹*Saint Petersburg State University, Earth Physics Department, Saint Petersburg, Russia*

²*Institute of Geophysics and Planetary Physics, University of California, Los Angeles, California, USA*

We obtain new parameter values for T96_01 model and project isotropic boundaries (IB) of energetic protons and electrons from the neutral current sheet to the NOAA satellites altitude. We compare the position of the calculated IB with observed. To determine the position of IB in the neutral current sheet used ratio $Rc/\rho=8$ (Rc — curvature radius of the field line, ρ — gyroradius of particles). The isotropic boundaries according to the NOAA was determined from the discrepancy between the trapped and untrapped particles.

We obtain significant discrepancy model and observed position of the IB (more than 1,5 degrees in corrected geomagnetic latitude). So it is necessary to use other methods to reaserch dipolization events (for example, including substorm current wedge module). However, the adaptive model can be used to describe the structure of the magnetic field in the region before the dipolization.

Magnetic reconnection site in the magnetotail during different solar wind streams

I.V. Despirak¹, A.A. Lubchich¹, R. Koleva²

¹*Polar Geophysical Institute, Akademgorodok 26a, Apatity, 184209, Russia, despirak@gmail.com*

²*Space Research and Technologies Institute, BAS, Sofia, Bulgaria*

In this work we discuss the problem of the location of magnetic reconnection site in the magnetotail during substorms associated with different solar wind streams. It was shown recently that solar cycle variations of the solar wind control the location of magnetic reconnection in the tail. A well-known fact is that solar wind high-speed streams have different nature during different phases of solar activity. During the declining phase and minima of the solar cycle predominate the recurrent streams (RS) originating from coronal magnetic holes. During solar cycle maxima the flare streams connected with coronal mass ejections prevail. We analyze the relationship between the locations of the tail magnetic reconnection site during substorms connected with solar wind magnetic clouds (MC) and recurrent streams. We use data from Geotail spacecraft in the magnetotail and solar wind parameters from Wind spacecraft observations; the auroral bulge parameters were obtained by the Ultra Violet Imager onboard Polar. We show that magnetic reconnection in the magnetotail takes place closer to Earth when substorm is observed during MC, and further in radial distance for substorms during solar wind recurrent streams.

The relation of equatorward-moving auroral traces with energetic particle injections at the geostationary orbit

N.P. Dmitrieva¹, M.M. Beloshkurskaya¹, T.A. Kornilova², I.A. Kornilov²

¹*Saint Petersburg State University, Saint Petersburg, Russia, e-mail: ndpshka@yandex.ru*

²*Polar Geophysical Institute, Apatity, Russia*

One of the main ionospheric substorm manifestations is the auroral bulge with bright arc at the polar boundary. During the substorm expansion phase the discrete aurora region expands not only poleward but also equatorward. Equatorward moving discrete aurora forms dynamic auroral bulge equatorial boundary. To find the magnetospheric source of equatorward drifting discrete auroral structures the spatio-temporal comparison with energetic particles' injection at geosynchronous orbit was done. It is shown that most of the drifting discrete structures observed by all-sky cameras correspond to energetic particle fluxes bursts at geostationary LANL satellites located in the same MLT sector. In the cases when the bursts are not observed at LANL spacecraft, the minimum latitude achieved by auroral structures is higher than the LANL ionospheric projection. The possible relation between discrete drifting auroras and non-stationary plasma streams in the tail plasma sheet is discussed.

Scheme of space-time distribution of auroral luminescence in the dayside sector

Y.I. Feldstein¹, V.G. Vorobjev²

¹*Pushkov Institute of Terrestrial Magnetism, Ionosphere, and Radiowave Propagation, Troitsk, 142190, Russia*

²*Polar Geophysical Institute, RAS, Apatity, Murmansk region, 184200, Russia*

Schematic illustration of dayside auroral forms distribution, often cited in scientific literature, was developed by Sandholt et al. (2002). The integrated scheme presents location of auroral forms for magneto-quiet (IMF $B_z > 0$) and magneto-disturbed (IMF $B_z < 0$) intervals. Sandholt et al. (2002) divided the dayside aurorae into five types depending on their morphological features and hypothesized origins. The midday sector is often dominated by one or both types 1 and types 2 forms. The type 1 aurora usually observed during southward IMF and is characterized by a quasiperiodic sequence of equatorward boundary intensifications (EBIs). Many EBIs are followed by poleward moving auroral forms (PMAF). These authors assumed that the type 1 aurora is a low-altitude manifestation of plasma entry from the solar wind in low-latitude boundary layer. The east-west component of these form motion is regulated by IMF B_y component. The type 2 forms occurred during northward IMF orientation. Sandholt et al. (2002) supported that type 2 forms represent an ionospheric signature of plasma and momentum transfer from the solar wind along the poleward boundary of the cusp. Auroral forms of types 4 and 5 are the pre noon and after noon multiple arcs. A belt of diffuse aurora, called type 3, is located on the equatorward side type 1 and 4 forms in the pre noon sector. Dominated green line emission at 557.7 nm and very weak red line emission at 630.0 nm is the pronounced feature of diffuse type 3 aurora optical spectra.

Available at present surface and satellite observations of auroral luminosity, precipitating at high latitudes plasma fluxes of auroral energies allow to improve the existing scheme. The modified schemes of distribution of auroral luminosity forms in the dayside sector are compiled taking into account both Sandholt et al. (2002), and Russian researches. Magneto-disturbed intervals ($B_z < 0$ nT). Ray arc in midday sector (type 1 aurora) with auroral luminosity intensity intensifications (AI) is located near the projection at ionosphere height of the boundary between low-latitude boundary layer (LLBL) and cusp (CU) at $\Phi \sim 75^\circ$. AI drifts poleward (poleward drifting auroral forms – PDAF), east-west component of this drift is controlled by the IMF B_y component. Auroral forms of types 4 and 5 are pre noon and after noon multiple arcs of the auroral oval, connected with the central plasma sheet (CPS) in the nightside magnetosphere. PDAF are observed inside the broad band of the red diffuse auroral luminosity (duplet (OI) 630.0 - 636.4 nm, type 6 aurora), and disappear inside the band not reaching its poleward border. The red band is about 1° - 2° wider than the auroral oval and with its poleward part is connected with the mantle (MA). A belt of diffuse aurora, called type 3 aurora, is located on the equatorward side type 1 and 4 forms in the pre noon and noon sectors. Dominated green line emission 557.7 nm is the pronounced feature of type 3 optical spectra. Magneto-quiet intervals ($B_z > 0$ nT). The whole system of auroral forms shifts poleward. Bundles of rays or ray arc in midday sector (type 2 aurora) are located near the boundary between CU and MA at $\Phi \sim 78^\circ$. Auroral forms of types 4 and 5 are pre noon and after noon single arcs of the auroral oval. PDAF are observed inside the band of the red diffuse auroral luminosity (type 6 aurora). East - west component of this drift is controlled by IMF B_y component. A belt of diffuse aurora with dominate green line emission (type 3 aurora) is located on the equatorward side type 2 and 4 forms in the pre noon and noon sectors.

The role of IMF B_x component in the global magnetotail dynamics

E. Gordeev, M. Amosova, V. Sergeev (*Saint Petersburg State University, St.Petersburg, Russian Federation*)

Various internal and external parameters such as dipole tilt angle, IMF B_y component, orientation of solar wind discontinuities, etc. can lead to global asymmetry in the magnetospheric system. The IMF B_x component is also among them but was neglected in previous studies mostly because of absence of its significant correlation with activity indices. Using global MHD simulations we found that IMF B_x considerably influences the pressure balance between magnetotail lobes that leads to the deviation of neutral sheet position and geometry from nominal. The effect is essentially transient and shows two different modes of vertical displacement of the tail neutral sheet. The first mode, due to pressure imbalance between two lobes, is launched by IMF southward turning and qualitatively agrees with Cowley's (1981) model. The second mode is observed during explosive growth of the near-Earth tail reconnection, it can be qualitatively treated in terms of the asymmetric reconnection theory (Semenov et al, 1998). On the observational side, the set of Geotail (1995-2005) and Cluster (2000-2006) data complemented with solar wind measurements was utilized to test Cowley's theory and MHD simulation results. This statistical study reveals clear IMF B_x - related displacement of magnetotail neutral sheet.

Ground and satellite observations of the SAR arc in the dusk-bulge region of plasmasphere

I.B. Ievenko, S.G. Parnikov, V.N. Alexeyev (*Yu. G. Shafer Institute of Cosmophysical Research and Aeronomy, Yakutsk, Russia*)

It is known that stable auroral red (SAR) arcs are the consequence of interaction of the outer plasmasphere (plasmapause) with energetic ions of the ring current. Arisen downward flux of the superthermal electrons along magnetic field lines increases the ambient electron temperature at the altitudes of ionosphere F2 region in the form Te-peak and as a result enhances the atomic oxygen red line intensity in SAR arc, which maps the plasmapause (cold plasma density radial gradient).

A plasmasphere boundary location in the dusk-bulge region strongly depends on LT and shifts toward the lower latitudes in the evening hours. The ground observer can register relative motion of this boundary projection at the height of the ionosphere F2 region if it is manifested in some phenomenon.

In this work the results of observations with the meridian scanning photometer of the SAR arc equatorward motion at 19-20 LT at the Yakutsk meridian (199°E geomagnetic longitude) during a weak magnetic storm recovery phase February 7, 2000 are presented. The data of simultaneous registration of Te-peaks aboard DMSP F14 and F15 at the meridian of optical observations and eastward of it shows that SAR arc maps the cold plasma density radial gradient in the dusk-bulge region. A wide band of ionospheric drift (SAPS) also observed by F14 and F15 is probably a specific signature of the dusk-bulge region of plasmasphere.

Visualisation tool for geomagnetically induced currents

Ju. Katkalov¹, M. Wik², A. Viljanen³

¹Polar Geophysical Institute, Apatity, Russia

²NeuroSpace, Malmö, Sweden

³Finnish Meteorological Institute, Finland

As part of the EU/FP7 project EURISGIC, a visualisation tool for geomagnetically induced currents have been created. This tool have been developed for the purpose of demonstrating GIC in the wide European power grid for a set of geomagnetic storms and artificial geoelectric field data.

Power grid data for Europe, consisting of substation coordinates, line- and transformer resistances, voltage levels etc, were collected and stored in a MySQL database. At present the database includes information of about 1800 transformer stations and 2400 high-voltage lines for more than 30 european countries.

The application consists of two main parts: a server-side application and a client-side web application. The power grid and GIC levels are visualised on an interactive map by the web-application, using Google Maps API and JavaScript code, that is available online at <http://www.eurisgic.eu/>. The GIC levels are calculated by Octave. The server-side application interact with the web-application and database and uses the JSON format for transmitting the data.

The tool is useful for demonstrating GIC but also as a test-platform for a stand-alone application aimed towards e.g. power companies, pipeline operators and universities.

The research leading to these results has received funding from the European Community's Seventh Framework Programme (FP7/2007–2013) under grant agreement 260330.

THEMIS observations of three similar dipolarization events

T.A. Kornilova, I.A. Kornilov (*Polar Geophysical Institute, Murmansk Region, Apatity, Russia, kornilova@pgia.ru*)

During one-hour time interval (11.02.2008, 00:00-01:15 UT) THEMIS spacecraft (X=-6 Re, Y=4 Re) detected three almost identical dipolarization events coupled with very similar auroral activity of pseudobreakup type and rather different dispersionless particle injections.

In the first event both electron and proton spectra are strongly oscillating (period about 2.5 minutes) and anticorrelating. Electron spectrum also demonstrates anticorrelation of electron fluxes with energies 10-500 eV and 2-20 keV correspondingly, so in this case all electrons are accelerated from the local cold plasma background by some active process at the front of dipolarization wave, and in this case dipolarization is a primary event.

In the second event electron fluxes were sharply increased without noticeable changes in electrons energy. Fine details of depolarization (Bz components variations) for several seconds delayed of electron flux variations, so we can suppose that dipolarization is a secondary process.

Geomagnetic storms and substorms

In the third events there was no substantial changes in the total electron flux, but average electron energy increased from 2 keV up to 12 keV.

Different electrons and ions energy spectra behavior and different time delays between particles injection and depolarization demonstrate that magnetospheric plasma can release redundant energy by different ways having rather similar external appearance in aurora and dipolarization.

Ground based, THEMIS and DMSP observations of 24.01.2012 CME event

I.A. Kornilov¹, F. Sigernes², T.A. Kornilova¹

¹*Polar Geophysical Institute, Murmansk Region, Apatity, Russia, kornilova@pgia.ru*

²*The University Centre in Svalbard (UNIS), N-9171 Longyearbyen, Norway, Fred Sigernes fred@unis.no*

On the base of auroral white light TV observations at Lovozero, Barentsburg and Canadian Themis ASI data magnetospheric and auroral effects of 24.01.2012 strong CME (Coronal Mass Ejection) event were investigated. ACE, WIND, THEMIS and GEOTAIL satellites traced solar wind parameters, and information on precipitating particles was taken from DMSP spacecraft data. Principally new feature in ours aurora study was using the data of recently developed hyperspectral all-sky cameras (NORUSCA project) installed in Longyearbyen and Barentsburg in 2011. Cameras use electro-optical tunable filters to image the night sky as a function of wavelength throughout the visible spectrum with no moving mechanical parts. Comparison of fine details of aurora dynamics detected by b/w cameras and spatio-temporal variations of 4278, 4861 (protons), 5577 and 6300 emissions with THEMIS and DMSP satellites data on magnetic and electric fields and particle fluxes in magnetosphere and upper ionosphere in energy range 10 eV – 500 keV allowed making some preliminary conclusions concerning details of solar wind shock interaction with magnetosphere.

Behavior of ions near the substorm onset from THEMIS observations

T.V. Kozelova, B.V. Kozelov (*Polar Geophysical Institute, Apatity, Russia*)

The substorm associated slow and fast changes of ions near the Earthward edge of plasma sheet is examined using data from THEMIS-C during the late growth and early expansion phases. The spacecraft at $r \sim 6-6.5$ Re observed two ion populations with different behavior during the growth phase. The convection boundary of 10-keV electrons was embedded in this ion region. A few minutes before the substorm onset, simultaneously with an intensification of auroral arc in same longitudinal sector, the oscillations of the E and B fields and particles with period $\sim 50-60$ s start near this convection boundary. The injection of higher-energy (81 -157 keV) ions occurs during substorm onset simultaneously with the sharp pressure drop of ions of energies less than 29 keV. Sudden appearance of the current disruption expressed by an equivalent downward current is observed in a transition between the inner magnetosphere and active plasma sheet. Our analysis supports the idea about the ballooning instability near the inner edge of the plasma sheet as associated with the initiation of substorm onset.

Extremely quiet 2009 state of geomagnetic field as a reference level amplitude of the local geomagnetic disturbances

A.E. Levitin, L.I. Gromova, S.V. Gromov, L.A. Dremukhina (*Pushkov Institute of Terrestrial Magnetism, Ionosphere and Radio Wave Propagation (IZMIRAN), Troitsk, 142190, Russia*)

Extremely quiet 2009 state of the geomagnetic field may be used as a reference level to create new technology of quantitative assessment of geomagnetic activity which could be more opportune than that of AE(AU, AL), Kp, Dst indices, out-of-date and not without drawback, since introduced more than half a century ago. Calculating the external geomagnetic field hourly amplitudes applicable for any hour and any day of the whole survey period of any observatory proceeding is basing on the ground based magnetometer measurements. The calculated values may be used to find the amplitudes of the most magneto-quiet hour (day, month, year) and the most magneto-disturbed one for the whole measurement period. These data allow to estimate and to draw maps of the recent geomagnetic activity and the activity during specific geophysical events in the past at any point on the Earth. A detailed description of the method is presented with examples for estimation of the local geomagnetic activity at Moscow observatory. For the period 1958-2009 we calculated hourly values of H-component of the external geomagnetic field at Moscow observatory, based on hourly values of H-component of extremely quiet 2009 as a reference level,

and estimated correction for secular variation of the Earth's magnetic field at the observatory location. Thus we were able to assess local current geomagnetic activity and that for any hour (day, month, year) of the observatory measurements, to study seasonal variations of geomagnetic activity, evaluate the external magnetic field contribution to annual values of H-component of the Earth's Main magnetic field which are used to estimate the rate of change of the Earth's magnetic field.

On significant additional contribution of "old" tail lobes to substorm power

V.V. Mishin, V.M. Mishin, Yu.A. Karavaev and S.B. Lunyushkin (*The Institute of Solar-Terrestrial Physics of Siberian Branch of Russian Academy of Sciences, Irkutsk, 664033, Russia, e-mail: lunyushkin@iszf.irk.ru*)

Each open tail lobe and polar cap (PC) during substorm (and storm too) consists of two different "old" and "new" parts, observed prior and during the substorm correspondingly. Magnetic fluxes through these PC parts are denoted Ψ_{02} and Ψ_1 , and total $\Psi = \Psi_{02} + \Psi_1$. My talk is about Poynting flux transported from solar wind into geomagnetosphere during substorms by corresponding two parts of geotail. Only the new variable magnetic flux Ψ_1 is usually taken into account in the transfer of magnetic flux, assuming Ψ_{02} to be constant and passive part of the tail lobe, not participating in the transfer processes. We study here the alternative approach, denoting it as that, accounting beta-effects. In this approach, Ψ_{02} is changed during substorm and contributes essential part of input energy flux ϵ' , exceeding that of Ψ_1 . The initial method to account beta-effects was described by Mishin et al (2012). This method have allowed to authors to obtain two values of ϵ' , the maximal and minimal possible values of ϵ' , but not the real (unique) solution. In addition to it, we consider in the present talk the complemented method, which gives unique solution of the equation system for calculation of the flux ϵ' . Also we obtain estimates of energy W^* , accumulated in the tail during growth phase and energy W consumed during the active phase of the 27.08.2001 substorm. The results will be compared with those based on the known Perreault-Akasofu and Kan-Lee equation.

The 27 Aug 2001 magnetospheric substorm: Field-aligned currents and mesoscale plasma vortices in the polar ionosphere

V.M. Mishin, V.V. Mishin and S.B. Lunyushkin (*The Institute of Solar-Terrestrial Physics of Siberian Branch of Russian Academy of Sciences, Irkutsk, 664033, Russia, e-mail: lunyushkin@iszf.irk.ru*)

We present new data, which confirms the results of recent studies that processes, initiating the substorm, start in the distant and the most distant open magnetotail, where medium-scale vortex plasma motions are appeared that travel toward the Earth. Our analysis of the system of field-aligned currents (FAC) and ionospheric convection during the 27 Aug 2001 substorm development shows that explosive substorm onset occurred almost simultaneously on the whole area of the night polar ionosphere and in the volume of the tail from the furthest from the Earth, where it was in the beginning of the process, until the closest to the Earth. We propose a substorm scenario, containing new elements: (1) the coherent development of a system of FACs and mesoscale convective vortices, (2) double-expansion onset; (3) the dominant contribution of the meridional ionospheric currents to the general system of currents, connecting the magnetosphere and ionosphere (4) expansion onset as a short circuit of currents in the tail current disruption region and in the magnetosphere-ionosphere system, (5) short-circuit coverage of the total area of polar cap and the oval and, therefore, the distant and the near tail.

The Magnetospheric Magnetic field deformation: Effects of double-loop Substorm Current Wedge

A.V. Nikolaev¹, V.A. Sergeev¹, N.A. Tsyganenko¹, H. Singer², V. Angelopoulos³

¹*St.-Petersburg State University, St.-Petersburg, Russia*

²*Space Weather Prediction Center (NOAA), Boulder, USA*

³*University of California, Los Angeles, USA*

Recent studies of magnetic field dipolarization amplitudes simultaneously observed by one GOES and four THEMIS spacecraft radially-distributed in the magnetotail have confirmed a double-loop (R1-like plus R2-like) geometry of the Substorm Current Wedge (SCW) and introduce and test the new magnetospheric quantitative model SCW2L. To demonstrate and quantify the double-loop current system field line twisting effect we map fixed neutral sheet points to the ionosphere using T89+DIP+SCW2L magnetic field model and show the possible shapes of active

Geomagnetic storms and substorms

ionospheric structures (such as auroral bulge) can appear when the substorm current system arise. Using quantitative SCW2L model and varying it's parameters (current intensities, I_2 / I_1 ratio, field line stretching amplitude and equatorial current radial distance) we investigate ionospheric footprints shifts of such magnetospheric structures as (1) streamers, (2) isotropic boundaries (IB), (3) region of tail current disruption and (4) region where the radial plasma flow, which generates dipolarization front (DF), stops and forms R2-like equatorial current segment. Based on these results, we discuss the dynamics of auroral forms which is contributed by the magnetic effects generated by double-loop current system.

Proton precipitation in the auroral zone during interplanetary shock on 24 January 2012

V.C. Roldugin, A.V. Roldugin, S.V. Pilgaev (*Polar Geophysical Institute, Apatity, Russia*)

The SC event on 24 January 2012 at 1503 UT was accompanied by proton precipitation in the auroral zone accordingly to appearance of H α emission in meridian spectrometer data in Lovozero. The H α emission shows up at 1506 and disappears at 1512 UT.

Other distinctive features of this event are cosmic noise absorption during the SC impulse, and absence of H α emission during long train of Pc5 pulsations, started immediately after vanishing of the hydrogen emission.

Modeling of GIC in the regional power system for strong geomagnetic storm

Ya. Sakharov¹, Ju. Katkalov¹, A. Viljanen², R. Pirjola^{2,3}, P. Wintoft⁴

¹*Polar Geophysical Institute, Apatity, Russia*

²*Finnish Meteorological Institute, Helsinki, Finland*

³*Natural Resources Canada, Ottawa, Canada*

⁴*Swedish Institute of Space Physics, Sweden*

The new version of program for calculation of geomagnetically induced currents (GIC) in power lines was developed in the Finish Meteorological Institute in frame of the EURISGIC project (European Risk from Geomagnetically Induced Currents). Successful validation of the model in 2012 get chance to estimate possible extremal value of GIC related with strong geomagnetic disturbances at former times. The geoelectric field was calculated at the nodes of the model using data from IMAGE magnetometer stations in North Europe and 1-D block models of the ground conductivity. Time-depending GIC was estimated then using the regional model of the power grid at NW of Russia. Calculated extreme values of GIC at selected transformer substations can be used for analyses of the impacts of strong geomagnetic storms on high-voltage systems.

The research leading to these results has received funding from the European Community's Seventh Framework Programme (FP7/2007–2013) under grant agreement 260330.

The structure of irregularities in disturbed high latitude ionosphere observed by GPS/GLONASS TEC measurements

I.I. Shagimuratov, Iu. Cherniak, I. Ephishov, I. Zakharenkova (*West Department of IZMIRAN, Kaliningrad, Russia*)

The radio signals of navigation systems that passing through the ionosphere have rapid variations of their amplitude and phase - signal scintillations. The scintillations are caused by the permanent existence in the ionosphere of the irregularities with wide range of scale. It is very important for performance of the GNSS navigation system (GPS/GLONASS) to know information about estimates of scintillation and phase fluctuation effects on the accuracy of the obtained position. Effects of the ionospheric irregularities on the GPS signals can be evaluated by measurements of the differential phase time rate of dual frequency GPS/GLONASS signals. The permanent observations carried out at the Arctic IGS (International GNSS Service) stations were used in order to study the development of TEC fluctuations in the high latitude ionosphere. Standard GNSS RINEX files with 30 s sampling rate data gives possibilities to detect the mid –and large-scale ionospheric irregularities.

For detection of ionospheric irregularities it was used the rate of TEC (ROT, in the unit of TECU/min, 1 TECU= 10^{16} electron/m 2) at 1 min interval. The temporal behavior of TEC fluctuations can be observed in time variations in the dual frequency carrier phase along satellite passes. As a measure of the fluctuation activity level the Rate of TEC Index (ROTI) based on standard deviation of ROT was also used. ROTI was estimated in 10-minute interval.

The ROT/ROTI techniques and IGS data were used to study the occurrence of TEC fluctuations at the northern latitude ionosphere for selected geomagnetic storms occurred at the end of 23rd and beginning of new 24th solar cycles.

Analysis demonstrates that fluctuation activity of GPS signals in the high latitude ionosphere is depended on geomagnetic conditions. Intensity of fluctuations essentially increases during geomagnetic storm. The strongest TEC fluctuations occurred as a short time rate of TEC enhancements of a factor of 2-5 relative to quiet time.

During geomagnetic disturbed conditions strong phase fluctuations can be registered at latitudes lower than 65°. The study showed that the operating high-latitudes GPS stations can conduct the monitoring of the irregularity oval in near real-time mode.

GPS observations of the Northern hemisphere were used as raw data for mapping the irregularities over the North Pole. These maps illustrate the spatial structure of the ionospheric irregularities, so called irregularity oval, which position is correlated with the auroral oval. During geomagnetic storms the intensity of the irregularities essentially increases and their location expands toward equator.

This work was supported by Presidium RAS Program N22.

We are grateful to International GNSS Service (IGS) for GPS data and products.

Analysis of the energetic particle observations during satellite passes over the auroral bulge

S.A. Timofeeva, V.A. Sergeev (*Institute of Physics, Saint Petersburg State University, Saint Petersburg, Russia*)

During the substorm explosive phase the conditions of particle scattering in loss-cone and structure of the auroral precipitation is changing because of the magnetic field reconfiguration. Interpreting the precipitation picture (regions of wave-induced precipitation and regions of non-adiabatic current-sheet precipitation) observed before and after the substorm onset and by comparing observation made inside and outside the active region we can obtain information about the magnetic field reconfiguration. Particularly, by analysing the distribution of particle flux and loss cone anisotropy as well as positions of the isotropic boundaries (IB) and their dynamics measured at low altitudes we can identify the areas of dipolarization and plasma injection in the magnetosphere and define the type of particle scattering mechanism.

In this paper we study 16 crossings of NOAA satellites across the nightside auroral oval near the substorm onset (8 cases before and 8 cases after the onset). In pre-onset crossings we observe the standard pattern of the isotropic boundary energy dispersion and the peak of auroral precipitation near the electron IB. In the post-onset crossings the same picture is observed if the satellite crosses the oval outside the active region. For crossing above the auroral bulge, we unexpectedly observe the equatorward shift of the proton IB with (often) absent energy dispersion. By contrast, the electron IB is shifted poleward by 4-5 degrees latitude (depending on the disturbance intensity), the region in between proton and electron IBs is filled by high fluxes of isotropic protons and anisotropic electrons suggesting a strong dipolarization and particle acceleration in the magnetosphere in the magnetic flux tubes of the auroral bulge.

Dynamics of the auroral precipitation zones during recurrent stream on 19-22 February, 2006

O.I. Yagodkina, I.V. Despirak (*Polar Geophysical Institute, RAS, Apatity, Murmansk region, Russia, e-mail: despirak@gmail.com*)

Dynamics of the electron precipitation boundaries during magnetic storms on 19-22 February, 2006 were investigated. The magnetic storm with a minimum in Dst of -40 nT was driven by solar wind high-speed recurrent stream. The locations of auroral precipitation boundaries from DMSP spacecraft observations were compared to those obtained by an empirical model (<http://apm.pgia.ru/>). In this model the locations of different auroral precipitation regions depend on geomagnetic activity level expressed by the AL- and Dst indices. It is shown a good agreement between the observed with DMSP spacecraft and calculated data for different MLT sectors. This allows us to use the model to examine the dynamics of auroral precipitation during the different intensity magnetic storms. The significant latitudinal displacements of the diffuse auroral zone (DAZ) and the auroral oval precipitation (AOP) along with an increase in magnetic activity were observed. The broadening of zones was more significant in the night sector (21-24 MLT). It has been shown a noon-midnight symmetry, which is controlled by an AL index. On the contrary, any differences in dawn-dusk widening (i.e., asymmetry) of the DAZ and AOP zones were not observed which were demonstrated during magnetic storms associated with solar wind magnetic clouds.

Как нам реорганизовать расчет геомагнитной активности

А.Е. Левитин, Л.И. Громова, С.В. Громов, Л.А. Дремухина (*Институт земного магнетизма, ионосферы и распространения радиоволн им. Н.В.Пушкина РАН (ИЗМИРАН), Троицк, 142190, Россия*)

Количественный расчет геомагнитной активности должен начинаться с её конкретного физического определения. Одновременно должен быть предложен конкретный метод расчета количественной величины этой активности, которая может быть или равна или пропорциональна её величине. Сегодня в Интернете можно найти только одно подобное конкретное физическое определение геомагнитной активности: геомагнитная активность ([англ. Geomagnetic activity](#)) – это возмущения магнитного поля Земли, связанные с изменениями магнитосферно-ионосферной токовой системы (Википедия). Правда, рядом с этим определением не указано как конкретно можно проводить количественный расчет этого возмущения. Вместо разработки современного количественного расчета геомагнитной активности, как на уровне земной поверхности, так и в околоземном пространстве, мы продолжаем пользоваться индексами геомагнитной активности, доставшимися нам от замечательных ученых до спутниковой эпохи. В докладе указываются значительные недостатки этих индексов, которые связанные с тем, что их замечательные авторы не владели информацией, которая появилась в период спутниковой эпохи. Одновременно предлагается метод количественной оценки локальной наземной геомагнитной активности переменного геомагнитного поля на основе расчета часовых амплитуд геомагнитного поля, регистрируемых мировой сетью магнитных обсерваторий. Он опирается на уникальное состояние солнечной и геомагнитной активности в 2009 году, что позволяет ввести уровень отсчета часовых амплитуд компонент векторов геомагнитного поля регистрируемых этими обсерваториями. Физическое содержание предлагаемой локальной наземной геомагнитной активности это – энергия магнитного поля, содержащаяся в часовых амплитудах компонент вектора переменного геомагнитного поля, регистрируемого магнитной обсерваторией. Такая энергия количественно определяется как сумма квадратов амплитуд часовых данных этих компонент или как только одной Н компоненты. Таким образом, имея данные геомагнитных измерений мировой сети обсерваторий, мы получаем возможность характеризовать наземную геомагнитную активность переменного геомагнитного поля.

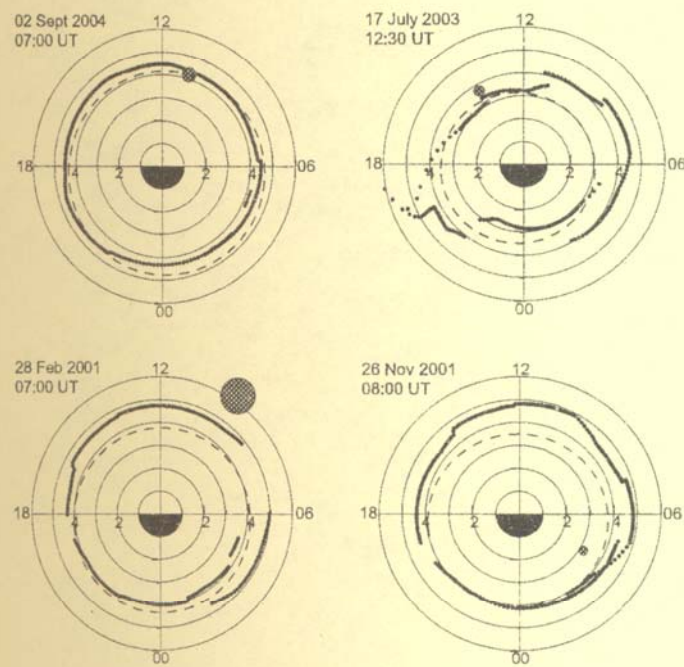
Исследование динамики положения плазмопаузы во время сильной магнитной суббури по данным меридиональной цепочки станций

Ю.А. Копытенко, В.С. Исмагилов, А.Л. Котиков, М.С. Петрищев, П.Е. Терещенко, А.В. Петленко, Д.Б. Зайцев, Д.Ю. Сарычев (*г. Санкт-Петербург, СПбФ ИЗМИРАН, ЕМ: office@izmiran.spb.ru*)

В августе-сентябре 2012 г. на территории Карелии была установлена меридиональная цепочка из пяти высокочувствительных трехкомпонентных магнитовариационных станций GI-MTS-1 в диапазоне исправленных геомагнитных широт $\Phi=59.5^\circ\text{--}62.0^\circ$. Расстояние между соседними станциями составляло $\sim 70\text{--}90$ км. Синхронизация записей вариаций магнитного поля осуществлялась с помощью GPS. Сильная магнитная суббури наблюдалась 05.09.2012 с 01:00 до 04:30 UT. На самой северной станции (Кузема) величина магнитного поля в Н-компоненте составляла ~ 600 нТл. Известно, что регистрируемые на земной поверхности геомагнитные вариации усиливаются в районе проекции плазмопаузы. Поэтому местоположение плазмопаузы на земной поверхности определялось по максимуму интенсивности геомагнитных возмущений в диапазоне частот $F=0.001\text{--}5$ Гц и по знаку разности этих интенсивностей на соседних станциях.

До начала суббури плазмопауза находилась севернее 62° . Установлено, что в течении суббури плазмопауза неоднократно смещалась на юг и достигала широты $\sim 60^\circ$. Наиболее четко положение плазмопаузы отслеживалось по данным горизонтальной Н компоненты. Определяемое положение плазмопаузы подтверждается также тем, что на данной широте регистрируется граница раздела западного и восточного электроджетов (разрыв Харанга), построенных по данным использованных магнитных станций.

Fields, Currents, Particles in the magnetosphere



SAR arc formation due to the interplanetary shock and substorm on December 14, 2006

I.B. Ievenko (*Yu. G. Shafer Institute of Cosmophysical Research and Aeronomy, Yakutsk, Russia*)

It is known that stable auroral red (SAR) arcs are the consequence of interaction of the outer plasmasphere with energetic ions of the ring current. The diffuse aurora is caused by the low-energy electron precipitation from the plasma sheet. Our studies at the Yakutsk meridian (199°E geomagnetic longitude) indicate that the SAR arc appears and/or brightening during the substorm expansion phase. The SAR arc formation begins in the equatorward boundary region of diffuse aurora (Ievenko, 1999; Ievenko et al, 2008). In this work the results of observations with all-sky scanning photometer of SAR arc formation during a substorm whose expansion phase has begun in 15 minutes after the onset of SC due to the impact of the strong interplanetary shock are presented.

The main development features of the phenomena in the event of December 14, 2006. At 1415 UT the SC has caused a dispersionless injection of energetic protons and electrons on the geosynchronous orbit in the morning MLT sector with a subsequent extension of proton flux into the dusk sector as a result of the gradient drift in the magnetic field. With a delay of 2 minutes an abrupt enhancement of the 427.8 nm emission in the nightglow in the premidnight MLT sector at the Yakutsk latitude (56°N geom.) caused, probably, by precipitation of energetic neutral atoms (ENA) has been observed.

At 1430 UT the intense substorm expansion phase with amplitudes of AL \sim -1300 and ASY-H \sim 200 nT indices has begun. At 1440 UT the photometer has registered the 630 nm emission intensification in the form of patch at 61°N latitude. The red patch with a diameter of \sim 300 km appears in a vicinity of diffuse aurora boundary and moves equatorward close to the Yakutsk meridian with the increase of velocity from 100 to 300 m / s. At 1510 UT the 630 nm emission intensification has been already observed in the form of SAR arc at \sim 57°N latitude.

Geosynchronous observations of the change of fluxes of energetic protons and electrons aboard the LANL spacecraft in the evening and midnight MLT sectors indicates to the location of substorm injection centre close to the Yakutsk meridian. This suggests that the dynamics of SAR arc formation in this event maps a prompt radial diffusion (electric drift) of energetic particles from the central region of substorm injection into the inner magnetosphere.

Dayside aurora

I. A. Kornilov¹, F. Sigernes², T. A. Kornilova¹

¹*Polar Geophysical Institute, Murmansk Region, Apatity, Russia, kornilova@pgia.ru*

²*The University Centre in Svalbard (UNIS), N-9171 Longyearbyen, Norway, Fred Sigernes fred@unis.no*

Four cases of noon auroral activity (11.00-13.00 MLT) were studied on Barentsburg TV camera and DMSP satellite data (07-08.12.2000, 22.12.2003, 12.12.2004). Keograms demonstrate poleward moving auroral forms (PMAFs) – indication of dayside magnetopause reconnection. Events analyzed have three common features:

1. Aurora has well-pronounced beam structure, similar to the nighttime breakup, where most of precipitating electrons are accelerated by field-aligned electric fields.
2. Tendency to anticorrelation of electron and proton fluxes was found - sure sign of electron acceleration by parallel electric field.
3. Electron energy spectra often show the presence of second high-energy component.

Seven cases of noon aurora detected by Barentsburg NORUSCA hyperspectral TV camera together with DMSP data were studied as well (December 2011 – January 2012). Camera recorded all-sky aurora images in 15 spectral lines between 4000A and 8000A. Previous conclusions were well confirmed, and synthesized NORUSCA RGB images (4278+5577+6300A emissions) directly demonstrate that diffuse and discrete beam-structured noon aurora caused by different mechanisms – diffuse aurora have mostly red color (soft-energy precipitation), but beams are mostly green (high energy of electrons).

We can suppose that low energy noon aurora caused by magnetopause field lines reconnection and direct penetration of solar wind particles, but high-energy beam-structured aurora is the result of field-aligned currents generation and electrostatic electron acceleration in parallel electric fields.

The study of magnetic barrier parameters dependence on the direction and intensity of the interplanetary magnetic field

K.Yu. Slivka, V.S. Semenov, and N.P. Dmitrieva (*Saint-Petersburg State University, Saint-Petersburg, Russia*)

The magnetic barrier is the region with enhanced magnetic field magnitude and depleted plasma. It is formed in the inner magnetosheath layer adjacent to the low-latitude dayside magnetopause.

Fields, currents, particles in the magnetosphere

There is a general point of view now that a magnetic barrier can persist only for the northward direction of interplanetary magnetic field (IMF) while it is absent for the southward direction. We make a special study to check appearance of magnetic barrier for different directions of IMF. To this end a data base consisting 63 events of low-latitude dayside magnetopause crossings by the THEMIS satellites was created and analyzed. In order to study the variations of key plasma parameters and the magnetic field in the magnetopause and the adjacent magnetosheath in a systematic way we used a superposed epoch analysis. It turns out that the magnetic barrier is the most pronounced for the northward IMF. For the southward IMF we still were able to find events with signatures of magnetic barrier. According to the theory magnetic barrier builds up more slowly than it collapses. Also we find out that the magnetic barrier field at the dayside magnetopause is about 80% of the magnetospheric value for southward IMF cases with a minimum magnetopause reconnection rate. In other hand, previous statistical studies showed that for southward IMF the magnetic barrier field is no more than 50% of the magnetospheric value.

The model calculations of the Poynting flux over the auroral arc

M.A. Volkov (*Murmansk State Technical University, 13 Sportivnaya Str., Murmansk, 183010, e-mail: volkovma@mstu.edu.ru*)

In this work the solution for the electric field across the auroral arc consistent with currents flowing into and from of the arc have been obtained. The model of the currents flowing into and from the arc has been specified but at the same time the currents across the arc have been calculated taking into account the ionization and recombination processes in the ionosphere. The solution for the auroral arc electric field depends on the background electric field or the field of the large-scale magnetospheric-ionospheric convection. The case where the current across the arc has opposite direction to the electric field has been considered. In this case, the arc is a generator of electromagnetic energy, and the Poynting vector is directed upward from the ionosphere. Using the model of the magnetospheric-ionospheric convection the areas where the arc can be the electromagnetic generator have been identified. The results of the calculation have been compared with the observations.

Long –lived proton auroras equatorward of the auroral oval on the dayside

A.G. Yahnin, T.A Yahnina (*Polar Geophysical Institute, Apatity, Russia (e-mail: ayahnin@gmail.com)*)

From the analysis of the IMAGE FUV instrument images we found a new (not described yet) type of sub-oval proton aurora on the dayside. This is long-lived (up to several hours) aurora that occurs during relatively quiet geomagnetic conditions and at relatively high latitudes in close relation with ground observations of geomagnetic pulsations Pc1. The latter means that both proton auroras (precipitation of protons) and pulsations are the result of the ion-cyclotron (IC) instability of the near-Earth plasma. Comparison with measurements onboard LANL spacecraft shows that the instability does not relate to the high cold plasma density, that is, the instability develops outside plasmasphere. The lack of the cold plasma explains the fact that related Pc1 frequency are always above equatorial gyrofrequency of He⁺ at the latitude of the proton auroras. We conclude that the IC instability is the result of the increased anisotropy of energetic ring current protons drifting around the Earth. The anisotropy increases in the day sector due to effect of the drift shell splitting.

Аномальные возмущения в вековых вариациях магнитного поля Земли перед катастрофическим землетрясением в Японии 11.03.2011

В.С. Исмагилов, Ю.А. Копытенко, Г.М. Попов (*г. Санкт-Петербург, СПбФ ИЗМИРАН, ЕМ: office@izmiran.spb.ru*)

11 марта 2011 г. у восточного побережья Японии произошло землетрясение с магнитудой M = 9. Это землетрясение оказалось сильнейшим за весь срок сейсмических наблюдений в Японии. Эпицентр землетрясения располагался под дном моря на расстоянии ~130 км от берега и на глубине ~24 км. По данным двух магнитных станций Есажи и Мизусава, расположенных на территории Японии на расстоянии ~180-200 км от эпицентра землетрясения исследовались вековые вариации главного магнитного поля Земли. Вековые (секулярные) компоненты главного магнитного поля Земли изменяются достаточно гладко в течение десятков и сотен лет. Однако в период 2000-2011 г. в районе катастрофического землетрясения на территории Японии обнаружены четыре аномалии в вековых вариациях главного магнитного поля Земли с длительностью от полугода до трех лет. Все аномалии развивались одновременно с возникновением и

развитием локальных сейсмоактивных зон в пределах ~ 100 км от использованных магнитных станций и предшествовали сильным землетрясениям ($M > 6$). Наиболее отчетливо аномалии видны в разностях соответствующих магнитных компонент измеренных на этих двух станциях расположенных на расстоянии ~ 19 км друг от друга. Последняя аномалия была самой сильной и проявлялась около 3 лет перед моментом катастрофического землетрясения ($M=9$) в Японии.

Возможной причиной аномального поведения магнитного поля перед землетрясениями может быть изменение проводимость в локальной области земной коры вследствие тектонических процессов. На начальном этапе тектонические процессы приводят к повышению температуры и, следовательно, повышению проводимости в области будущего гипоцентра землетрясения, что приводит к перераспределению земных токов и изменению магнитного поля на земной поверхности. В дальнейшем тектонические процессы приводят к усилению трещиноватости в области будущего гипоцентра и к уменьшению проводимости перед моментом землетрясения.

Анизотропия пространственного скейлинга в полярных сияниях по наземным наблюдениям в Апатитах

Б.В. Козелов (ПГИ КНЦ РАН, г. Апатиты, Россия, Boris.Kozelov@gmail.com)

По данным наземных наблюдений комплекса авроральных камер анализировались спектры пространственных флуктуаций аврорального свечения в анизотропных формах (дуги, полосы и системы дуг). Спектры рассчитывались по одномерным сечениям наблюдаемого двумерного распределения методом логарифмических диаграмм с использованием дискретного вейвлет-разложения по вейвлетам Добеши 3-5 порядков. Получены зависимости спектральных индексов от ориентации сечения. Проведено сравнение с аналогичными характеристиками, полученными из теоретических представлений.

Отождествление долгопериодных МГД пульсаций в магнитосфере методами вейвлет-скелетонного анализа как предвестников протонных солнечных вспышек

С.Е. Ревунов, Д.В. Шадруков, Н.В. Косолапова (Нижегородский Государственный Педагогический Университет, Нижний Новгород)

Ранее было замечено [Быстров М.В., Кобрин М.М., Снегирев С.Д. Квазипериодические пульсации магнитного поля Земли с периодами 20-200 минут и их связь с аналогичными пульсациями в радиоизлучении Солнца перед протонными вспышками // Геомагнетизм и аэрономия, 1979, Т.2, с.306], что за несколько дней до развития солнечной вспышки в магнитосфере могут наблюдаться долгопериодные (~ 20 мин) МГД пульсации, обнаруживаемые в компонентах геомагнитного поля наземных обсерваторий. Методы анализа данных, основанные на алгоритме преобразования Фурье в данном случае малопригодны, т.к. они не содержат информации о динамике частотного режима быстро изменяющегося сигнала. В связи с этим, в исследовании выполняется вейвлет-анализ компонент геомагнитного поля, позволяющий отслеживать эволюцию МГД пульсаций в магнитосфере на разных масштабах. Более того, нами использована вейвлет-скелетонная техника обработки данных, что делает интерпретацию результатов максимально наглядной. В работе рассматривается возможность использования этих результатов в качестве предвестников возникновения мощных протонных солнечных вспышек.

Исследование выполнено на минутных данных для компонент геомагнитного поля шести среднеширотных (310-640) обсерваторий Leirvogur, Valentia, Kanoya, Hatizyo, Kakioka, Memambetsu в широком диапазоне координат, полученных с ресурса <http://wdc.kugi.kyoto-u.ac.jp>. Также анализировались одновременные минутные данные о мощности рентгеновского излучения, предоставленные ресурсом <http://spidr.ngdc.noaa.gov/spidr>, минутные данные параметров солнечного ветра: модуль ММП, плотность потока, давление (<http://cdaweb.gsfc.nasa.gov>). Анализ данных выполнен за полные 5 магнитоспокойных дней предшествующие регистрации конкретных протонных вспышек на Солнце по данным каталога NASA (<http://cdaw.gsfc.nasa.gov>).

Вейвлет-скелетонная техника, с разложением по базисной функции Добеши четвёртого порядка, применялась для обработки и сопоставительного анализа компонент геомагнитного поля, фиксируемых наземными обсерваториями. В результате в полученных скелетонах были обнаружены долгопериодные МГД пульсации, регистрируемые за несколько дней до развития протонной вспышки. Аналогичные пульсации удалось обнаружить и в модуле скорости потока солнечного ветра. Выполненный анализ двух протонных солнечных вспышек показал, что вспышке X3.9 (11.03.2003, 09:43-10:19 UT) предшествовали колебания горизонтальной компоненты геомагнитного поля на всех исследуемых станциях за ~ 48 -60 часов

Fields, currents, particles in the magnetosphere

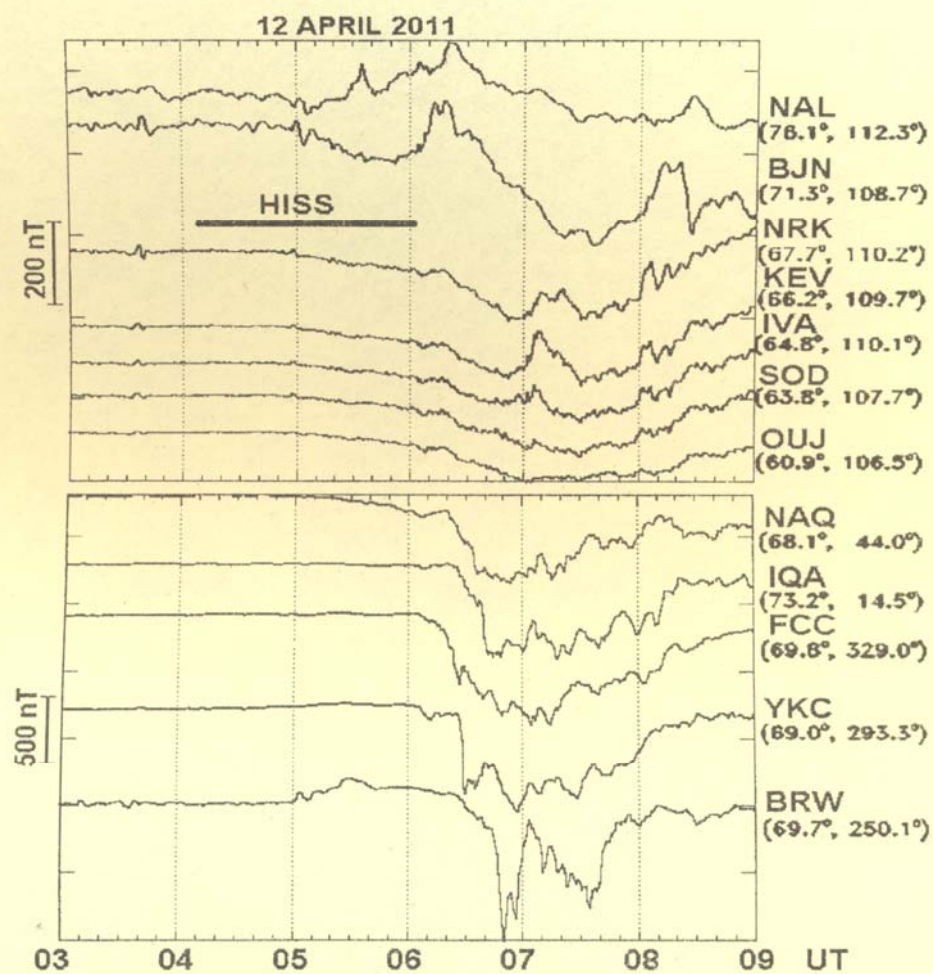
до начала события, а вспышке X3.6 (16.07.2004, 13:49-14:00 UT) – колебания горизонтальной компоненты геомагнитного поля на всех исследуемых станциях за ~30-40 часов до начала события.

Новый тип высыпаний энергичных протонов к экватору от изотропной границы

Т.А. Яхнина, А.Г. Яхнин, Т.А. Попова (*Полярный геофизический институт КНЦ РАН, Анадырь, tyahnina@gmail.com*)

По данным наблюдений потоков энергичных протонов на спутниках NOAA обнаружен новый тип высыпаний протонов к экватору от изотропной границы – высыпания на широтах 65°-70° на дневной стороне. Характерный широтный размер таких высыпаний – более 2° градусов, что также, кроме широты наблюдения, отличает их от известных типов локализованных (~1°) высыпаний протонов, связанных с геомагнитными пульсациями Pc1 и КУП. Высыпания наблюдаются за плазмопаузой после периодов повышенной геомагнитной возмущенности (например, геомагнитных бурь). Рост потока высыпающихся протонов часто наблюдается при скачках динамического давления солнечного ветра. При превышении потока протонов величины ~105 (см² ср с)-1 в области протонных высыпаний могут наблюдаться протонные сияния. Повышенные потоки высыпающихся протонов коррелируют с геомагнитными пульсациями диапазона Pc1. Высказано предположение, что этот тип высыпания протонов обусловлен взаимодействием ионно-циклотронных волн с протонами кольцевого тока, которое наиболее эффективно в дневном секторе, где в результате расщепления дрейфовых оболочек на относительно высоких широтах возникает область повышенной поперечной анизотропии энергичных протонов.

Waves, Wave-Particle Interaction



Pg wave detected by array of satellites

V.B. Belakhovsky¹, V.A. Pilipenko², S.N. Samsonov³, D.Yu. Klimushkin⁴

¹*Polar Geophysical Institute, Apatity, Russia*

²*Institute of the Earth Physics, Moscow, Russia*

³*Institute of Cosmophysical research and Aeronomy, Yakutsk, Russia*

⁴*Institute of Solar-Terrestrial Physics, Irkutsk, Russia*

Pg geomagnetic pulsations in the Pc4-5 frequency range during 2007 were studied using the magnetometer and particle data from geostationary GOES, LANL, and ETS-8 satellites, augmented by THEMIS satellite data. The recorded pulsations had monochromatic wave forms and were observed during quiet geomagnetic conditions. However, in contrast to the previously reported Pg wave events, these pulsations practically could not be seen by the ground-based magnetometers. The geostationary observations showed that Pg pulsation had dominant radial and field-aligned components. The cross-correlation between the GOES-10 and GOES-12 data yielded the azimuthal wave number $m \approx 20-25$. The observations from the LANL satellites indicated that these Pg pulsations may be generated by a cloud of protons with energies 50-75 keV due to some kinetic instability.

The investigation of the spatial distribution of auroral Pc5 pulsations and its connection with simultaneous Pc5 pulsations in geomagnetic field and CNA

V.B. Belakhovsky¹, V.A. Pilipenko²

¹*Polar Geophysical Institute, Apatity, Russia*

²*Institute of the Earth Physics, Moscow, Russia*

The coupling between the auroral Pc5 pulsations and simultaneous Pc5 pulsations in geomagnetic field and cosmic noise absorption (CNA) has been studied using the data from magnetometer array CARISMA, riometer network NORSTAR, and Barentsburg station. The aurora observations were made with meridian scanning photometers (MSP). Geomagnetic Pc5 pulsations reveal the resonance properties: the decrease of the pulsations frequency with the increase of the geomagnetic latitude, and the apparent propagation from low to high latitude. The geomagnetic Pc5 pulsations were accompanied by corresponding auroral Pc5 pulsations in 557.7, 630.0, and 471 nm emissions. The auroral Pc5 pulsations were found to propagate from low to high latitudes. Auroral and geomagnetic Pc5 pulsations were accompanied by the pulsations in CNA with the same frequency. Auroral Pc5 pulsations were observed in a more narrow latitudinal interval than geomagnetic Pc5 pulsations. This fact shows that geomagnetic Pc5 pulsations are the source for the auroral Pc5 pulsations. The ratio of 557.7/630.0 emissions indicates that auroral Pc5 pulsations may be generated by accelerated magnetospheric electrons.

Comparative analysis of the ULF emissions fractal characteristics in quiet and disturbed conditions

T.V. Bondareva, N.A. Smirnova (*Institute of Physics, St. Petersburg University, St. Petersburg 198504, Russia, e-mail: b.ndareva@gmail.com*)

In our previous presentations, a statistical analysis of the ULF emissions fractal characteristics versus Kp-index of geomagnetic activity was introduced. On the basis of magnetic data obtained on a network of the 210 MM stations, we have shown that the ULF emissions fractal dimension D decreased and the corresponding spectral exponent β increased with increasing of the Kp-index. Here we continue to consider the dependence of the ULF emissions fractal characteristics on geomagnetic activity, fulfilling the case study of the D and β dynamics in quiet and disturbed conditions, as it follows from the Dst-index variations. It is revealed that ULF emissions fractal dimension drops sharply under transition from quiet to disturbed conditions, which means a change of the ULF emissions behavior from antipersistent regime (during quiet conditions) to persistent regime (during geomagnetic disturbances). The results obtained are discussed on the basis of the SOC (Self-organized criticality) consideration. A possibility of using of the revealed peculiarity as a precursory signature of geomagnetic disturbance is considered.

Cyclotron acceleration of radiation belt electrons by whistler-mode chorus waves

A.G. Demekhov (*Institute of Applied Physics, Nizhny Novgorod, Russia*)

We study the efficiency of nonlinear gyroresonant interaction of radiation-belt electrons with VLF chorus wave packets. Model wave packets with linear and parabolic frequency drift and artificially imposed amplitude modulation are used along with a realistic wave packet taken from Cluster data. It is shown that the amplitude modulation in a wave packet decreases significantly the number of particles which are accelerated in the regime of trapping by the wave field. We calculate the net energy balance between a particle population and a wave packet and discuss its dependence on the wave amplitude and frequency drift.

Interplay of Alfvénic and electrostatic ion-cyclotron processes in the magnetosphere-ionosphere coupling on small scales

I.V. Golovchanskaya (*Polar Geophysical Institute, Apatity, Russia*)

The role of the EIC waves in the development of the broadband ionospheric turbulence is considered. These waves can be involved (a) by producing density variations, which alter the propagation of shear Alfvén waves, leading to the appearance of small spatial scale sizes in the plane perpendicular to the external magnetic field, and (b) by producing a kind of anomalous perpendicular diffusion, which is important in the non-linear interaction of Alfvénic coherent structures. On the other hand, the non-uniform electric fields (transverse velocity shears) of Alfvénic turbulence change the dispersive properties of the medium and thereby influence the propagation of the EIC waves, modifying their dispersion relation.

Application of extremely low frequency electromagnetic waves for subsurface-surface communication in mines

V.A. Lubchich (*Polar Geophysical Institute, Murmansk, Russia*)

The report deals with problems of organization of extremely low frequency wireless subsurface - surface communication in mines. In 2011 the experiment was carried out in the mine "Barentsburg" in the Spitsbergen. The extremely low frequency radio signal, radiated by subsurface mobile low-power source of electromagnetic waves, was recorded on the surface of the Earth. The radio signal was generated at frequencies of 10.9, 36.7, 76.2 and 159.4 Hz. The transmitter was located at a distance of 3.4 km from the receiver. The measured amplitudes of magnetic field components, normalized on the current, amounted to $|Hz| = (3.7 \pm 1.7) \cdot 10^{-9}$ A/m, $|Hx| = (6.3 \pm 1.7) \cdot 10^{-9}$ A/m and $|Hy| = (1.7 \pm 0.6) \cdot 10^{-9}$ A/m, the X axis is directed along the magnetic meridian to the North. It was found, that the measured values of the magnetic field greatly exceeded the normal values, computed for subsurface vertical magnetic dipole. The normal values of magnetic field amounted to $|Hz_0| = 2.4 \cdot 10^{-10}$ A/m, $|Hx_0| = 2 \cdot 10^{-11}$ A/m and $|Hy_0| = 1.7 \cdot 10^{-12}$ A/m. It was suggested, that the high values of the observed magnetic field amplitudes were caused by influence of geoelectric heterogeneities in the Earth. Three dimensional modeling of nonhomogeneous ground was performed by the method of grid approximation of Maxwell's equations in order to estimate this influence. The model took into account the relief of the area, the proximity of sea bays and the presence of thin high conducting coal seam. The model values of magnetic field amplitudes amounted to $|Hz_m| = 2.1 \cdot 10^{-9}$ A/m, $|Hx_m| = 7.8 \cdot 10^{-10}$ A/m и $|Hy_m| = 3.7 \cdot 10^{-10}$ A/m. So it was demonstrated, that the largest increase of observed magnetic field amplitudes can be determined by high conducting areas in the ground, for example, the coal seam.

Spectacular quasi-periodic VLF emissions in the auroral latitudes

J. Manninen¹, N.G. Kleimenova², O.V. Kozyreva²

¹*Sodankyla Geophysical Observatory, Sodankyla, Finland*

²*Institute of the Earth Physics of RAS, Moscow, Russia*

The new type of the long-lasting quasi-periodic (QP) VLF emissions in the frequency range of 1–5 kHz was found during the winter Finnish VLF campaign ($L = 5.3$) in December 2011. These emissions were not accompanied by geomagnetic pulsations. The considered QP emissions were recorded as unusually spectacular events with a

duration of several hours, observed during the night-time under very quiet geomagnetic conditions ($K_p \sim 0-1$), although the typical QPs usually occur during the daytime. The spectral structure of these QP events represented an extended, complicated sequence of the repeated discrete rising VLF signals with duration of about 2–3 min each. The repetition signal periods ranged from about 1 min to about 10 min. At least 5 such non-typical events are observed during this campaign. A fine structure of the separated QP elements represented a mixture of the different frequency band signals, which seem to have independent origins. It was found that the periodic signals with lower frequency appear to trigger the strong dispersive upper frequency signals. The temporal dynamics of the spectral structure of the QPs studied were controlled by some disturbances in the solar wind and interplanetary magnetic field. The generation mechanism of the discussed QP emissions is not yet understood.

Quasi-periodic VLF emissions: An analysis of the periods on different time scales

J. Manninen¹, E.E. Titova², A.G. Demekhov³, A.E. Kozlovsky¹, D.L. Pasmanik³

¹*Sodankyla Geophysical Observatory, Sodankyla, Finland*

²*Polar Geophysical Institute, Apatity, Russia*

³*Institute of Applied Physics, Nizhny Novgorod, Russia*

Quasi-periodic (QP) VLF emissions are characterized by periodic modulation of wave amplitude with periods from a few seconds to minutes. During the ground-based campaign on VLF measurements in Northern Finland (Kannuslehto, $L=5.3$) in December 2011–January 2012 different types of QP VLF emissions were observed [Manninen et al., 2012].

In this report, we discuss observations of December 24, 2011, during which multiple characteristic time scales of the magnetospheric whistler-mode waves manifested themselves especially clearly in the QP emissions. In particular, we roughly determine the location of the QP source in the magnetosphere by analyzing the polarization and frequency range of the VLF waves detected on the ground. We present observational evidence of the transition from the linear to the nonlinear regime of magnetospheric wave-particle interactions. We also consider substorm-related changes in the QP periods which differed from those discussed by Manninen et al. [2012], and propose an explanation of the observed difference.

Manninen J., et al., Non-typical ground-based quasi-periodic VLF emissions observed at $L \sim 5.3$ under quiet geomagnetic conditions at night, JASTP <http://dx.doi.org/10.1016/j.jastp.2012.05.007>

Modulation of the total electron content by geomagnetic Pc5 pulsations

V.A. Pilipenko¹, V.B. Belakhovsky², D. Murr³, M. Terramoto⁴

¹*Institute of the Earth Physics, Moscow, Russia*

²*Polar Geophysical Institute, Apatite, Russia*

³*Center of Atmospheric and Space Physics, Minneapolis, USA*

⁴*Nagoya University, Japan*

The intriguing effect was found while analyzing the small-scale variations of total electron content (TEC) derived from global positioning system (GPS) signals. We have searched for a possible response in TEC variations to intense global Pc5 pulsations with period about few mHz covering the CGM latitudes $\sim 58^\circ$ – 75° during the recovery phase of the strong magnetic storms on Oct. 30–31, 2003. Earlier studies demonstrated that the GPS-TEC technique is a very powerful method to study the propagation pattern of transient disturbances in the ionosphere, generated by seismic or internal gravity waves. This technique has turned out to be unexpectedly sensitive to ULF waves as well. During periods with intense Pc5 geomagnetic wave activity very clear pulsations with the same periodicity were found in the TEC data from high-latitude GPS receiving stations in Scandinavia and Arctic Canada. The wavelet and cross-spectral analysis show a high coherence (~ 0.9) between the periodic geomagnetic and TEC variations. Moreover, the relative amplitude of TEC periodic fluctuations $\Delta \text{TEC}/\text{TEC}$ was even larger than relative amplitude of geomagnetic variations $\Delta B/B$. So far, the effect of TEC modulation by Pc5 waves is not well understood and is still a challenge for the MHD wave theory. Various possible modulation mechanisms have been estimated, but no mechanism was firmly identified.

ELF electromagnetic disturbances in the outer ionosphere produced by the HAARP heating facility

E.E. Titova¹, A.G. Demekhov², A.A. Mochalov¹, A.B. Pashin¹, M.M. Mogilevskiy³

¹*Polar Geophysical Institute, Fersmana 14, 184209, Apatity, Russia*

²*Institute of Applied Physics, Ulyanov 46, 603950, Nizhny Novgorod, Russia,*

³*Space Research Institute, Profsoyuznaya 84/32, 117997, Moscow, Russia,*

Strong heating of the ionospheric plasma by high-power high-frequency radio waves can lead to the generation of electromagnetic and plasma disturbances. We study characteristics of electromagnetic ELF turbulence at altitudes of about 700 km, measured by DEMETER satellite above the HAARP heating facility. It is demonstrated that the amplitude of the ELF noise increased 2-8 times above the HAARP transmitter during daytime passes of the DEMETER spacecraft. The horizontal extent of the ELF disturbance region at the DEMETER altitude was about 50-70 km. We analyze the spectra of the ELF signals related to the HAARP operation and discuss possible mechanisms for the excitation of ELF noise by HAARP heating facility at altitudes of the DEMETER spacecraft.

Unusual proton aurora correlated with unusual “Pc1”

A.G. Yahnnin¹, T.A. Yahnnina¹, E.N. Ermakova², A.G. Demekhov³, F. Soraas⁴

¹*Polar Geophysical Institute, Apatity, Russia*

²*Radio-Physical Institute, Nizhniy Novgorod, Russia*

³*Institute of Applied Physics, Nizhniy Novgorod, Russia*

⁴*University of Bergen, Bergen, Norway*

Unusual proton aurora form was observed on 10 November 2004 by the IMAGE spacecraft - a long narrow arc in the night-early morning sector at CGLat = 50 (L ~ 2.4). Observations from the low-orbiting NOAA satellite showed that this arc is related to the localized precipitation of energetic (E>30 keV) protons. Such precipitation typically correlates with EMIC waves associated with geomagnetic pulsations in the Pc1 range, and is believed to result from ion-cyclotron interaction in the equatorial plane of the near Earth magnetosphere. Analysis of data of ground-based magnetometers regularly observing the magnetic fluctuations in the range of Pc1 (0.2-5 Hz) did not show any signatures of the pulsations. However, an emission at higher frequencies (10-12 Hz) correlated with observations of the proton arc was detected in data of the search-coil magnetometer at Novaya Zhizn station (L=2.6) near Nizhniy Novgorod. This frequency does not match the classical Pc1 range, and is higher than the He⁺ gyrofrequency at the location of the equatorial projection of the proton arc. We interpret the emission as the H + band of the EMIC waves generated near the extremely low-latitude plasmapause. The location of the plasmapause at L-shells close to that of the proton arc is confirmed by the plasmapause modeling and IMAGE RPI observations.

Характеристики потоков высывающихся частиц в пульсирующих полярных сияниях по триангуляционным наблюдениям в Апатитах

Б.В. Козелов, Е.Е.Титова (*ПГИ КНЦ РАН, г. Апатиты, Россия, Boris.Kozelov@gmail.com*)

Данные наземного комплекса авроральных камер анализировались для определения пространственно-временных характеристик потоков высывающихся частиц в пульсирующей ауроре. Весь комплекс состоит из 5 авроральных камер с различным полем зрения, что позволяет регистрировать как крупномасштабные пульсирующие пятна, так и мелкие (~100 м) детали в пульсирующих формах. Наблюдения из двух точек вблизи магнитного зенита дают возможность определить высоту максимума интенсивности авроральной формы, а абсолютная калибровка интенсивности свечения – оценить поток высывающихся частиц.

Результаты анализа наблюдаемой тонкой пространственно-временной структуры пульсирующих сияний сравниваются с существующими теоретическими представлениями.

Использование фазовых скоростей УНЧ геомагнитных вариаций для исследования геоэлектрической структуры земной коры

Ю.А. Копытенко, В.С. Исмагилов, А.Л. Котиков, М.С. Петрищев, П.Е. Терещенко, А.В. Петленко, Д.Б. Зайцев, Д.Ю. Сарычев, А.Г. Коробейников, Г.М. Попов (г. Санкт-Петербург, СПбФ ИЗМИРАН, ЕМ: office@izmiran.spb.ru)

Для обнаружения глубинных аномалий электропроводности земной коры в районе п. Толвуя (Карелия) проведены синхронные наблюдения вариаций электромагнитного поля Земли. В этом районе наблюдаются выходы высокопроводящих шунгитоносных пород на земную поверхность. В процессе эксперимента были установлены 5 высокочувствительных трехкомпонентных магнитовариационных станций GI-MTS-1 разнесенных на 5-10 км друг от друга. Дискретность регистрации данных составляла 50 Гц. Для исследования изменения каждого удельного сопротивления с глубиной на всех 5 пунктах выполнена обработка данных двумя методами - магнитотеллурического (МТЗ) и фазово-градиентного зондирования (ФГЗ). Метод ФГЗ разработан в СПбФ ИЗМИРАН и для его применения необходимо наличие трех магнитовариационных станций расположенных треугольником на земной поверхности.

Фазовая скорость между парами станций определяется следующим образом:

$$V_{12} = 2\pi f d_{12} / \ln[B_1(t)/B_2(t+\tau_{12})] \quad V_{13} = 2\pi f d_{13} / \ln[B_1(t)/B_3(t+\tau_{13})] \quad (1)$$

Здесь f – частота вариаций, $d_{12} = x_2 - x_1$ – расстояние между двумя точками на земной поверхности, B_1 , B_2 и B_3 – значения индукции магнитного поля в момент времени, τ_{12} и τ_{13} – фазовые задержки при использовании соответствующих пар станций в треугольнике.

Зная фазовые скорости V_{12} и V_{13} можно определить вектор скорости вдоль земной поверхности:

Для вектора фазовой скорости вдоль земной поверхности:

$$\alpha = \arctg[(V_{12}\cos(a_1) - V_{13}\cos(a_2)) / (V_{12}\cos(a_1) - V_{13}\cos(a_2))] \quad |V| = V_{12}\cos(\alpha + a_1) \quad (2)$$

Для вектора градиента вдоль земной поверхности:

$$\alpha = \arctg[(G_{12}\cos(a_1) - G_{13}\cos(a_2)) / (G_{12}\cos(a_1) - G_{13}\cos(a_2))] \quad |G| = G_{12}/\sin(\alpha + a_1) \quad (3)$$

В выражениях (2) и (3) V_{12} , V_{13} , G_{12} , G_{13} – величины фазовых скоростей и градиентов в направлении между парами магнитных станций 1 и 2, 1 и 3. α – направление соответствующего вектора относительно оси юг – север, $|V|$ и $|G|$ – величины фазовой скорости и градиента вдоль земной поверхности. Углы a_1 и a_2 определяются через координаты магнитных станций 2 и 3 (базовая станция 1 расположена в начале системы координат): $a_1 = \arctg(x_2/y_2)$, $a_2 = \arctg(x_3/y_3)$.

По величине фазовой скорости можно определить кажущееся удельное сопротивление в Ом·м:

$$\rho = 0.1 \cdot V^2 T, \text{ где } V \text{ – фазовая скорость в км/сек, } T \text{ – период в сек.}$$

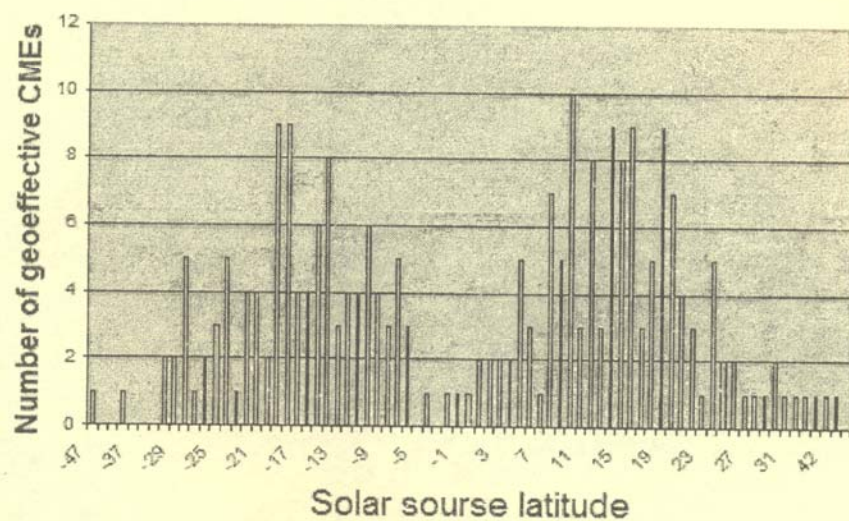
Сопоставление результатов интерпретации методов МТЗ и ФГЗ показало хорошее их соответствие.

Генерация колебаний убывающего периода облаком дрейфующих протонов

А.А. Любич (Полярный Геофизический институт КНЦ РАН)

С целью изучения механизма генерации геомагнитных колебаний убывающего периода (КУП) проведены расчеты инкремента циклотронных волн, возбуждаемых при контакте дрейфующих в долготном направлении энергичных протонов, инжектированных во время суббури, с холодной плазмосферной плазмой. Исследована зависимость характеристик геомагнитных пульсаций КУП (длительность, наклон, частотный диапазон пульсаций) от свойств питч-углового распределения фоновых и дрейфующих частиц. Питч-угловое распределение моделируется, в частности, полиномами Лежандра разного порядка. Определены условия, при которых возможна генерация КУП на частотах выше экваториальной гирочастоты гелия.

The Sun, Solar Wind, Cosmic Ray



Аномальный барометрический коэффициент микросекундных интервалов для нейтронного монитора

Ю.В. Балабин (*Полярный геофизический институт КНЦ РАН, Апатиты, Россия*)

Высокоскоростная система сбора данных нейтронного монитора (НМ), разработанная в ПГИ, ведет непрерывную фиксацию появления каждого импульса с точностью 1 мкс на станциях Баренцбург (Шпицберген) и Баксан (Сев. Кавказ). За прошедшие годы накоплено более $3 \cdot 10^{10}$ импульсов на каждой станции. В этом огромном массиве данных специальными программа по заданному алгоритму производится поиск различных событий – определенных последовательностей импульсов. В предыдущих работах, рассказывающих об этой системе, было показано, что распределение временных интервалов в данных НМ с высокой точностью подчиняется закону Пуассона.

Известно также, что счет НМ зависит от атмосферного давления; барометрический коэффициент для стандартного НМ составляет 0.72 %/мб. Как показывают измерения атмосферного давления на НМ, типичная вариация давления при изменении погоды составляет ± 20 мб, а в течение года случаются вариации до ± 40 мб. Вариация давления в 20 мб создает вариацию в счете НМ $\sim 15\%$, что намного больше суточных вариаций первичных космических лучей ($\sim 0.5\%$). Изменения в темпе счета НМ ведут к изменению среднего интервала между импульсами НМ, соответственно, изменяются значения распределения Пуассона, описывающего флуктуации счета НМ при данном атмосферном давлении.

Были выполнены как теоретические расчеты зависимости параметра распределения Пуассона на НМ от атмосферного давления, так и экспериментальные измерения этого параметра при вариациях давления. Обнаружено полное соответствие рассчитанных величин с реально наблюдаемыми в широком диапазоне значений интервалов. При этом наличие огромной базы данных позволило определять барометрический коэффициент не в целом по НМ, а для различных временных интервалов между импульсами. Например, определить барометрический коэффициент только для тех интервалов между импульсами, которые лежат в пределах 1100-1110 мкс, 1110-1120 мкс и т.д.

Однако, для малых интервалов (менее 1000 мкс) между импульсами барометрический коэффициент резко отклоняется от расчетной зависимости и начинает расти. В то же время из прежних работ известно: значение интервала в 1000 мкс является граничным. Именно при значениях менее 1000 мкс основной вклад в количество коротких интервалов вносят множественности; при значениях < 100 мкс доля интервалов, созданных множественностью, более чем на порядок превосходит число таких же интервалов, определяемое распределением Пуассона.

Исследование барометрической зависимости в разных микросекундных интервалах показывает, что короткие интервалы имеют отличный от стандартного для НМ барометрический коэффициент. Пределы действия этого аномального барометрического коэффициента соответствуют пределам влияния множественности на счет НМ. Отметим, что барометрический коэффициент является индивидуальной характеристикой компонентов вторичных космических лучей, определяющей степень их взаимодействия с атмосферой. Таким образом, получено свидетельство, что множественности на НМ производятся другой компонентой вторичных космических лучей с иным барометрическим коэффициентом.

New middle latitude station with multiplicity recording

Yu.V. Balabin, E.V. Vashenyuk, A.V. Germanenko, B.B. Gvozdevsky (*Polar Geophysical Institute of RAS, Apatity, Russia*)

High-speed data acquisition system for a neutron monitor (NM), developed in PGI, by the present moment is installed at the fourth station – in Moscow (cutoff rigidity 2.4 GV). Previously, similar systems were installed in Barentsburg (Spitsbergen, cutoff rigidity 0 GV), Apatity (cutoff rigidity 0.6 GV) and Baksan (North Caucasus, cutoff rigidity 5.4 GV). Due to this system multiplicity events of M from M = 5 to M = 100, which (as has been shown in previous studies) are produced by individual energetic particles (M $\approx 5-10$) or local hadronic showers (M > 10), were studied. Earlier observations were actually performed only for two distinct zones: at sea level near the Polar Cycle and at high mountain middle latitude zone. However, the interaction of cosmic rays with the atmosphere and the generation of multiplicity at sea level and at 2000 m are significantly different. Now we have the opportunity to explore the events of multiplicity in different points with different cut-off rigidity at sea level. At the same time the stations have the same type design of NM, except Apatity.

The results obtained on three stations show that the events of M > 10 can be produced only by the local hadronic showers in the atmosphere over NM. This is supported by the same time profiles of multiplicity events at these stations and the difference in the numerical values due to different cut-off rigidity.

All GLEs in one package

Yu.V. Balabin, E.V. Vashenyuk, B.B. Gvozdevsky, A.V. Germanenko (*Polar Geophysical Institute of RAS, Apatity, Russia*)

Using the data of the worldwide network of neutron monitors (NM) it is possible to determine parameters of the solar cosmic ray (SCR) flux (spectrum, direction and pitch-angle distribution) during a ground level event (GLE). This task involves the solution of an inverse problem using one or another model of the SCR flux. We have developed a new advanced model for this problem. It is well suited for such complicated cases as two-directional fluxes in loop-like structures of the interplanetary magnetic field or temporal separation of the SCR particles in pitch-angles in regular interplanetary magnetic structures. We use a modern magnetospheric model T01 for calculations of asymptotic cones of NM stations.

The worldwide NM network during its existence registered totally 71 GLEs. The first one was in 1942 (18th solar cycle) and the last one was on 17.05.2012 (24th solar cycle). We have selected 51 events (from GLE05 (23.02.1956) to GLE71 (17.05.2012)) suitable for modeling. There are no enough stations in skipped GLEs. Selected GLEs have huge range of increases from ~2 % up to ~5000 %. For the selection and processing of these GLEs we used a unified methodology. The analysis of results showed that the majority of events have two components of the SCR flux: the prompt component has an exponential spectrum and a narrow pitch-angle distribution, the delayed component has a power-law spectrum and almost isotropic pitch-angle distribution. The prompt component is registered on the initial phase of a GLE. It is generated on the Sun in the pulse phase of a flare. The delayed component comes to the Earth later. It is generated by the stochastic acceleration mechanism. Moreover, the spectra of both prompt and delayed components can be divided into distinct groups, i.e. values of E0 (characteristic energy of exponentials) and γ (spectral index of power law) are formed groups, but are not scattered on the wide ranges.

The first GLE of new 24th solar cycle

Yu.V. Balabin, E.V. Vashenyuk, B.B. Gvozdevsky, A.V. Germanenko (*Polar Geophysical Institute of RAS, Apatity, Russia*)

The first event of the solar cosmic rays in the new 24th solar cycle after 5 years pause has occurred 17.05.2012. It was associated with a solar flare in NOAA region 1476 located at N11W76. It was also registered in soft X-rays as a weak eruption 1F/M5.1. Ground level enhancement (GLE) was observed on the worldwide network of neutron monitors (NM).

This GLE is odd in some points. It was produced in a small active region (its square is 230) of beta type after weak flare 1F. GLE started at 01:54 UT (Oulu), maximum was 18 % on Oulu and Apatity stations at 02:08 UT. South Pole station recorded around 7 % increase reduced to sea level. This is the third magnitude station. Total duration of GLE was around 1.5 hour.

Due to our advanced methodics (which was applied to more than five tens of GLE.) we derived main parameters of GLE like spectrum, pitch-angle distribution and direction of anisotropy. There were used data of the worldwide network (27 stations). To calculate asymptotic cones of the stations the magnetosphere model T-01 was applied. Pitch-angle distribution has a gap near 90 degrees and the gap is real present according to NM data. We explain it the next way. Relativistic protons passed from the Sun to the Earth along Parker's line and didn't scatter into quiet interplanetary environment. In this case there can be lack of protons on $\sim 90^\circ$ pitch-angles due to time delay because such protons spread along magnetic line with low velocity.

The results of our modelling are presented at <http://pgia.ru:81/cosmicray/GLE/>

Fluctuations in the solar wind density and IMF and their ground effects

O.V. Kozyreva, N.G. Kleimenova (*Institute of Physics of the Earth RAS, Moscow, Russia*)

We studied the level of the ULF fluctuations in the solar wind density (Np) and IMF by applying the special ULF-index, based on 1-min OMNI data. The data obtained during the solar activity minimum (2006-2009) have been analyzed. It was shown that the strongest ULF fluctuations in the solar wind density and IMF were observed at the forward fronts of the high speed solar wind streams in the compression solar plasma region which leads to development of an initial phase of magnetic storm. We found that the amplitude of the fluctuations in the frequency range of the 2-7 mHz very strongly increased with increasing the solar wind density. The same tendency was found for the ULF fluctuations in the B IMF.

The similar ULF-index (ULFgr), based on the 1-min data of the global magnetometer network in the Northern Hemisphere, has been calculated and applied to study ground effects of discussed above ULF fluctuations in the solar wind density and IMF in the high speed solar wind streams. We found that these effects depend on the sign of the IMF B_z component. We showed that at the forward fronts of the high speed solar wind streams under IMF B_z<0, the strongest ground effects in the geomagnetic pulsations generation were observed in the night-early morning sector of the high latitudes of closed magnetosphere. However, under IMF B_z>0, the strongest geomagnetic pulsations were observed in the morning or day-time sector of the polar latitudes, corresponded to the open magnetic field lines. These pulsations could be, probably, caused by a penetration to the polar ionosphere and nonlinear transformation of the solar wind hydromagnetic waves. In the maximum of magnetic storms, the IMF and N_p fluctuations suddenly dropped, however, the ground ULF pulsation activity in the closed magnetosphere became stronger. The source of these ULF waves likely have an inside magnetosphere origin.

Simulation of the lead-free neutron monitor response function

E.A. Maurechev, A.V. Germanenko, Yu.V. Balabin, E.V. Vashenyuk, B.B. Gvozdevsky (*Polar Geophysical Institute of RAS, Apatity, Russia*)

On Apatity Neutron Monitor Station for many years works a background radiation monitoring system. An important part of one is a lead-less neutron monitor needed to expand an investigated neutron energy range. It should be noted that unlike other detectors, such as a muon telescope with efficiency $\mathcal{E} = 1$ in a wide energy range, the efficiency of neutron detectors is highly dependent on the incident particles energy. Exactly for this purpose it is necessary to study in detail a characteristics of the detectors of this type with a numerical simulation.

The aim of this study is to simulate the lead-free neutron monitor response on the particles in the energy range 10^{-2} - 10^{10} eV and the efficiency calculation of the neutron detector.

To determine the lead-less neutron monitor response function a simulation of propagation of a neutron incident on the detector have been carried out with GEANT4 toolkit. For this simulation a software package including a geometric model (4 counters surrounded by a polyethylene moderator), physical processes of particle interactions with matter and a sensitive detectors implementation was created. As a source of particles a modeling particle generator is used, which generates a parallel flow of monoenergetic neutrons incident on the detector. Model neutron source is located at a height of 30 cm above the detector. It should be noted that with the available experimental and theoretical data of other authors there is good agreement.

The search of positions of X-ray emission sources in the magnetic field obtained by solar flare MHD simulation in a real active region

A. I. Podgorny¹ and I. M. Podgorny²

¹*Lebedev Physical Institute RAS, Moscow, Russia*

²*Institute for Astronomy RAS, Moscow, Russia.*

The primordial energy release takes place in the solar corona above an active region at the height 15 - 30 thousands kilometers. It is proved by precise flare X-rays observations on the solar limb. Flare energy accumulation can occur in the current sheet magnetic field created by disturbances focusing in the vicinity of an X-type singular line. Several others solar flare mechanisms are considered in many publications, majority of them are based on assumption of a magnetic rope appearance in the corona. To define what mechanism is responsible for solar flare, the 3D MHD simulations are done in the solar corona without any assumptions about the flare physics. The initial and boundary conditions are taken from observations of a real active region before the flare. The calculations are initiated several days before the flare, when strong disturbances in the corona are absent. Therefore, the potential magnetic field in the corona, calculated from the field distribution observed on the photosphere, is used for setting initial conditions. The magnetic field distributions measured on the photosphere are used for setting boundary conditions during period of simulated active region evolution. Others boundary conditions are approximated by free-exit conditions. The flare mechanism is shown by results of numerical simulation, instead of its artificially introducing in setting the initial or boundary conditions. The main goal of MHD simulation in the solar corona is finding-out of the physical mechanism of solar flare. The simulation shows that the current sheet appears in the preflare state in the corona above an active region. The electrodynamic model of the solar flare based on current sheet mechanism, which explains main flare manifestations, is proposed. The Hall electric field generates field-aligned electric currents in the corona along the magnetic field lines that are crossing a current sheet. The hard X-ray emission is caused by the electrons bremsstrahlung in the chromosphere, which are accelerated in field-aligned

The Sun, solar wind, cosmic rays

currents. The positions of sources of X-ray radiation can be found from magnetic field configuration obtained by MHD simulation. According to the solar flare electrodynamic model the position of thermal X-ray is situated in the current sheet, and positions of nonthermal hard X-rays are places of crossing of photosphere with the magnetic lines, which are going out of the current sheet. The graphical system is developing, which can find these possible positions of sources of X-ray radiation. For further study of the solar flare mechanism it is necessary to compare the possible positions of sources of X-ray radiation founded from MHD simulation with X-ray observations.

The magnetic field dynamics of large active regions in the pre-flare state and during solar flares

I.M. Podgorny¹, A.I. Podgorny², and N.S. Meshalkina³

¹*Institute for Astronomy RAS, Moscow, Russia, podgorny@inasan.ru*

²*Lebedev Physical Institute RAS, Moscow, Russia*

³*Institute of Solar Terrestrial Physics SD RAS, Irkutsk Russia*

Publications of the active region behavior before flares and during flares are controversial. In our report in Apatity Seminar 2012 the preliminary data were demonstrated that the growth of the magnetic flux of the active region before flares is appeared. The flares of X class are recorded, when the magnetic flux of an active region becomes bigger than 1022 Mx. Apparently the new magnetic flux flowing up from the Sun surface is responsible for energy accumulation in the corona. During a solar flare, when the accumulated energy is fast released, there are no specific magnetic flux changes in the active region. This surprising fact follows from the analysis of the array data obtained in recent years for big flares on the SOHO and SDO spacecrafts. It is shown the conservation of the magnetic field distribution in active regions during the majority of flares. Some small magnetic field changes in the distribution of the field appear that are typical for the time interval at the flare absence. A scheme for the formation and decay of the flare current sheet is proposed, which shows that the dissipation of the current sheet magnetic field in the corona must not lead to a perturbation of the magnetic field distribution on the Sun surface. These results are consistent with the flare theory based on the slow accumulation of the magnetic energy in the current sheet and its explosive realize due to current sheet instability.

Role of tilt orientation of BMRs and meridional circulation in the polar magnetic field reversal on the Sun

N.V. Zolotova, D.I. Ponyavin (*St-Petersburg State University, St-Petersburg, Russia*)

Using Greenwich catalogue of sunspots and magnetic field observations it was shown that impulses of sunspot activity during a course of solar cycle are responsible for residual magnetic field transported by meridional circulation toward the poles. This, in turn, is related to the polarity reversal of the axisymmetric large-scale magnetic fields. We perform parameter study of tilt angle orientation of the Bipolar Magnetic Regions (BMRs) with imposed meridional flow profiles to model poleward magnetic field surges. Simulation was done in terms of point density distributions of leading and following sunspots according to Hale and Joy polarity rules. It was demonstrated that latitudinal profile of tilt orientation of BMRs is crucial in polar field reversal. A faster meridional velocity reduces polar field. However results depend on size of the mesh grid. Latitudinal profile of meridional flow influences the polar field strength as well.

Конфигурация магнитных облаков и сезонная зависимость геомагнитной активности

Н.А. Бархатов^{1,2}, А.Е. Левитин³, Е.А. Ревунова¹

¹*Нижегородский государственный архитектурно-строительный университет, Нижний Новгород*

²*Нижегородский государственный педагогический университет им. Козьмы Минина, Нижний Новгород*

³*Институт земного магнетизма, ионосферы и распространения радиоволн им. Н.В.Пушкиова, Москва*

Работа посвящена анализу причин сезонной зависимости геомагнитной активности с учетом ориентации крупномасштабных плазменных структур типа магнитных облаков солнечного ветра.

Длительное наблюдение геомагнитной активности показало существование ее полугодовых вариаций, которые проявляются в периоды весеннего и осеннего равноденствия в виде максимумов в долгосрочных средних значениях различных индексов геомагнитной активности. В настоящее время для объяснения этих

вариаций предложено и проверено несколько гипотез: осевая гипотеза, в которой основную роль играет гелиографическая широта Земли, и гипотеза равноденствия, согласно которой геомагнитная активность увеличивается, когда угол между земным диполем и потоком солнечного ветра составляет 90^0 . Однако ни одна из предложенных гипотез не учитывает пространственную структуру геоэффективных плазменных потоков. Вместе с тем, форма и структура возникающего плазменного потока определяется типом солнечного источника, а его действие на земную магнитосферу зависит еще и от взаимного расположения солнечного источника и Земли. Такие геоэффективные структуры как магнитные облака, в отличие от других плазменных потоков, обладают выраженной ориентацией в пространстве, поэтому именно они могут становиться источниками магнитных бурь различной интенсивности в периоды равноденствия и солнцестояния.

В работе на реальных событиях предложена и проверена модель сезонной зависимости геомагнитной активности, учитывающей ориентацию магнитных облаков солнечного ветра относительно плоскости эклиптики. Согласно данной модели, ориентация магнитных облаков в пространстве должна отражаться в их геоэффективности вследствие изменения значения проекции магнитного поля на оси облака на земной диполь в периоды равноденствия и солнцестояния. Таким образом, в периоды солнцестояния наибольший вклад в геомагнитную активность должны давать облака с большими значениями угла наклона оси облака к плоскости эклиптики, которые по статистике являются довольно редкими событиями в околоземном пространстве. В то время как в периоды равноденствия облака любой ориентации должны давать примерно равнозначный вклад в геомагнитную активность. В связи с этим число и интенсивность геомагнитных бурь в периоды равноденствий должно увеличиваться за счет многочисленных событий с небольшими углами наклона оси облака к плоскости эклиптики.

Проверка предложенной гипотезы проведена на 52 магнитных облаках различной ориентации, зарегистрированных в околоземном пространстве с 1980 по 2004 гг. Расчет изменения значения проекции величины магнитного поля облака на земной диполь показал, что в периоды равноденствия действительно больший вклад в геомагнитную активность дают облака с небольшими значениями угла наклона оси к плоскости эклиптики. В периоды солнцестояния данный тип облаков оказывается практически не геоэффективным, что и отражается в снижении уровня геомагнитной активности зимой и летом.

Взаимодействие малых магнитогидродинамических возмущений с вращательным разрывом в плазме низкого давления

А.А. Любич (Полярный Геофизический институт КНЦ РАН)

Анализируется взаимодействие падающих МГД-волн малой амплитуды с вращательным разрывом в сильно замагнченной плазме, когда магнитное давление много больше плазменного давления. Определены амплитуды уходящих от разрыва волн в зависимости от свойств вращательного разрыва, типа падающей волны и угла падения. Показано, что вращательный разрыв в сильно замагнченной плазме остается нейтрально устойчивым – отсутствует возможность спонтанного излучения им МГД-волн постоянной амплитуды.

Отражение динамики солнечных плазменных потоков в вейвлет-скелетонных картинах параметров околоземного космического пространства

С.Е. Ревунов, Д.В. Шадруков, Н.В. Косолапова (Нижегородский Государственный Педагогический Университет, Нижний Новгород)

Исследование посвящено установлению спектральных особенностей солнечных плазменных потоков в форме магнитных облаков (МС), областей взаимодействия потоков (CIR), ударных волн (Shocks) и высокоскоростных потоков от корональных дыр (HSS), регистрируемых на орбите Земли патрульными космическими аппаратами. Подобный подход к вопросу диагностики ближнего околоземного космического пространства позволит на ранних этапах идентифицировать геоэффективные структуры в потоке солнечного ветра с целью прогнозирования эволюции магнитосферного возмущения. Вейвлет-скелетонная обработка представляет одномерный сигнал в развертке по времени и частоте, что делает ее наиболее подходящим методом для использования в режиме онлайн мониторинга плазменных потоков.

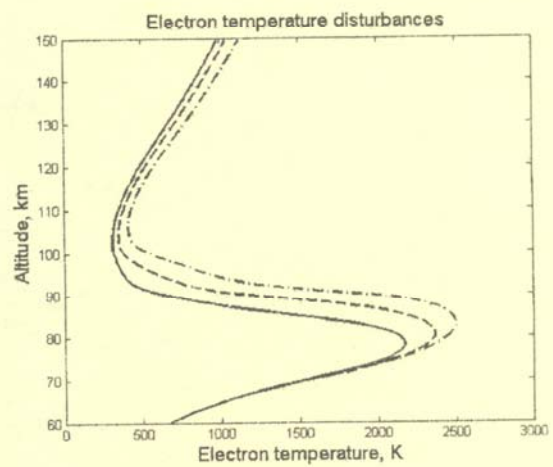
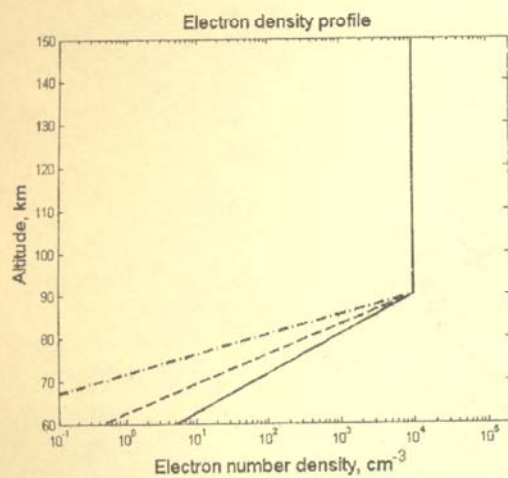
Для постановки численных экспериментов отобрано по 6 случаев разнотипных событий, зарегистрированных в период с 2000 по 2007 гг. по данным каталогов NASA (<http://cdaw.gsfc.nasa.gov>) и NOAA (<http://ngdc.noaa.gov>). Всего отобрано 24 события МС (28.07.2000, 29.12.2000, 12.04.2001, 28.05.2001, 09.08.2001, 17.04.2002), CIR (27.07.2003, 05.04.2005, 07.05.2007, 20.09.2007, 27.09.2007, 25.10.2007), Shocks

The Sun, solar wind, cosmic rays

(19.12.2002, 27.02.2003, 14.07.2003, 17.07.2003, 12.04.2004, 22.07.2004), HSS (01.03.2000, 26.07.2003, 20.11.2004, 04.07.2006, 29.07.2007, 17.12.2007). С вэб-узла CDAW (<http://cdaweb.gsfc.nasa.gov>) для каждого из них были получены минутные данные параметров солнечного ветра: N (плотность), V (скорость), T (температура), P (динамическое давление) и данные о величине межпланетного магнитного поля (ММП) $|B|$, B_x , B_y , B_z в солнечно-эклиптической системе координат, зарегистрированные на патрульных космических аппаратах.

Полученные для рассматриваемых событий скелетонные картины возмущений выше указанных параметров отражают внутреннюю динамику плазменных потоков разных типов и масштабов. Так, потоки типа MC характеризуются долгопериодными изменениями в компонентах магнитного поля, быстрыми изменениями на всех масштабах колебаний в параметрах скорости, плотности, температуры и давления на переднем крае таких событий. Потоки типа CIR можно отождествить по относительно быстрым изменениям во всех параметрах и во всех анализируемых масштабах колебаний. Потоки типа Shocks вызывают резкие изменения во всех параметрах и особенно это заметно при анализе низкочастотной части спектра. Потоки типа HSS можно идентифицировать как долгопериодные изменения в параметрах скорости, плотности, температуры, давления и быстрые изменения в компонентах магнитного поля.

Ionosphere and Upper Atmosphere



Spatial distribution of NOx components during geomagnetic storms

F.S. Bessarab, Yu.N. Koren'kov, M.V. Klimenko, V.V. Klimenko (*West Department of Pushkov IZMIRAN, Kaliningrad, Russia*)

Such minor neutral components as $N(^4S)$, $N(^2D)$, NO and non-thermal particles "hot N and O" take important place in the thermodynamic regime of the Earth's thermosphere and ionosphere. This contribution presents the model calculation results of the global spatial distributions of metastable components $N(^4S)$, $N(^2D)$, NO and hot O in the disturbed geomagnetic conditions. During geomagnetic storms Joule heating dissipation is the dominant form of the magnetospheric energy input responsible for many chemical and dynamical variations in the thermosphere. Another source of the energy in the high latitudes is a charged particle precipitation. This energy input leads to the dramatic increasing of thermospheric temperature and nitric oxide (NO) density and thus radiative emission by NO. We give for the first time a quantitative assessment of the relationship between the global Joule heating power and global NO, $N(^4S)$, $N(^2D)$ distribution in comparison with particle precipitation power. It is found a global NO part of cooling power under disturbed conditions. We also present a global distribution of another metastable particles and their deposit in the thermodynamical regime of the thermosphere and ionosphere during geomagnetic storms.

Investigation of the polar cap soft electrons fluxes' influence on the latitudinal variations of the ionosphere total electron content and peak F2-layer electron density

M.G. Botova¹, A.A. Namgaladze¹, B.E. Prokhorov^{2,3}

¹*Murmansk State Technical University, Murmansk, Russia, e-mail: botovamg@gmail.com*

²*Helmholtz Centre Potsdam, GFZ German Research Centre for Geosciences, Telegrafenberg, 144734 Potsdam, Germany*

³*University Potsdam, Applied Mathematics, Interdisciplinary Center for Dynamics of Complex Systems (DYCOS), 14476 Potsdam, Germany*

The paper presents the investigation of the polar cap soft electrons fluxes' influence on the latitudinal variations of the ionosphere total electron content (TEC) and peak F2-layer electron density (NmF2).

The computer modeling was performed using the global three-dimensional self-consistent numerical model of the Upper Atmosphere of the Earth (UAM).

The model calculations have been carried out for equinox and solstice conditions and different levels of solar activity (F10,7 ~ 90 and F10,7 ~ 180). The latitudinal variations of the NmF2 and TEC were analyzed for the meridional section 15–03 of the magnetic local time (MLT).

In UAM calculations with soft electrons fluxes ("polar rain") set according to Hardy et al. [1985], model TEC and NmF2 values underestimate (except for summer conditions) both the GPS observed TEC values and IRI-2007 simulations at the main ionosphere trough region. To improve the agreement between model case and observation it is necessary to increase the intensity of the "polar rain" for an order.

Auroral ovals and the irregularity ovals on the base of optical and GPS measurements

S.A. Chernouss¹, I.I. Shagimuratov², I.I. Efishev²

¹*Polar Geophysical Institute of KSC RAS, Apatity, Russia*

²*West Department of IZMIRAN, Kaliningrad, Russia*

Some authors studied the dependence of a Total Electron Content (TEC) fluctuations on auroral activity mostly during great planetary storms (Aarons et al., 2000; Afraymovich and Perevalova, 2006; Shagimuratov et al, 2008). Comparison of the auroral oval and the oval of the TEC fluctuation at different activity presents in this report on basis of auroral and GPS measurements at Arctic and Antarctic stations. The statistics of number and intensity of the TEC fluctuations over polar ionosphere for quiet and disturbed geophysical conditions presented. The auroral oval, depending on geomagnetic activity indices, presented by Feldstein, Starkov and Zverev data, used in the report. Authors present the auroral oval and the oval of the TEC fluctuations as circular diagrams for better comparison of them. As well as auroral oval the spatial and temporal occurrence of the irregularities can be visually presented in

Ionosphere and upper atmosphere

coordinates-of the geomagnetic local time and corrected geomagnetic latitude. We used high-precision dual-frequency GPS phase measurements, as measurements of phase fluctuations activity, The rate of the TEC (ROT) was used and fluctuation intensity was evaluated by using ROTI index calculated with 10 min resolution to measuring of fluctuations activity. These images demonstrate the irregularity oval, similar to the auroral oval. The occurrence of the irregularity oval relates both with auroral oval and cusp. It was revealed that location of the equator-ward edge of the irregularity oval at magnetic midnight was 65°-68° CGL, for dayside, higher than 70° CGL for quiet conditions. The irregularity oval expands equatorward with increase of the auroral and magnetic activity. We show also structure and dynamics of aurora and some GPS parameters in case studies during high activity. The study showed that the operating high-latitudes GPS stations can provide a permanent monitoring tool for the irregularity oval in near real-time. The GPS measurements of northern and southern hemispheres were used to study storm-time development of TEC fluctuations at conjugate area in polar cusp, auroral and subauroral ionosphere. During magnetic storm the intensity of irregularities essentially increases and strong TEC fluctuations can be registered at subauroral ionosphere. Maximal activity of both aurora and TEC fluctuations follow to a large negative IMF Bz component. Storm time development of TEC fluctuations, caused by ionospheric irregularities, controlled by UT. The results demonstrated that dynamics and structure of the irregularity ovals and the auroral ovals well matched.

Case study of disturbed polar ionosphere impact on navigation systems by auroral and GPS data

S. Chernouss, M. Shvec, M. Filatov, O. Antonenko (*Polar Geophysical Institute of the KSC RAS, Apatity-Murmansk, Russia*)

First part of this report devote to the experimental results of the effect of ionospheric disturbances, which marker is an aurora, on GPS signal received by simplest single-frequency receivers "Garmin." These experiments were carried out in Murmansk and Apatity and they features are under consideration. As it follows from these observations, in a situation, when the aurora completely cover the field of view of GPS receiver, positioning quality should deteriorate. This hypothesis could be checked by the precision observational data from dual-frequency receiver "Javad" installed and work in the Polar Geophysical Institute station at Spitsbergen. This Barentsburg station on Spitsbergen is rather convinion to study the effects of auroral disturbances on GPS signals, measured on the Earth's surface since, often, even during a small perturbation of the polar ionosphere, navigation satellite signal must pass through the auroral oval. Thus, the signals of all satellites in working constellation, both equatorial and polar ones, should pass through the disturbed ionosphere. Therefore, if we will to analyze together data from the GPS receiver, magnetometers and all-sky cameras, we must obtain direct results of the effect. Day of 24.11.2009 characterized by a magnetic storm, and the aurora, which covered the entire sky. We provided an analysis of pictures of all-sky camera installed at the station Barentsburg. We can see aurora take up most of the sky, and completely cover the field (radiation pattern) of the receiver in the images at 18:10 UT and at 18:20UT Maps of the navigation satellites positions and the aurora was constructed over the point of both devices in different times. It was concluded that, in the time series of positioning errors, these errors increase with the navigation signal propagation through the disturbed polar ionosphere, which characterized by occurrence of the aurora.

The results are discussed in physical terms of high frequency waves propagation in the polar ionosphere.

VLF direction finder in Lovozer

M. Filatov, S. Chernouss, M. Shkrabalyuk, A. Nikitenko, A. Larchenko, S. Pilgaev, and Yu. Fedorenko (*Polar Geophysical Institute of the KSC RAS, Apatity, Russia*)

The direction finding technique in very low frequency range is widely used to determine an exit point of magnetospheric VLF emissions from ionosphere. There are two methods: i) method based on multistation observations, the group velocity vector here is estimated from time delays of VLF signals recorded at several spatially separated sites; and ii) method that uses the simultaneous recordings of three field components (Hx, Hy, and Ez) observable on the ground. We present VLF direction finder that may implement both methods. It offers extremely accurate time synchronization of data stream to UTC that after post-processing of recordings is about several tens of nanoseconds so it may be used in multistation measurements. VLF recorder equipped with two magnetic loop antennas and vertical dipole measures three electromagnetic field components in frequency range from 700 Hz to 6.5 kHz. The latter VLF direction finder is now installed in the Lovozer observatory. These kind of observations could be successfully used in experimental verification of the Flow Cyclotron Maser model in the "Resonance" project.

This work is supported by the Programme 22 of the Presidium of Russian Academy of Sciences

Auroral ionosphere dynamics during the two types of geomagnetic storms (CIR and CME)

D.A. Kargapolov, L.N. Makarova A.V. Shirochkov (*Arctic and Antarctic Research Institute, St-Petersburg, Russia*)

Auroral ionosphere dynamics during the geomagnetic storms is still not completely studied. Due to radio signals total absorption (blackout) in the high latitudinal ionospheric lower layers the experimental study is not possible during strong geomagnetic activity. In this work we studied the dynamics of auroral ionosphere during two different types of geomagnetic storms: CME (Coronal Mass Ejection) and CIR (Corotating Interaction Regions - recurring magnetic storms). Vertical sounding data and riometer absorption from Lovozero (Russia), Tromso (Norway) and Sodankyla (Finland) sites were used. EISCAT incoherent scattering radar data (Tromso) was also taken into consideration. CME type storms are connected with the Sun coronal mass emissions and increasing high energy proton flux intensity causing polar cap absorption. Consequently there is a high level ionization in the lower layer of the ionosphere and decreasing of the electron concentration in E and F-regions. At the same time there are no changes in F2 layer structure. During the CIR storms, connected with high-speed solar wind stream without high-energy particles interactions, changes in the ionospheric dynamics are associated with the auroral particles precipitation from the magnetosphere tail during activation of the substorm activity controlled by the value of magnetic PC-index. The experimental data shows changes in the auroral ionosphere occur with a ten minutes period, determined by the time variations of the electric field and particles precipitation in the auroral zone. Data analyses presented in this study demonstrates quite different response of the auroral ionosphere between these two kinds of the geomagnetic storms.

Modeling of the TEC disturbances generated by seismogenic electric currents for different seasons

M.I. Karpov, A.A. Namgaladze (*Murmansk State Technical University, Murmansk, Russia*)

Numerical calculations of the ionosphere Total Electron Content (TEC) disturbances have been performed using global Upper Atmosphere Model (UAM) for conditions corresponding to the Haiti (January, 2010) and Japan (March, 2011) earthquakes. Vertical electric currents with the density of 20 nA/m² and flowing over area of about 250 by 2000 km have been setup as the sources of the seismogenic impact at the height of 80 km in the UAM electric potential. Their action resulted in relative (%) TEC disturbances with the same key features as the TEC variations observed before both these earthquakes. Deviations appeared mostly at night near the epicenter and magnetically conjugated area; they were 20-40% by magnitude; and did not move during their lifetime. Maximum of both modeled and observed TEC variations was pronounced in the area magnetically conjugated to the epicenter for the Haiti case. Concerning Japan case, both modeled and observed disturbances were more symmetrical relative to the geomagnetic equator. According to the UAM simulations, disturbances that are symmetrical relative to the geomagnetic meridian of the epicenter were obtained by setting up vertical electric currents flowing to the Earth at one side from the meridian and acting simultaneously with back currents set up at the opposite side from the meridian.

Yakutsk Anomaly (YA) according to the satellite and ionosonde network observation data and its representation using the GSM TIP model

V.V. Klimenko¹, A.T. Karpachev², M.V. Klimenko¹, K.G. Ratovsky³

¹*West Department of Pushkov IZMIRAN, Kaliningrad, Russia*

²*Pushkov IZMIRAN, Moscow, Russia*

³*ISTP, Irkutsk, Russia*

Recently a great attention is given to the longitudinal variations in the Earth's ionosphere. One of the most interesting manifestations of such variations is the Mid-latitude Summer Nighttime Anomaly (MSNA). In the summer Southern Hemisphere the MSNA is known as Weddell Sea Anomaly (WSA) and extensively investigated both experimentally and theoretically. The main feature of the WSA is that near the location of Weddell Sea the summer nighttime critical frequencies of the ionosphere F2 region exceed the daytime values. A similar-to-WSA structure occurs in the Northern Hemisphere nearest the longitude of Yakutsk during local summer and named as the Yakutsk anomaly (YA). The YA is much less studied in comparison to the WSA. We present the observations of the IK-19 and CHAMP satellites and ionosonde network in Siberia for summer conditions at different levels of solar activity. For a more detailed study of the YA and its comparing with WSA we present the calculation results performed for the same conditions using the GSM TIP model. Based on this study, we conclude that the YA and WSA have the same nature and are formed by the same mechanisms.

Ionosphere and upper atmosphere

Geomagnetic activity influence on the global changes in the ionospheric parameters during 2009 Sudden Stratospheric Warming

V.V. Klimenko, M.V. Klimenko, F.S. Bessarab, Yu.N. Koren'kov (*West Department of Pushkov IZMIRAN, Kaliningrad, Russia*)

We present the GSM TIP simulation results of the ionospheric effects of 2009 Sudden Stratospheric Warming. These results were obtained using the neutral atmosphere parameters (neutral density, temperature, and vector velocity horizontal components of the neutral gas mass-average motion) at the GSM TIP lower boundary (80 km) that are given with 6-hour intervals on the basis of TIME GCM model output data involving the data measurements of the lower atmosphere parameters. Our research was initiated by the existing assumption that variations in the upper atmosphere parameters at heights of *F* region observed during Sudden Stratospheric Warming can be related not only with changes in the neutral atmosphere, but with the changes in the Earth's magnetosphere. To test this assumption, we performed model runs both without and with taking into account the geomagnetic activity during the considered period. We took into account the geomagnetic activity changes by specifying the potential difference through polar caps and R2 FAC, depending on the *AE* index and high-energy particle precipitation as a function of the *K_p* index. The conclusion is made regarding the geomagnetic activity contribution to the changes of the ionosphere *F* region parameters during 2009 Sudden Stratospheric Warming.

Ionospheric response on May 2, 2010 geomagnetic storm and its influence on HF radio wave propagation at high-latitudes

D.S. Kotova¹, M.V. Klimenko², V.V. Klimenko², V.E. Zakharov¹

¹*I. Kant BFU, Kaliningrad, Russia*

²*West Department of Pushkov IZMIRAN, Kaliningrad, Russia*

At the previous seminar we presented the numerical calculation results of the ionospheric effects of geomagnetic storm on May 2, 2010 obtained using the GSM TIP model. In the given report we used these model results as an inhomogeneous anisotropic medium for simulation of the HF radio paths using the model developed in the I. Kant BFU. Calculations were performed for several hypothetical high-latitude transmitters located in the different places on the Earth's surface emitting HF radio waves of different frequencies in the zonal and meridional direction at different elevation angles. The calculation results of radio paths in an active phase of the storm on May 2, we compared with calculation results for the undisturbed conditions on May 1 and during the recovery phase of geomagnetic storm on May 3. It is shown that the geomagnetic storm leads to significant changes in HF radio paths at high-latitudes associated with changes such large-scale ionospheric irregularities as the main ionospheric trough and tongue of ionization and, in particular, with the stratification of the main ionospheric trough, resulting from non-stationary magnetospheric convection.

Practice of CCD cameras' calibration by LED low-light source

B.V. Kozelov¹, B.U.E. Brandstrom², F. Sigernes³, A.V. Roldugin¹, S.A. Chernouss¹

¹*Polar Geophysical Institute, Apatity Murmansk region, 184209 Russia*

²*Swedish Institute of Space Physics, Kiruna, Sweden*

³*The Kjell Henriksen Observatory, UNIS, Longyearbyen, Norway*

Two CCD cameras used for auroral observations (Kozelov et al., 2012) have been calibrated by LED low-light source PGI-Chernouss-38AM. The calibration factor as a function of the wavelength and the camera gain was deduced. Previously the light source PGI-Chernouss-38AM (SID 105) was absolutely calibrated during the intercalibration of optical low light sources (Brandstrom et al., 2012), and it was found some issues motivated additional studies of the light source. The current-voltage and emission intensity characteristics of the light source have been measured. It have been found recommendation for the light source users: i) the current value should be measured; ii) the light source should be equipped by external stabilized electric power source; iii) the setting "3" of the lamp and region of wavelengths < 500 nm should be avoided due to peaked spectrum.

The measuring of induction magnetometer transfer function

A.V. Larchenko, O. M. Lebed, Yu. V. Fedorenko (*Polar Geophysical Institute, Apatity, Russia*)

Observations of natural and artificial electromagnetic fields in ELF frequency range typically aim to acquire spectral and temporal behavior of field components. To evaluate power spectra, amplitudes and phases one have to know transfer function of a data acquisition system. Although this transfer function may be theoretically calculated from sensor parameters and sensor preamplifier circuitry, a common practice is to obtain it by calibration procedure. The main difficulties arise from the fact that it is not possible to screen the sensor under calibration from external electromagnetic noise. It places a limit to calibration accuracy, especially at lower frequencies below 1-2 Hz where geomagnetic pulsations sometimes are so strong that make calibration if not impossible but unacceptably long to reach desired accuracy by averaging. In the frequency range 50-300 Hz most of interference comes from impulsive electromagnetic signals (atmospherics) produced by thunderstorms around the World.

In this work, we present a calibration procedure used in PGI to evaluate transfer functions of data acquisition system that comprises three-component induction magnetometer. Atmospherics impulsive noise in the frequency range 50-300 Hz is suppressed by median filter. In contrast to conventional method which includes estimation of amplitudes and phases at number of frequencies considering them as an independent samples we make use of an a-priory information that the transfer function of any sensor with preamplifier is a rational function of $j\omega$. Transfer function may be expressed in terms of several zeros and poles of rational function. We calculate zeros and poles using the Continuous Minimization by Simulated Annealing, and weight of each sample is not the same because noise influence is altered with frequency. Our method has better accuracy against conventional one and more convenient in use because it utilizes a-priory information of the transfer function form and expresses it in a small number of poles and zeros.

Field structure of natural electromagnetic signals in ELF range in March 2012

O. Lebed, A. Larchenko, S. Pilgaev, O. Akhmetov and Yu. Fedorenko (*Polar Geophysical Institute, Apatity, Russia*)

In March 2012 a large sunspot unleashed several solar flares that affect propagation of ELF signals in Earth-ionosphere waveguide and alter electromagnetic field structure in Lovozer (67.97N, 35.02E) and Barentsburg (78.093N, 14.208E). We investigate jointly a response of magnetic field polarization in Lovozer and Barentsburg to disturbances caused by flares, and E_z/H_t ratio and Poynting vector in Lovozer in March 3rd -10th compare to quiet time since March, 20. Results show that electromagnetic field structure differs from that predicted by a simple mode theory and required realistic propagation model including inhomogeneous lower and anisotropic upper boundaries of the Earth-ionosphere waveguide.

Vertical electric field measurements in ELF range

O. Lebed, A. Larchenko, S. Pilgaev, and Yu. Fedorenko (*Polar Geophysical Institute, Apatity, Russia*)

Simple mode theory of electromagnetic field in Earth-ionosphere waveguide in the frequency range below 1000 Hz predicts two main components – horizontal magnetic (H_ϕ) and vertical electric (E_z) while most of observatories measure only horizontal and vertical magnetic components. We present the data acquisition system now installed in Lovozer that records E_z component as complementary to H_x , H_y , and H_z measurements. The transfer function of newly installed E_z component matches that of H_x , H_y , and H_z . The circuitry of the electrical antenna amplifier is adapted to operating conditions in Arctic. Here we discuss method of calibration that allows representing of transfer function of both magnetic and vertical electric channels via combination of poles and zeros and present recordings of natural and artificial signals.

A model study of the influence of artificial heating of the nighttime high-latitude ionosphere on the spatial distributions of the ionospheric parameters

G.I. Mingaleva, V.S. Mingalev (*Polar Geophysical Institute, Apatity, Russia*)

It is well known that high-power high-frequency radio waves, pumped into the ionosphere, cause the variety of physical processes in the ionospheric plasma. Some of such processes can result in the disturbances of the height profiles of the ionospheric parameters at F-layer altitudes. It may be expected that these disturbances can cover some area in the horizontal plane. To study the dimension of this area the numerical modeling can be applied.

In this study, the mathematical model of the high-latitude ionosphere, which can be affected by powerful high-

Ionosphere and upper atmosphere

frequency radio waves, developed earlier in the Polar Geophysical Institute, is utilized to calculate three-dimensional distributions of the ionospheric parameters in the nighttime high-latitude F-region ionosphere. The model takes into account the convection of the ionospheric plasma, strong magnetization of the plasma at F-layer altitudes, and geomagnetic field declination. In the model calculations a field tube of plasma is traced as it moves along a convection trajectory through the moving neutral atmosphere. The profiles against distance from the earth along the geomagnetic field line of ionospheric quantities are obtained by solving the appropriate system of transport equations of ionospheric plasma. By tracing many field tubes of plasma, it is possible to construct three-dimensional steady distributions of ionospheric quantities. The model is based on numerical solution of the system of transport equations, which consists of the continuity equation, equation of motion for ion gas, and heat conduction equations for ion and electron gases. The model is able to take into account artificial heating of the ionosphere by powerful HF waves.

The calculations were made for two cases. Firstly, we obtained the distributions of the ionospheric parameters under natural conditions without a powerful high-frequency wave effect. Secondly, the distributions of the ionospheric parameters were obtained on condition that the ionospheric high-frequency heating facility near Tromsø, Scandinavia, has been operated during the period of five minutes, with the heater being located on the night side of the Earth on the magnetic meridian of 01.20 MLT. In the second case, powerful high-frequency waves lead to a decrease of about 40% in the electron concentration at the level of the F2-layer peak over the ionospheric heater. The cross section of the density depletion region has a diameter of about 100 km in the horizontal direction at the level of the F2-layer peak.

This work was partly supported by the RFBR grant 13-01-00063.

Numerical modeling the influence of magnetic activity on the global circulation of the middle atmosphere for January conditions

I.V. Mingalev, G.I. Mingaleva, V.S. Mingalev (*Polar Geophysical Institute, Apatity, Russia*)

The non-hydrostatic model of the global neutral wind system of the Earth's atmosphere, developed earlier in the Polar Geophysical Institute, is utilized to investigate how magnetic activity affects the formation of the large-scale global circulation of the middle atmosphere and lower thermosphere. This model produces three-dimensional global distributions of the zonal, meridional, and vertical components of the neutral wind and neutral gas density in the troposphere, stratosphere, mesosphere, and lower thermosphere. The peculiarity of the utilized model consists in that the internal energy equation for the neutral gas is not solved in the model calculations. Instead, the global temperature field is assumed to be a given distribution, i.e. the input parameter of the model, and obtained from the NRLMSISE-00 empirical model. Moreover, in the model calculations, not only the horizontal components but also the vertical component of the neutral wind velocity is obtained by means of a numerical solution of a generalized Navier-Stokes equation for compressible gas, so the model is non-hydrostatic. Simulations are performed for the winter period in the northern hemisphere (16 January) and for two distinct values of magnetic activity ($K_p=1$ and $K_p=4$). The simulation results indicate that magnetic activity ought to influence considerably on the formation of global neutral wind system in the mesosphere and lower thermosphere. However, this influence is not straightforward. From the simulation results obtained, we can see that the atmospheric temperature, calculated with the help of the NRLMSISE-00 empirical model, does not depend on the magnetic activity below approximately 80 km. Nevertheless, the effect of magnetic activity on the global circulation of the atmosphere below 80 km exists. This effect is conditioned by the vertical transport of air from the lower thermosphere to the mesosphere and stratosphere. This transport may be rather different under distinct magnetic activity conditions. It can be noticed that the utilized mathematical model was able to simulate this effect due to the fact that the model is non-hydrostatic.

This work was partly supported by the RFBR grant 13-01-00063.

Dynamics of the precipitation spectral characteristics during sawtooth substorms

V.D. Nikolaeva^{1,2}, A.L. Kotikov^{2,3}, A.V. Shirochkov¹, L.N. Makarova¹, T. Raita⁴

¹*Arctic and Antarctic Research Institute, Saint Petersburg, Russia*

²*Saint Petersburg State University, Saint Petersburg, Russia*

³*SPbF IZMIRAN, Saint Petersburg, Russia*

⁴*SGO of the University of Oulu*

Sawtooth substorms are magnetic disturbances in the polar cap and the auroral zone under conditions of steady and strong solar wind. Sawtooth substorm displays features other than the classical substorm parameters.

Electron and proton precipitation of different energies during sawtooth substorms of March 20, 2001 and August 28-

29, 2000 are examined in this paper. Synchronous changes of riometer absorption in the western and eastern hemispheres superimposed on ionospheric current system, restored by Canadian and Scandinavian meridian chain of magnetometers are taken into consideration.

Electron fluxes with energies from 6 eV to 30 keV (DMSP - 12, 13, 14, 15, satellite data) and proton fluxes from 1 to 100 MeV (GOES satellite data) are analyzed for different phases of sawtooth substorms. Vertical profiles of the electron density along the satellites trajectories were calculated from DMSP data and compared with EISCAT incoherent scatter radar measurements for substorms of March 20, 2001. Convection system and the potential across the polar cap are obtained by SUPERDARN system.

This analysis allows to determine different spectrum regions responsible for the various physical processes in the auroral ionosphere for different sawtooth substorms phases.

Estimation of artificially enhanced electron temperature in lower ionosphere with absorption of the HF electromagnetic wave

A.B. Pashin, A.A. Mochalov (*Polar Geophysical Institute, 184200 Apatity, Murmansk region, Russia*)

In spite of long-time history of the experiments on ionosphere heating at present we have no direct measurement of primary modified parameter, namely enhanced electron temperature. Our knowledge on its value is based on theory, numerical modeling, or observation of disturbances being results of the temperature increasing. One of these measurements is amplitude of artificial low frequency emissions excited under modulated heating of D-region electrons. The generation of artificial magnetic pulsations – the emissions in frequency range around 1 Hz – shows their sporadic nature. Sometimes during experiments detection of the pulsations is finished without significant variations of parameters of the ionosphere. This peculiarity demonstrates incomplete of our knowledge on the emission excitation and it requires to develop more direct experimental method of the enhanced temperature estimation.

Clear dependence of absorption of HF electromagnetic wave on electron temperature gives an opportunity to consider the measurements of the absorption value as a candidate for diagnostic of this parameter. Numerical modeling shows that the value of the additional absorption during the heating should be significant enough for the measurements and interpretations. The possibility to employ of the probe waves at different frequencies has an advantage, unknown parameters such as electron density and undisturbed electron temperature may be excluded from the solution. As a source of HF waves one may use a cosmic radio noise or transmitter based on a satellite.

Southern boundary of the ultra relativistic electron precipitation on May 13, 1987

G. F. Remenets, A. M. Astafjev (*Physics Department of St.-Petersburg State University, Russia*)

Phenomenon of the ultra relativistic electron precipitation (UREP with energy is about 100 MeV) was analyzed in a cycle of publications [1-5] since 1985 year. Today we know about these electrons that their flux density such, that they, generating X- and gamma ray bremsstrahlung, create a sporadic D-layer of electric conductivity at the altitudes of 10 – 40 km. Such sporadic layer forms a reflected signal (due to the partial reflections from the altitude intervals where the conductivity gradient differs from zero) from the on ground monochromatic radio sources of very low frequency (VLF) range (10 – 16 kHz). The effective height h of radio wave reflection is changing during a disturbance since normal undisturbed value ~ 60 km to ~ 30 km in the maximum of powerful disturbance (Pwd's) at daytime. For weaker disturbances (for strong (StD's) and moderate disturbances (MdD's)) the effective height variations are less. These values were gotten due to the solution of the VLF inverse problem, in which according to the time variations of the amplitudes and the phases of 3 radio signals for the auroral radio pass the effective height and the reflection coefficient R were calculated as functions of time. It was supposed that at every moment of the disturbance the radio pass was homogeneous, i. e. it was considered that the spacious horizontal scale of a disturbance was greater than the length of the auroral radio pass (10.2, 12.1, 13.6 kHz) with its 885 km length. The pointed VLF inverse problem is called here as an inverse problem of first kind. This problem for an event on 13 May was solved in [6], and it turned out that the variations of conductivity parameters were the following: $h = 64 - 38 - 61$ km, $R[\psi^1(h)] = 0.60 - 0.45 - 0.55$, where ψ^1 is an angle of incidence of the first ray on the top boundary of wave-guide with height h and where the middle values correspond to the maximum of disturbance. Uncertainty of h and R was estimated at several km and 0.03 correspondingly.

The presented report is devoted to an inverse VLF problem of second kind, in which we used the amplitude and phase variations of a radio signal (16 kHz) during the same disturbance but for a long partly auroral radio pass (England – Kola peninsula, $S=2497$ km) for the determination of the southern boundary of the UREP on May 13, 1987. From direct comparison of the phase variations for the pointed auroral and the partly auroral radio passes it was estimated earlier that the long radio pass was disturbed only partly from the northern end and that the disturbed part was about 1/3 of its length [3, 4, 7]. But every disturbance is individual. It is necessary to have an algorithm for

Ionosphere and upper atmosphere

finding the position of a boundary between the disturbed and undisturbed parts of the radio pass for a given disturbance.

So let us imagine a model of a wave-guide, which consists of two homogeneous parts at every moment of a disturbance. The southern part of a wave-guide with length S^2-d was modeled with the help of the middle latitude ionosphere and did not depend on time. The northern part of the wave-guide (with length d) is characterized by the changes in time (the same for all points) of the electric properties of the sporadic D-layer of conductivity, which the VLF inverse problem of first kind had given. The position of a boundary between these two parts is an object of search by the help of the inverse problem of second kind. For the pointed model we calculated the relative changes of the amplitude and the phase variation for 16 kHz radio-signal as function of time. We included these two functions into a function-discrepancy $GG(d)$, which characterizes the difference between the experimental and calculated functions of time, demanding that the initial values of experimental and calculated curves coincided with each other before the disturbance. Such function GG we minimized relative to the value of d . In the case of our event on May 13, 1987 to the values $GG_{min} \pm 0.1$ GG_{min} corresponded the values of relative distance $d/S^2 = (18 \pm 5.00)\%$ and of the latitudes $(65^\circ \pm 0.8^\circ)N$. correspondingly. A function-discrepancy $G(d)$, which contained only phase data, was minimized, and the corresponding results were the same: $d^1/S^2 = (18 \pm 5.00)\%$; $(65^\circ \pm 0.8^\circ)N$. Continuation of the calculations for a function-discrepancy $G^{amp}(d)$, which contained only the amplitude data, gave the following: $d^2/S^2 = (30 \pm 6.00)\%$; $(63^\circ \pm 1^\circ)N$. It concludes, that even the most rough estimation according to the $G^{amp}(d)$ – calculations indicates on the fact that on 13 May 1997 the southern boundary of UREP did not lowed then 63° of North latitude for the radio-pass Ragby- Apatity.

So we have got an approximate solution of a problem about the latitude of the southern boundary of ultra relativistic electron precipitation. The solution is approximate, because nothing is known about a possible movement of the boundary while a disturbance. So the position of precipitation boundary founded is an effective one and equal to $65^\circ N$.

The same estimation may be fulfilled for the cases of proton precipitations but nobody has done it yet.

References

1. Remenets, G. F., and M. I. Beloglazov, (1985) Reflection properties of the low polar ionosphere, the peculiarities of intoxication and propagation of the VLF waves at high latitudes, *Izvestija Vuzov. Radio Physics*, 28, 1491–1504 (in Russian).
2. Remenets, G. F. and M. I. Beloglazov, (1992) Dynamics of an auroral low ionospheric fringe at geophysical disturbances on 29 September 1989, *Planet Space Sci.*, 40, 1101-1108.
3. Remenets, G. F., (2001) Investigation of the dynamics of high latitude upper atmosphere ionization due to the VLF experimental data, *Vestnich of the St. Petersburg University*, series 4, issue 3, (no. 20), 23–38 (in Russian).
4. Beloglazov, M. I. and G. F. Remenets, (2005) Investigation of powerful VLF disturbances, *Intern. J. Geom. Aeronom.*, 5, No. 3, April issue, GI3004, doi: 10.1029/2005GI000101.
5. Beloglazov, M. I. and G. F. Remenets, (2010) Phenomenon of ultra-relativistic electron precipitation in the middle polar atmosphere, in *Science Conference "The State and Perspectives of Development of the Geophysical Investigations at High Latitudes"*, edited by V. G. Vorobiov, (Polar Geophys. Inst. of RAS, Murmansk-Apatity, Russia) 20–22 (in Russian).
6. Remenets G. F., Kustov A. A. Southern boundary of the ultra-relativistic electron precipitation on May 13, 1987. In: 9th International conference "Problems of Geocosmos". Book of abstracts. St. Petersburg, 2012. P. 222-224.
7. Beloglazov, M. I. and G. F. Remenets, (2010) Ultra-relativistic electron precipitations as a main cause of the most powerful disturbances in the middle polar atmosphere, in *Proceedings of the 8th International Conference "Problems of Geocosmos"* held in St. Petersburg, Russia, edited by V. S. Semenov (St Petersburg, 2010) 51–56. ISBN 978-5-9651-05045, <http://geo.phys.spbu.ru/> .

Auroral riometer absorption may be caused by auroral protons

V.C. Roldugin, M.E. Shkarbalyuk, A.V. Roldugin, S.V. Pilgaev (*Polar Geophysical Institute, Apatity, Russia*)

Several events of riometer absorption in Lovozero. Sodankyla and Kiruna during H-positive magnetic bays are investigated. We suppose that such auroral absorption cases are caused by auroral proton precipitation. This hypothesis is verified by spectral observations of hydrogen emissions with meridian spectrometer in Lovozero.

Horizontal scale of the Ionospheric Alfvén Resonator inferred from simultaneous auroral and magnetic observations

N.V. Semenova, A.G. Yahnin (Polar Geophysical Institute, Apatity)

Analysis of induction-coil magnetometer observations of the resonance structure in spectra of electromagnetic noise in the 0.1-10 Hz frequency range along with simultaneous auroral TV camera observations showed that the resonant structure could be observed when relatively intense aurora is far enough from the magnetometer location. When the auroral precipitation approaches the magnetometer site as close as ~ 150 -200 km, the observations of the resonant structure cease. The resonant structure, as believed, is related to the existence of the Ionospheric Alfvén Resonator (IAR). The disappearance of the resonant structure related to close approach of the aurora is, evidently, due to fast

variations of the ionospheric parameters, which prevent the formation of stationary IAR, or to the increase of the electron density in the E-region, which leads to the decrease the IAR quality. Thus, a minimal distance between auroras and the magnetometer observing the resonant structure determines the horizontal scale of the IAR responsible for the resonant structure seen on the ground.

Mesosphere temperature profile retrieval based on the wide-angle polarization measurements of scattering radiation during the twilight period

O.S. Ugolnikov, I.A. Maslov (*Space Research Institute, Russian Academy of Sciences, Moscow, Russia*)

The work is devoted to the study of Earth's mesosphere optical properties based on the measurements of twilight sky intensity and polarization conducted at the latitude 55°N during the spring-summer period of 2011 and 2012 with wide-angle polarization camera (field of view is about 140°). The developed method of single scattering separation and calculation of its scattering function is based on observational data over the whole measured part of the sky. The analysis of multiple scattering properties helps to subtract it from the total background. Single scattering field is retrieved at the altitude range from 70 to 85 km.

Observational analysis had shown that the single scattering polarization in the mesosphere is usually close to Rayleigh value, revealing the domination of molecular scattering. For this case the altitude dependency of pressure and temperature can be obtained.

The temperature values based on the twilight measurements are compared with the satellite infrared emission data (experiment SABER onboard the TIMED satellite, experiment MLS onboard the EOS Aura satellite). The comparison shows that the twilight values are little bit less than SABER ones, but exceed the MLS temperatures (the difference between SABER and MLS data was found straight after the start of EOS Aura mission and reaches 5-10K in the northern hemisphere during the summer).

The accuracy of temperature measurements and agreement with satellite data show the efficiency of twilight method for the mesosphere temperature control. The problem is actual due to the increase of mesosphere trace gases (first of all, CO₂) density and their influence to the temperature by the radiative cooling process.

The work is done with the financial support of Russian Foundation for Basic Research, grant No.12-05-00501-a.

Optical characteristics of aurorae during undulation events on December 12, 2010

V.G. Vorobjev, V.K. Roldugin, O.I. Yagodkina (*Polar Geophysical Institute, Apatity, Murmansk region 184200, Russia*)

Large-scale undulations on the equatorward edge of diffuse aurora observed from two all-sky cameras at the Kola Peninsula on Dec.12, 2010 were examined. Undulations appeared near 1400 UT about 12 min later the thumb-like variation in the solar wind dynamic pressure with the duration of about 15 min and value changes from about 2 to 17 nPa. Undulations were observed about two hours up to 1610 UT, i.e. from about 1640 to 1850 of the geomagnetic local time (MLT). According to triangulation measurements the height of undulations is evaluated to be 120 ± 10 km. Luminosity waves of 100-300 km amplitude propagated westward with the velocity of about 0.7 - 0.8 km/s. According to TV observations and results of MIRACLE project, undulations were generated at the equatorward edge of the broad eastward electrojet, near the poleward edge of which discrete auroral forms were observed. The eastward electrojet occupied all region of diffuse auroral luminosity of about 6°-7° of latitude. N-S oriented rayed auroral bands, separated rays, patches and luminosity inhomogeneities moved inside of diffuse luminosity with the average velocity of ~2.0 km/s that corresponds to the poleward electric field of about 100 mV/m. This auroral velocity was in two and more time larger than velocity of undulations that testifies about different driving mechanisms.

Модель распространения ультра и сверх низкочастотных сигналов в волноводе Земля–ионосфера, основанная на численном решении уравнений Максвелла с учетом реалистичной тензорной проводимости ионосферы

О.И. Ахметов, И.В. Мингалев, О.В. Мингалев, Ю.В. Федоренко, В.С. Мингалев, О.М. Лебедь (*Полярный геофизический институт КНЦ РАН, Апатиты, mingalev_o@pgia.ru, akhmetov@pgia.ru*)

Начиная с 1994 года за рубежом опубликовано большое число работ, в которых для исследования распространения электромагнитных сигналов в нижнем диапазоне частот используются различные численные модели, основанные на конечно-разностной аппроксимации уравнений Максвелла на

Ionosphere and upper atmosphere

пространственной сетке со 2-м порядком точности. Такие модели в англоязычной литературе принято называть FDTD–models. Рассматривались как локальные модели для определенного отрезка в нижней части диапазона частот, так и глобальные FDTD–модели для низкочастотных сигналов. Имеется несколько научных групп, которые последовательно развивают свои версии глобальных моделей.

Авторами разработана глобальная 3-мерная численная модель распространения ультра и сверх низкочастотных сигналов (ниже 100 Гц) с малой амплитудой в волноводе Земля–ионосфера, основанная на разностной аппроксимации уравнений Максвелла. По сравнению с зарубежными глобальными FDTD–моделями впервые учитывается реалистичная тензорная проводимость ионосферы, используются в разы меньшие шаги пространственной сетки, реалистичное граничное условие на границе атмосфера–литосфера, а также новая более эффективная методика численного решения уравнений Максвелла. Был выполнен набор расчетов распространения образовавшегося на экваторе атмосферика – сигнала от сильного разряда молнии, а также сравнение результатов расчетов с имеющимися в ПГИ экспериментальными данными, которое обнаружило хорошее качественное и количественное соответствие между ними. В частности, получена наблюдаемая в эксперименте зависимость сигналов от времени в данной точке и затухание антиподного (обошедшего вокруг Земли) сигнала по сравнению с прямым сигналом, а также совпадающая с экспериментальными данными различная скорость распространения сигналов на дневной и на ночной стороне.

Кроме того, выполненные расчеты продемонстрировали принципиальное влияние тензорной проводимости нижней ионосферы, в особенности её холловской составляющей, на распространение сигналов, в том числе и в приземном слое.

Создание модели открывает принципиально новые возможности в диагностике состояния нижней высокоширотной ионосферы по данным наземных измерений на радиотрассе длиной 1300 км между Баренцбургом (на о. Шпицберген) и Ловозеро (на Кольском п-ве).

Работа выполнена при поддержке гранта РФФИ № 13-01-000-63.

Обнаружение магнитогравитационных волн по данным о вариациях концентрации ионосферного слоя F2 и магнитным наблюдениям в периоды высокоэнергичных геофизических событий

О.М. Бархатова^{1,2}, Н.В. Косолапова², Р.И. Серебрякова¹

¹*Нижегородский государственный архитектурно-строительный университет, Нижний Новгород, Россия*

²*Нижегородский государственный педагогический университет, Нижний Новгород, Россия*

Проанализированы данные критических частот ионосферных слоев E, Es и F2, а также X, Y, Z компоненты геомагнитного поля со станции Learmonth (21,9° ю.ш., 114° в.д.) в период сильного подземного землетрясения, которое произошло на глубине 10 км 17 июля 2006 г. в 08:19:25 UT на западном побережье Индонезии (9.33° ю.ш., 107.26° в.д.). Магнитуда события составляла 7.7 баллов по шкале Рихтера. В результате землетрясения образовалась цунами высотой более 5 метров.

В пределах временного интервала, включающего 3 дня до события, день события, и 3 дня после него выполнен спектральный анализ ионосферных и магнитных возмущений в диапазоне $10^{-5} \div 10^{-3}$ Гц. Сопоставление полученных динамических спектров для всех указанных выше параметров демонстрирует синхронность ионосферных и магнитных возмущений в течение двух дней до землетрясения и двух дней после него на близких характерных частотах в диапазоне $(2\text{--}4)\cdot 10^{-4}$ Гц. Это может свидетельствовать о существовании в данные периоды возмущений, обусловленных волнами магнитогравитационного типа.

В течение двух дней до рассматриваемого события также зарегистрировано увеличение интенсивности спектра критической частоты слоя F2 ионосферы ($f0F2$) и X-компоненты геомагнитного поля на характерной частоте. За день до события в то же время возрастает и интенсивность спектра критической частоты спорадического слоя Es ($f0Es$). Выявленные спектральные особенности могут рассматриваться в качестве возможных проявлений физических процессов, предшествующих развитию землетрясения. В день землетрясения совпадений спектральных особенностей ионосферных и геомагнитных параметров не отмечается, однако имеет место заметное усиление интенсивности спектра $f0Es$. В течение двух дней после землетрясения на динамических спектрах наблюдается синхронное возмущение $f0F2$, и Y-компоненты геомагнитного поля, причем на следующий день после землетрясения в то же время возрастает и интенсивность спектра $f0Es$. Обнаруженные совпадения могут свидетельствовать о генерации магнитогравитационных волн и после высокоэнергичных событий. За три дня до и после рассматриваемого события совпадения спектральных особенностей не обнаружено.

Таким образом, обнаруженные особенности плазменной и магнитной возмущенности свидетельствуют о том, что возмущенность спорадического слоя Es заметно возрастает за несколько часов до события и

сохраняется в течение суток. Синхронные возмущения слоев ионосферной ионизации и геомагнитного поля в периоды, предшествующие высоконергичному геофизическому событию свидетельствуют о наличии в эти времена магнитогравитационных возмущений, которые могут служить предвестниками этих событий.

Исследование вклада локальных грозовых очагов в формирование РСС и вариаций поляризации фонового магнитного шума

Е.Н. Ермакова¹, Д.С. Котик¹, А.В. Рябов¹, А.А. Панютин²

¹*Научно-исследовательский радиофизический институт, Н. Новгород, Россия.*

²*Нижегородский ЦГМС-Р, Н. Новгород, Россия*

В работе исследовано влияние маскирующего фактора от локальных грозовых очагов на спектры КНЧ полей при существовании структур ИАР и суб-ИАР в локальной ионосфере.

На основе оригинальной методики обработки данных по регистрации горизонтальных магнитных компонент на среднеширотном приемном пункте «Новая Жизнь» исследован вклад источников, удаленных на разные расстояния от приемного пункта, в формирование РСС и вариаций поляризации фонового шума. Метод предполагает задание определенного порога (0.1 до 0.9) от максимального значения импульсной составляющей шума, при котором она заменяется «белым» шумом, с амплитудой, не превышающей порога. Результат записывался в новый файл и подвергался спектральному анализу. Далее проводился сравнительный анализ вновь полученных и первичных спектров при разных уровнях порога. По глубине осцилляций резонансных структур делался вывод о вкладе источников, расположенных на различных расстояниях от приемного пункта в формирование этих структур. Для определения положения локальных очагов привлекались данные с метеорологического радиолокационного комплекса МРЛ-5АКСОПРИ, расположенного в Н. Новгороде.

Работа поддержана грантами РФФИ 11-02-00419-а и Министерства образования и науки Российской Федерации, государственный контракт № 16.518.11.7066.

Околополуденное авроральное свечение на высоких широтах

В.Л. Зверев¹, В.Г. Воробьев¹, Я.И. Фельдштейн²

¹*Полярный геофизический институт, Анадырь, Россия*

²*Институт земного магнетизма, ионосферы и распространения радиоволн, Троицк, Россия*

Оптические наблюдения полярных сияний меридиональным сканирующим фотометром (MSP), телевизионной камерой всего неба (TV-камера) на ст. Баренцбург (BAB; $\Phi'=75.2^\circ$, $MLT=UT+2.4$) и одновременные наблюдения вторгающихся частиц спутниками DMSP F12-F16 использованы для исследования связи дневных полярных сияний с плазменными структурами вторгающихся частиц. Детально исследованы два события, когда орбиты спутников пересекали дневную авроральную зону от полярной границы мантии до диффузной зоны.

(1). 22 декабря 2003 г. одновременные наблюдения полярных сияний и вторжений авроральных частиц на спутнике DMSP F16 проводились в интервале 09:01–09:04 UT.

Особое внимание обращалось на положение аврорального свечения во время пересечения высоколатитных плазменных доменов в магнитосфере: мантии (MA), каспа (CU) и низкоширотного граничного слоя (LBL) в 09:01:30–09:02:30 UT. Такие события достаточно редки, так как пролеты спутников DMSP происходят со скважностью ~ 102 мин, а наблюдения за свечением в области каспа возможны только вблизи зимнего солнцестояния в интервале 08–11 UT. Анализ спектрограммы электронов и ионов вдоль траектории пролёта спутника и спектров вторгающихся частиц показал, что положение границы между мантией и каспом, определённым автоматическим методом APL, необходимо сместить на более высокие широты ($\sim 0.4^\circ$). Дуга полярного сияния в 09:02:05 UT в предположении высоты 240 км проектируется на геомагнитную широту $\sim 73^\circ$. Её положение хорошо совпадает с положением границы мантия – касп. В 09:01 UT. отношение интенсивностей эмиссий 630.0/557.7 в дуге равно 4, что соответствует средней энергии высыпающихся электронов ~ 0.2 keV. Спектры с максимумом на этих энергиях наблюдаются по DMSP на приполюсном крае электронных высыпаний. Согласно этим данным высота дуги должна быть ~ 250 км.

(2). 8 декабря 2000 г. одновременные наблюдения полярных сияний и вторгающихся частиц по данным спутника DMSP F13 проводились в 08:10:47–08:21:31 UT. Траектория спутника пересекала поле зрения TV камеры вблизи Z станции и проходила практически вдоль геомагнитной параллели E-W. Полярные сияния в 08:12:00 UT располагались широкой полосой в области Z ст. BAB. В проекции на поверхность Земли они находились в пределах плазменных областей магнитосферы: мантия - касп – LBL – касп - LBL, которые

Ionosphere and upper atmosphere

были определены автоматическим методом APL, и чередуются через небольшие интервалы широт. Полярные сияния имели слабо выраженную лучистую или волокнистую структуру. На основе анализа реальных спектров вторгающихся электронов и ионов предложена другая идентификация доменов вдоль траектории DMSP F13: мантия, касп, LLBL.

Вывод. Автоматический метод APL для определения границ плазменных доменов в дневном секторе требует корректировки по реальным спектрам вторгающихся частиц. Полярные сияния наблюдаются в области границы вторжения частиц мантия/касп на высотах ~ 250 км.

Особенности распространения радиоволн в периоды высыпания частиц в мини-магнитосферах Марса

А.П. Киреев, А.М. Крымский (*Южный Федеральный Университет*)

В эксперименте по радиозондированию Марса MARSIS AIS были определены области, в которых обычно регистрировались сигналы на частотах выше f_{\max} ионосферы Марса, отраженные от поверхности планеты. Однако в этих областях сигналы отраженные от поверхности Марса не регистрировались в нескольких временных интервалах протяженностью несколько дней каждый, что коррелировало с периодами возмущенного солнечного ветра. Исчезновение отражений от поверхности может быть объяснено столкновительным поглощением сигнала (Morgan et al, 2012). Рассеяние радиоволн, связанное с образованием неоднородностей в концентрации электронов при высыпании частиц в мини-магнитосферах Марса, также ослабляет проходящий сигнал. Вследствие нагрева атмосферы высыпающимися энергичными частицами (Johnson, 1990) исчезновение отраженного сигнала должно сопровождаться подъемом ионосферного максимума и ростом шкалы высот нейтралов. Сравнительный анализ данных магнитометрических экспериментов и данных акселерометра (Krymskii et al, 2004) показал, что в окрестности внешних границ мини-магнитосфер Марса и их потенциальных каспов, где возможно высыпание частиц, шкала высот нейтралов обычно выше ее среднего по поверхности планеты значения. Таким образом, при прохождении радиосигнала через нижнюю ионосферу в окрестности границ мини-магнитосфер Марса можно ожидать роста его поглощения.

Влияние возмущений в полярной ионосфере на вариации атмосферного электрического поля

А.Л. Котиков¹, А.В. Франк-Каменецкий², А.А. Круглов², Н.Г. Клейменова³, О.В. Козырева³, М. Кубицки⁴, А. Оджимек⁴

¹*Санкт-Петербургский филиал института земного магнетизма, ионосферы и распространения радиоволн РАН, г. Санкт-Петербург, Санкт-Петербургский государственный университет, г. Санкт-Петербург*

²*ФГБУ Научно-исследовательский институт Арктики и Антарктики, г. Санкт-Петербург*

³*Институт физики Земли РАН, г. Москва*

⁴*Институт геофизики Польской Академии Наук, г. Варшава*

Величина атмосферного электрического поля (E_z) в условиях «хорошей погоды» определяется величиной разности потенциалов (в дальнейшем потенциала) между ионосферой и земной поверхностью над точкой наблюдения. В высоких широтах потенциал ионосферы (U_i) создается как метеорологическими генераторами (U_{int}) (преимущественно грозами), так и внешними источниками магнитосферного происхождения (U_{ext}). Соответственно, измеряемое атмосферное электрическое поле можно представить как $E_z = E_{zint} + E_{zext}$. Многолетние наблюдения E_z на ст. Восток в Антарктиде позволили разработать метод разделения этих источников. Значения E_{zint} , полученные по данным ст. Восток, позволили вычислить значения E_{zext} для обс. Хорзунд на арх. Шпицберген, где регулярно регистрируются вариации E_z . Выполнен анализ одновременных наблюдений вариаций приземного электрического поля (E_z), нормированного на среднесуточное значение, в различных областях высоких широт. Установлено, что в полярной шапке (ст. Восток) вариации атмосферного электрического поля контролируются вариациями потенциала ионосферы над точкой наблюдения с высоким коэффициентом корреляции ($R \sim 0.7-0.9$). В обс. Хорзунд, расположенной вблизи границы полярной шапки, ситуация сложнее. В интервалы, когда Хорзунд находился в области западного электроджета, эта корреляция обычно положительная с $R \sim 0.60-0.85$, а когда Хорзунд оказывался в области восточного электроджета знак корреляции может изменяться на отрицательный.

Влияние гравитации на распространение магнитозвуковых волн в нижней ионосфере Земли

В.Д. Терещенко (*Polar Geophysical Institute, Murmansk, 183010, e-mail: vladter@pgi.ru*)

На основе решения уравнений магнитной гидродинамики получено локальное дисперсионное соотношение для собственных низкочастотных колебаний частично ионизованного газа, находящегося в магнитном и гравитационном полях, которое имеет следующий вид:

$$\omega^4 - \omega^2(\omega_A^2 + \omega_s^2 + N_a^2 - N_A^2) + N^2 \omega_s^2 \sin^2 \varphi + (\omega_A^2 - N_A^2)(\omega_s^2 \cos^2 \vartheta + N_a^2 \cos^2 \eta) = 0,$$

где $\omega_A^2 = k^2 V_A^2$, $\omega_s^2 = k^2 c_s^2$, $N_a = c_s/2H$, – предельная акустическая частота, $N_A = V_A/2H$, – предельная альвеновская частота, H – приведённая высота атмосферы, V_A и c_s – альвеновская и адиабатическая звуковая скорости, ω – частота, φ – угол между волновым вектором \mathbf{k} и ускорением силы тяжести \mathbf{g} , η – угол между геомагнитным полем \mathbf{B}_0 и \mathbf{g} , ϑ – угол между \mathbf{k} и \mathbf{B}_0 .

Построены поляры и определены частоты, фазовые и групповые скорости собственных колебаний нижней ионосферы над геомагнитным полюсом, экватором и в промежуточной зоне. Показано, что тип низкочастотных колебаний, возбуждаемых и распространяющихся в ионосфере Земли, зависит от геомагнитных координат точки наблюдения и направления распространения волны.

Двухпараметрический характер термо-аномалии запылённого ночного аврорального динамо слоя

Е.Е. Тимофеев¹, С.Л. Шалимов^{2,3}, О.Г. Чхетиани^{2,3}, М.К. Валлинкоски⁵, Й. Кангас⁵

¹*Государственная морская академия им. адм. С.О. Макарова, С.-Петербург*

²*Институт физики земли им. О.Ю. Шмидта, РАН, Москва*

³*Институт космических исследований, РАН, Москва*

⁴*Институт физики атмосферы им. А.М. Обухова, РАН, Москва*

⁵*Отдел космофизики университета г. Оулу, Финляндия*

С целью дальнейшего изучения эффекта аномального охлаждения электронов динамо слоя (ДС) в настоящей работе анализируются пространственные и временные вариации ионной (Ти) и электронной (Тэ) температур, а также величины электронной плотности (Ne) и компонент вектора ионосферного электрического поля (Е-поля). Вариации всех параметров, измеряемых системой радаров EISCAT в ходе 2-х авроральных суббурь 15 и 23 марта 1988 в зените обс. Тромсё, сглаживаются методом скользящего среднего с выбором оптимальной ширины корреляционного окна. Показано, что: 1) температурная аномалия с охлаждением электронов по отношению к температуре ионов (Ти - Тэ) на величину от $\sim 15\text{K}$ до $\sim 140\text{K}$ регистрировалась в более чем в половине всего интервала измерений. 2) При этом в областях аномалии величина Ne постоянно превышала пороговый уровень $\sim 5 \cdot 10^4 / \text{см}^3$, а при кратковременных (5-15 минут) инверсиях к режиму ФБ-перегрева (Тэ > Ти), наоборот, была ниже указанного порога. 3) Подобные инверсии знака величины (Ти - Тэ) наблюдались в каждом из 4-ёх ~ 2 -х часовых интервалах измерений с характерным времененным масштабом от 40 до 70 минут. 4) В периоды противофазных волновых вариаций Тэ и Ne охлаждение электронов примерно вдвое превышало нагрев ионов при типичной величине (Ти - Тэ) $\geq 50\text{K}$, а величины Е-поля не превышали порога ФБ-неустойчивости (15-20 мВ/м). 5) При резком росте Ne до величины $\sim 25 \cdot 10^4 / \text{см}^3$ за время ~ 7 -10 минут, импульсное охлаждение электронов начиналось и при величинах Е-поля заметно превышающих ФБ-порог. 6) В периоды медленных (~ 1 -2 мВ/м в минуту) вариаций модуля вектора ионосферного электрического поля, регистрировались квазистационарные тепловые структуры с пространственными масштабами от 7 до 45 км. При этом вектор Е-поля находился преимущественно в юго-западном квадранте.

Дана физическая интерпретация основной части описанных выше результатов, основанная на гипотезе о конкуренции двух факторов. кулоновских сил заряженных макро-частиц пыли, обеспечивающих жёсткость структуры плазменно-пылевого кристалла, и порождаемой неустойчивостью Фарлея-Бунемана (ФБ) плазменной турбулентностью, стремящейся разрушить эту структуру. Механизмом генерации тепловых структур может быть, например, нелинейная стадия неустойчивости эмановского типа.

Связь некоторых характеристик ППШ с температурой верхней мезосферы

В.А. Ульев¹, О.А. Данилова², О.И. Шумилов³

¹*Арктический и Антарктический Научно-исследовательский институт (ААНИИ, СПб), vauliev@yandex.ru*

²*Санкт-Петербургский филиал Института Земного Магнетизма, Ионосферы и Распространения*

радиоволн (СПбО ИЗМИРАН), md1555@mail.ru

³*Институт проблем промышленной экологии Севера Кольского научного Центра РАН, oleg@aprec.ru*

В работе анализируется долговременный тренд двух характеристик ППШ: величины поглощения в максимуме ППШ (по данным станций внутри полярной шапки) и амплитуды эффекта полуденного восстановления (по данным станций в авроральной зоне). Установлено, что в течение рассматриваемого периода (с 70-х по 90-е годы) происходило уменьшение относительной амплитуды ППШ и амплитуды полуденного восстановления. Данные по поглощению сопоставлены с изменением спектра потоков солнечных протонов, уровня геомагнитной активности и температуры мезосферы за указанный период. Физический анализ и расчёты позволили сделать вывод о том, что основной причиной отрицательного тренда данных по поглощению является понижение температуры верхней мезосферы.

Электронные и ионные высыпания в утреннем и вечернем секторах в зависимости от уровня магнитной активности

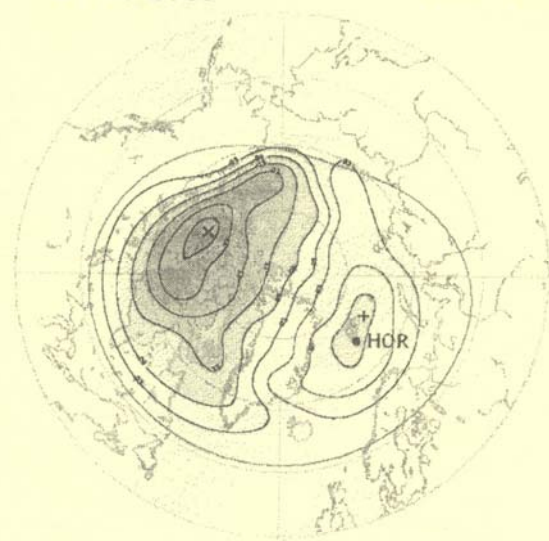
О.И. Ягодкина, В.Г. Воробьев (*Полярный геофизический институт КНЦ РАН, Анадырь*)

Исследованы сравнительные характеристики электронных и ионных высыпаний в утреннем (0300-0600 MLT, 0600-0900 MLT) и вечернем (1500-1800 MLT, 1800-2100 MLT) секторах в зависимости от уровня магнитной активности. Показано, что в утреннем секторе доминируют электронные высыпания. Здесь в области структурированных высыпаний (AOP) потоки энергии ионов (Fi) составляют менее 5% от потока энергии электронов (Fe). В области диффузных высыпаний (DAZ) доля Fi уменьшается с ростом магнитной активности от ~25% при AL=-100 нТл до ~5% при AL=-1000 нТл. В вечернем секторе в области AOP также преобладают электронные высыпания, в то время как в DAZ потоки энергии ионов значительные. Отношение Fi/Fe изменяется от 0.8 до ~3.5 при росте AL от -100 нТл до -1000 нТл.

Low Atmosphere, Ozone

27.10.2005

00.30 UT



Variations of sea level pressure in the Northern and Southern hemispheres in association with Forbush decreases of galactic cosmic rays

I.V. Artamonova, S.V. Veretenenko (*Saint-Petersburg State University, Saint-Petersburg, Russia*)

The investigation of atmospheric pressure variations during Forbush decreases of galactic cosmic rays (GCR) was carried out; the data of NCEP/NCAR reanalysis for the cold half of year of the period 1980-2006 years were used. The research showed that Forbush decreases of GCR are accompanied by significant variations of sea level pressure in the North and South Atlantic regions and over the South Ocean in the latitudinal belts 45-70° in both hemispheres. The maximum pressure values were revealed on the 3rd-4th days after Forbush decrease beginning over the North Atlantic, Scandinavia and North Europe in the Northern hemisphere. In the Southern hemisphere the maximum pressure was observed on the 4th-5th days after Forbush decrease onset in two regions: the first is over the South Ocean between South Africa and Antarctica, the second is between Australia and Antarctica. It was assumed that the revealed atmospheric pressure variations are caused by intensification of anticyclone activity associated with Forbush decreases under study. The results obtained in this work showed that short-time variations of GCR may contribute to the evolution of extratropical baric systems, as well as about an important role of galactic cosmic rays in the Sun-Earth relations.

Modeling of the lower and upper atmosphere interconnection

K.E. Beloushko (*Physics Department, Murmansk State Technical University, Sportivnaya St., 13, 183010 Murmansk, Russia; e-mail: Beloushko@mail.ru*)

Attempt to develop the united numerical model of the Earth's atmosphere is undertaken. At the moment there is a need to create a single numerical model of the gaseous envelope of the Earth, which would advance in the study of the global electric circuit, the meteorological effects on the lower ionosphere, atmospheric tides, acoustic-gravity waves, stratospheric anomalies, etc. Purpose of the project is development of the general methodologies and technologies of coupling of models with use of the so-called frame approach. Coupling of the upper and lower atmosphere models will allow not only to develop united model, but also thus to remove the uncertainty, connected with assignment of the upper boundary conditions in lower atmosphere and lower boundary conditions in upper atmosphere. As a result of named problem analysis the following algorithm for coupling of models is offered: in the area, where the model grids intersect, it is proposed to carry out an iterative exchange of data. Results of some joined simulations on the basis of model of upper atmosphere UAM and model of general circulation of INM RAS are presented and discussed.

Sensitivity of the tropospheric circulation to the GLE

V.I. Demin (*Polar Geophysical Institute, Apatity*)

The atmospheric circulation processes belonged into one of elementary circulation processes (ESP) types, if the following criteria were met:

- 1) similar development and geographical distribution of the leading (directing) pressure areas;
- 2) similar direction of prevailing winds;
- 3) similar attributes of the main invasions of air masses.

Thus change of ESP is indicator of transformation of large-scale atmospheric circulation. This suggests the use of ESP for estimation the sensitivity of the tropospheric circulation to the GLE.

Research shows that frequencies of changes of ESP before and after the GLE are similar. This proves the weak influence of GLE on the troposphere circulation. At least this influence is not detected by the standard techniques of synoptical analysis.

Long-term changes in the vertical air temperature profile in the Khibiny Mountains

V.I. Demin¹, P.A. Chernous², V.N. Moroz²

¹*Polar Geophysical Institute, Apatity*

²*Centre of Avalanche Safety, "Apatit" JSC, Kirovsk*

Average summer temperatures in the Khibiny mountains for period of 1961-2011 years are more than ones for period of 1881-1960 years by 0.3-0.4°C. This corresponds to movement of summer isotherms by 30-50 m upward. At the same time since end of 19th century the upper tree-line in the Khibiny Mountains has risen up by

Low atmosphere, ozone

100-150 m. It is suggested that the observed rise of upper tree-line limits in the Khibiny is mainly due to long-term (centuries) climate changes and to a lesser degree is response to short-term (decades) climatic variations including the present-day warming.

Seasonal changes of diurnal variation of atmospherics ELF-VLF range on observations at the Kola Peninsula

V.I. Kirillov, V.V. Pchelkin, M.I. Beloglazov, A.A. Galakhov (*Polar Geophysical Institute, Apatity*)

The results of measurements of the pulsed component of atmospheric electromagnetic noise at the 600 and 6000 Hz which were performed in June-November 2012 at the observatory PGI "Lovozero" were study. The measurements were carry out using atmospherics registrator developed in the PGI. Two orthogonal frame used as antennas oriented along and across the magnetic meridian. For analysis were selected days, during which the AE - index does not exceed 300 nT.

In addition, we considered only atmospherics with amplitudes levels over 100 relative units (range of amplitudes measured from 0 to 833 relative units).

Based on the analysis, the following conclusions concerning the atmospherics of this type:

1. Density recorded atmospherics N_{hour} (number of pulses in 1 hour) at frequency of 6000 Hz is much larger than 600 Hz.
2. Pronounced daily maximum observed in the summer months at both frequencies and in both components ("N-S", "E-W"). Nearest thunderstorms of midlatitude is the most likely source daily high.
3. In contrast to the ELF range, does not show significant difference in the diurnal variations of atmospherics at both frequencies in the components of the "N-S" and "E-W" both N_{hour} , and on the average hourly amplitudes.
4. Probability distribution of the levels of atmospherics can be approximated by the formula known from the literature form: $P(X) = [1 + (X/X_{50}) k]^{-1}$, where the parameter k of this relationship varies from 2.2 to 3.2 for the 600 Hz and from 1.5 to 2 for 6 kHz.

Influence is artificial the indignant ionosphere on mesospheric ozone

Y.Y. Kulikov¹, V.L. Frolov²

¹*Institute of Applied Physics, N. Novgorod, Russia*

²*Radiophysical Research Institute, N. Novgorod, Russia*

The experiments, carried out at the SURA heating facility in 2009 – 2012 allow revealing a new physical phenomenon: the decrease of the microwave intensity in the line of the atmosphere ozone at frequencies of about 110836.04 MHz during modifications of the Earth's ionosphere by powerful HF radio waves. Features of this phenomenon are the following:

The decrease of the ozone line spectral intensity is observed not only in a region located directly over the SURA facility but also in a region spaced of about 150 km and more to the south from it. The value of the ozone spectral intensity varies proportionally to the pump wave power. Quantity evaluation of vertical density profiles, made basing on ozone line spectral intensity measurements, gives a decrease by 18% in the ozone density at altitudes of about of 60 km relatively to its background value, which is of about 50% of its daily variations due to sunset and sunrise.

As interpretation of observably effect are considered:

1. Amplification of formation of negative ions mesospheric ozone owing to increase of electron temperature at heating the low ionosphere by high-power radio waves [1].
2. Action on mesospheric ozone by internal gravity waves generated in the ionosphere E-region heating by its HF heating [2-4].
3. Impact of ion chemistry on correlation between changes of mesospheric ozone and the total electron content in an ionosphere Impact of ion chemistry on correlation between changes of mesospheric ozone and the total electron content in an ionosphere [5]. It is necessary to note, that the total electronic contents appreciably changes at modification an ionosphere by powerful HF radio waves [6].

1. Kulikov Y.Y., Frolov V.L., Influence of HF powerful radio waves on the ozone number density in the Earth's atmosphere. The Seventh International Kharkov Symposium on Physics and Engineering of Microwaves, Millimeter, and Submillimeter Waves (MSMW'10) Proceedings, Kharkov, Ukraine, June 21 – 26, 2010. doi:10.1109/MSMW.2010.5545979

2. Grigor'ev G.I. and Trakhtengerts V.Yu., Emission of internal gravity waves during operation of high-power heating facilities in the regime of time modulation of ionospheric currents. *Geomagnetism and Aeronomy*, V. 39, No. 6, P. 90-94, 1999.

3. Kulikov Y.Y., Grigor'ev G.I., Krasilnikov A.A., Frolov V.L., Variations of mesospheric microwave emission by modification of the low ionosphere by powerful HF radio waves. *Radiophysics and Quantum Electronics*. V. 55, No. 1-2, P. 57-65, 2012.
4. Kulikov Y.Y., Frolov V.L., Grigor'ev G.I., Demkin V.M., Komrakov G.P., Krasilnikov A.A., Ryskin V.G., Response of the mesospheric ozone on low ionosphere heating by powerful HF radio waves. *Geomagnetism and Aeronomy*. V. 53, No. 1, P. 102-109, 2013.
5. Muscari G., Pezzopane M., Romaniello V., de Zafra R.L., Bianchi C., Fiocco G., On the potential impact of large electron concentrations on mesospheric ozone. *Mem. S. A. It. V 76*, P. 1007-1010, 2005.
6. Kunitsyn V.E., Padokhin A.M., Vasiliev A.E., Kurbatov G.A., Frolov V.L., Komrakov G.P. Study of GNSS-measured Ionospheric Total Electron Content variations generated by powerful HF heating. // *Adv. Space Res.*, 2010, doi: 10.1016/j.asr.2010.03.031.

Numerical simulation of the initial stage of the formation of large-scale cyclonic vortices in the vicinity of the intratropical convergence zone

I.V. Mingalev¹, N.M. Astafieva², K.G. Orlov¹, V.S. Mingalev¹, O.V. Mingalev¹, V.M. Chechetkin³

¹*Polar Geophysical Institute, Apatity, Russia*

²*Space Research Institute, Moscow, Russia*

³*Keldysh Institute of Applied Mathematics, Moscow, Russia*

The regional non-hydrostatic mathematical model of the neutral wind system of the lower atmosphere, developed earlier in the Polar Geophysical Institute, is utilized to investigate the initial stage of the origin of large-scale cyclonic vortices in the vicinity of the intratropical convergence zone. The mathematical model is based on the numerical solution of the system of transport equations containing the equations of continuity for air and for the total water content in all phase states, momentum equations for the zonal, meridional, and vertical components of the air velocity, and energy equation. The model produces time-dependent three-dimensional distributions of the atmospheric parameters in the height range from 0 to 15 km over a limited region of the Earth's surface. Simulations are performed for the cases when this region is intersected by the intratropical convergence zone. It was supposed that, at the initial moment, the intratropical convergence zone contains the convexity in the north direction, moreover, the zonal wind velocities at more northern latitudes relatively the centerline of the intratropical convergence zone are larger than those at more southern latitudes relatively it, with the west crook of the convexity being sharp while the east crook of the convexity being gently sloping. Simulation results indicated that the twin tropical cyclones were formed during the period for about three days. The cyclones were formed one after another in the course of time. The rotational center of the first cyclone is close to the northern edge while the center of the second cyclone is close to the southern edge of the initial intratropical convergence zone to a moment of 70 hours after the beginning of calculations. The radii of these cyclones are about 600 km. The horizontal wind velocity in the cyclones achieved values of 15-20 m/s during the period of about three days.

This work was partly supported by the RFBR grant 13-01-00063.

Simulation study of the mechanism of the formation of polar cyclones at high latitudes of the northern hemisphere

I.V. Mingalev, K.G. Orlov, V.S. Mingalev (*Polar Geophysical Institute, Apatity, Russia*)

To investigate the initial stage of the formation of polar cyclones at high latitudes of the northern hemisphere, the regional mathematical model of the neutral wind system of the lower atmosphere, developed earlier in the Polar Geophysical Institute, is applied. The mathematical model is based on numerical solving of non-simplified gas dynamic equations and produces three-dimensional distributions of the wind components, temperature, air density, water vapor density, concentration of micro drops of water, and concentration of ice particles in the height range from 0 to 15 km over a limited region of the Earth's surface. The dimensions of this region in longitudinal and latitudinal directions are 36° and 25°, respectively. The southern boundary of the simulation region was located at 55° N. It was supposed that, at the initial moment, this region is intersected by an arctic atmospheric front. Simulations were performed for various cases in which the initial forms of the arctic atmospheric front were different and contained convexities with distinct shapes, with the distributions of wind velocity in the vicinity of the arctic atmospheric front having been chosen different. Simulation results indicated that the origin of a convexity in the configuration of the arctic atmospheric front can lead to the formation of a polar cyclone during the period for about one day. The cyclone has a horizontal extent of about 1000 km. The horizontal wind velocity in this polar cyclone can achieve values of 15-20 m/s during the period of 25 hours. The simulation results show that the key factor in the mechanism of the formation of polar cyclones is the origin of a convexity in the configuration of the arctic atmospheric front. As a consequence, instability of the shear air flow arises. This instability leads to considerable transformation of the wind field. As a result, polar cyclones may be formed in the vicinity of the initial position of the arctic atmospheric front in the course of time.

This work was partly supported by the RFBR grant 13-01-00063.

On one kind of anomalies in angular distributions of the natural electromagnetic emissions in the ELF range from measurements in Lovozero observatory

V.V. Pchelkin (*Polar Geophysical Institute, Apatity, Russia*)

Using continuous measurements of magnetometers in Lovozero observatory (2006-2009 years), arrival directions of registered natural electromagnetic emissions in the ELF range were calculated and analyzed. Abnormality continuous tracks in angle distribution of high - amplitude signals were found. Estimate of azimuth and time range of this tracks have made. It was suggested that the cause of this anomaly is the thunderstorm activity near the observation point (up to 500 km).

Investigations of Antarctic stratosphere gas composition based on the high-resolution spectroscopy of the Moon during the lunar eclipse

O.S. Ugolnikov¹, A.F. Punanova², V.V. Krushinsky²

¹*Space Research Institute, Russian Academy of Sciences, Moscow, Russia*

²*Kourovka Astronomical Observatory, Ural Federal University, Ekaterinburg, Russia*

The work is devoted to the southern polar stratosphere investigations based on the high resolution spectroscopy of the Moon inside the umbra of the Earth. During the eclipse the Moon is emitted by the radiation refracted in the atmosphere of the Earth. The altitude and coordinates of the ray perigee are determined by the moon surface point position inside the umbra. The radiation transfer geometry is analogous to the space limb atmosphere measurements allowing to scan the distant atmosphere regions at several thousand kilometers from the observation point. Lunar eclipse is the only ground-based possibility to hold such measurements. Using the large-aperture astronomical technique and high resolution spectrographs we can hold the line-by-line analysis of the polar stratosphere components.

The work is based on the spectral measurements of the Moon near the southern umbra border during the total eclipse of December, 10, 2011. The radiation was transferred through the Antarctic stratosphere near the seasonal ozone depression, that makes the investigation especially interesting. The observations were held at 1.2-meter telescope of Kourovka observatory with fiber high resolution spectrograph (R about 30000). Measurements covered the spectral range from 450 to 780 nm and were calibrated by the analogous spectra of uneclipsed Moon and standard star. This allowed to hold the correct account of atmospheric lines above the observation point.

Observational spectra contain a lot of atmospheric lines (O_2 , O_3 , O_4 , H_2O , NO_2). Three oxygen bands (630, 690 and 765 nm) together with O_4 absorption features between 450 and 600 nm were used to retrieve the effective trajectory of the radiation transfer through the Antarctic stratosphere depending on the wavelength and estimate the influence of aerosol scattering. Other gases bands give the values of tangent column densities of these gases in the lower Antarctic stratosphere. The accuracy is especially high for ozone, since the observational range covers the majority of Chappius bands, where absorption by the tangent trajectory is very strong (up to a factor of 6).

The work is done with the financial support of Russian Foundation for Basic Research, grant No.12-05-00501-a.

Comparison of air quality in Moscow and London megacities

A.M. Zvyagintsev¹, I.N. Kuznetsova²

¹*Central Aerological Observatory, Dolgoprudny, Russia*

²*Hydrometeorological Research Center of Russia, Moscow, Russia*

Economic and social activities in megacities lead there to concentrated emissions of air pollutants. The negative impact of megacities on local air quality has long been recognized. We give an overview of air quality in two biggest European megacities: London and Moscow. Using long-term data bases we analyzed there periodical and aperiodical (trends) variations of trace gases (CO , $NO_x=NO+NO_2$, SO_2 and ozone) and aerosols (PM10 and PM2.5). Mean long-term diurnal and seasonal variations of concentrations of pollutants are presented. Concentrations of primary pollutants and aerosols at nearest (ca. 1 km) urban roadside and background stations may differ up 10 times and more, concentrations of secondary pollutant (ozone) may differ 2-3 times. The lowest concentrations of primary pollutants and highest ones of secondary pollutant are observed during weekends. In London remarkable decreasing of concentrations of most primary pollutants and some increasing of primary one are observed in the past 15 years, in Moscow no conclusion on long-term changes of concentrations of pollutants don't be done due to fewer period of observations and higher variations of concentrations of pollutants.

Сезонные вариации в различных компонентах вторичных космических лучей

Ю.В. Балабин, А.В. Германенко (*Полярный Геофизический институт КНЦ РАН*)

В лаборатории космических лучей в течение нескольких лет ведется непрерывный мониторинг различных компонентов вторичных космических лучей. К настоящему времени помимо стандартного нейтронного монитора (18-НМ-64) работают детектор гамма-квантов на сцинтилляционном кристалле, бессвинцовая секция нейтронного монитора (БСНМ), детекторы заряженной компоненты (ДЗК) и тепловых нейтронов (ДТН). Сцинтилляционный детектор регистрирует кванты с энергиями от 20 кэВ до 5 МэВ, нейтронный монитор (НМ) чувствителен к нейтронам с энергиями более 50 МэВ, БСНМ – к нейтронам с энергиями сотни кэВ – единицы МэВ, ДТН – тепловые нейтроны (порядка 0.03 эВ), ДЗК регистрирует все заряженные частицы (мюоны, электроны, позитроны) с энергиями более 2 МэВ.

Данные со всех приборов поступают в общую систему регистрации. Их анализ за последние несколько лет показал наличие сезонных вариаций в некоторых компонентах космических лучей. В ряду «нейтронный монитор – бессвинцовая секция – детектор тепловых нейтронов» амплитуда вариации нарастает с уменьшением энергетического диапазона принимаемых нейтронов. На НМ вариация нулевая, на ДТН – около 10 %. Плотность потока нейтронов больших энергий определяется космическими лучами, тогда как нейтроны меньших энергий получаются в результате торможения высокозернистых, следовательно, их поток существенно зависит от условий состояния среды. Наибольшая по амплитуде и четко выраженная вариация наблюдается в канале сцинтилляционного детектора – более 20 %. Гамма-излучение в приземном слое атмосферы возникает как тормозное излучения энергичных электронов, появляющихся от распада мюонов, и можно предположить, что электрическое поле атмосферы влияет на полную энергию мюонов, что, в конечном счете, сказывается на потоке гамма-квантов.

Баланс энергии и происхождение возрастаний приземного гамма-фона

Ю.В. Балабин, А.В. Германенко, Э.В. Ващенюк, Б.Б. Гвоздевский (*Полярный Геофизический институт КНЦ РАН*)

В течение 2012 года было продолжено исследование вариаций приземного гамма-фона, связанных с атмосферными осадками. В настоящей работе представлены результаты ряда новых экспериментов, проведенных на усовершенствованной системе регистрации гамма-излучения. Основой системы является набор из трех приборов для измерения радиации: малого и большого сцинтилляционных детекторов на основе кристаллов *NaI(Tl)* а также детектора заряженных частиц на основе счётчиков Гейгера-Мюллера. Малый сцинтилляционный детектор имеет размеры $Ø63 \times 20$ мм и энергетический диапазон 20-300 кэВ, большой – размеры $Ø150 \times 100$ мм и энергетический диапазон 0.2-5 МэВ. С помощью большого сцинтилляционного детектора и многоканального амплитудного анализатора непрерывно ведутся измерения дифференциального спектра гамма излучения с временным разрешением в 30 минут в диапазоне 0.2-5 МэВ. Была проведена серия экспериментов, состоящих в том, что на длительный срок один из детекторов обкладывался со всех сторон свинцовыми кирпичами (закрытое состояние). Малый детектор под свинцовой защитой не показывает возрастаний во время осадков, в то время как в открытом состоянии регистрируются возрастания практически при каждом случае выпадения осадков. Детектор заряженных частиц, как в открытом состоянии, так и в закрытом не обнаруживает никаких возрастаний. Большой детектор в открытом состоянии показывает такие же вариации гамма-фона, как и малый, однако, и в закрытом состоянии обнаруживаются вариации, связанные с осадками, но амплитудой в несколько раз меньше. Измерения дифференциальных спектров гамма-излучения на большом детекторе в закрытом и открытом состояниях показывают, что форма спектров добавочного излучения, вызывающего возрастания, не изменяется, лишь уменьшается абсолютное значение потока.

Толщина свинцовой защиты (5 см) такова, что ни электроны, ни гамма-кванты до энергий в десятки МэВ проникнуть через нее не могут. Следовательно, результаты серии проведенных экспериментов указывают на то, что в наблюдаемых вариациях гамма-фона их первичным источником являются мюоны, рождающиеся в атмосфере от первичных космических лучей и обладающие высокой проникающей способностью. Также следует вывод, что вариации обусловлены той же причиной, что и подобные события в умеренных и тропических широтах – доускорение мюонов в электрических полях дождевых облаков. Именно мюоны являются теми частицами, которые набирают дополнительную энергию в электрических полях в облаках и переносят ее в нижние слои атмосферы.

Исходя из результатов наблюдений был подсчитан энергетический баланс. Дополнительный поток энергии, возникающий при возрастании гамма-фона, составляет около 23 кэВ·см⁻²·с. При существующей плотности потока мюонов у земли и средней толщине облака такой дополнительный поток энергии обеспечен будет при напряженности поля в облаке всего 1.2 кВ/м. Это вполне реальная величина, большинство измерений электрического поля в облаках дают величину 2-5 кВ/м.

Возрастания гамма-фона и состояние атмосферы в приземном слое

А.В. Германенко, Ю.В. Балабин, Э.В. Ващенюк, Б.Б. Гвоздевский (*Полярный Геофизический институт КНЦ РАН*)

На основе многолетней базы данных, накопленной на станции космических лучей в Апатитах и содержащей сотни событий с возрастаниями гамма-фона в приземном слое атмосферы, проведено исследование с целью поиска возможных корреляций этих возрастаний с состоянием атмосферы. Подавляющее большинство этих события сопровождаются осадками и плотной облачностью, однако, ранее такое заключение основывалось на субъективных оценках. Подробная база метеоданных, содержащая параметры атмосферы и метеоусловия за период с начала 2010 года по 2013 год, была взята с сайта RP5.RU. Использовано около десятка параметров, описывающих метеоусловия и состояние атмосферы, которые могли бы оказаться важными факторами, влияющими на возрастания. Выявлена корреляция между скоростью ветра и высотой нижней границы облачности, а также от типа облачности. Для возрастаний характерна, помимо осадков, тихая погода и низкая облачность. Бури, штормы, метели, а также мелкая морось не сопровождаются возрастаниями гамма-фона. Проведенное исследование подтверждает и обосновывает на фактическом материале предположение, что для событий возрастания важным фактором является состояние именно приземного (до 600 м) слоя атмосферы.

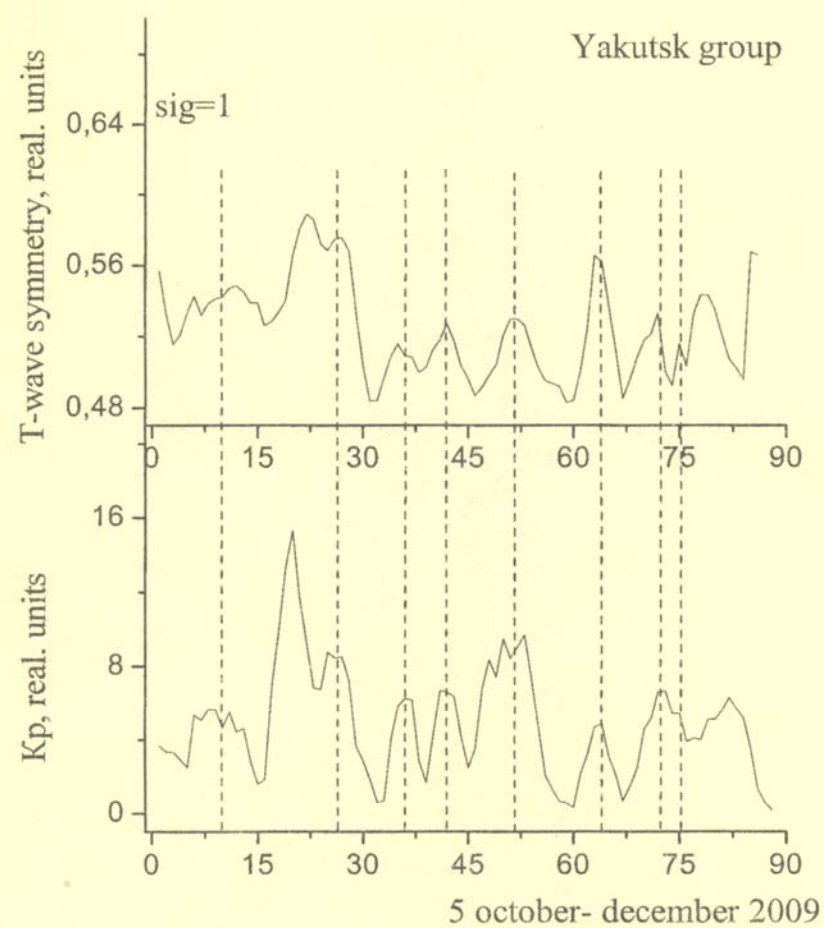
Метод расчета радиационных потоков в атмосферах Земли и других планет, удобный для применения параллельных вычислений

И.В. Мингалев, Е.А. Федотова (*Полярный геофизический институт КНЦ РАН, Россия*)

В данной работе излагается новый метод расчета радиационных потоков в планетных атмосферах с учетом собственного излучения атмосферного газа и с учетом молекулярного и аэрозольного рассеяния. Метод использует традиционное 1-мерное приближение горизонтально однородной атмосферы. Метод основан на представлении поля излучения в узком спектральном интервале в виде суммы излучения не испытавшего рассеяния, излучения, испытавшего однократное рассеяние, излучения, испытавшего двукратное рассеяние, и так далее до излучения, испытавшего m -кратное рассеяние включительно. При этом число m определяется необходимой точностью в расчете скоростей нагрева. Проведенные тестовые расчеты показали, что для точности 2% в расчете скоростей нагрева-охлаждения атмосферы как правило достаточно учитывать 50 порядков рассеяния, а учет 100 порядков рассеяния обеспечивает как правило точность не хуже 1%. Данный метод расчета достаточно прост в программной реализации и позволяет эффективно использовать параллельные вычисления при расчете радиационных потоков в одном спектральном интервале, чего не позволяет например метод дискретных ординат. Главная особенность данного метода состоит в том, что он допускает эффективное применение параллельных вычислений как на обычных процессорах, так и на графических процессорах фирмы NVIDIA.

Работа выполнена при финансовой поддержке гранта РФФИ № 13-01-00063.

Heliosphere



Biological effects, neutron fluxes and ambient equivalent doses near the Earth surface during GLE events in October 1989

N.K. Belisheva¹, E.A. Maurehev², E.V. Vashenyuk²

¹*Kola Science Centre RAS, Apatity, Russia*

²*Polar Geophysical Institute KSC RAS, Apatity, Russia*

A direct evidence of biological effects of solar cosmic rays (SCR) is demonstrated in experiments with three cellular lines growing in culture during three events of Ground Level Enhancement (GLEs 43,44,45) in the neutron count rate detected by ground-based neutron monitor in October 1989. Various phenomena associated with DNA lesion on the cellular level demonstrate coherent dynamics of radiation effects in all cellular lines coincident with the time of arrival of high-energy solar particles to the near-Earth space and with the main peak in GLEs. Cluster damages, local clusters of the disorders of nuclear structure such as multinuclear cells (MNC), gigantic cells (GC), apoptosis, necrosis, cell aggregation and “free space” around MNC and GC were observed in the all cellular lines. These results were obtained in the course of six separate experiments, with partial overlapping of the time of previous and subsequent experiments, which started and finished in the quiet period of solar activity (SA). A significant difference between the values of MNC in all cellular lines in the quiet period and during GLE events indicates that the cause of radiation effects in the cell cultures is an exposure of cells to the secondary solar CR near the Earth’s surface. Time coincidence of numerous disorders of nuclear substances in three cell lines with solar proton events and Ground Level Enhancement gives the basis to consider the increase of secondary component of SCR as a reason of discovered phenomena. For examination of this version, the calculation of the cascades of particles in the atmosphere on the level of Apatity (950 g/cm³) by using the PLANETOCOSMICS 2.0 package based on GEANT4 (Maurehev et al, 2011) has been performed. Since the flux of particles at sea level is more than 97% neutrons, we took into account only the neutron fluxes. Two-component structure of increase of high energy particles were detected in solar proton intensity associated with GLE 43, 44, 45. This structure included a fast component and a delayed component, which together contributed to increase in proton intensity. In this research, neutron fluxes generated by fast and delayed components of solar protons were considered separately. Spectrum of the secondary neutrons typically consists of four major components: “cascade peak” with energy at about 100 MeV, when a minimum of cross-sections under inelastic neutron scattering with the nuclei of the matter show a minimum (Abfalterer et al., 2001); “evaporation peak” at energies of about 1 MeV, due to emission of evaporation neutrons from nuclei excited by collisions with other particles; third peak are produced by thermalized neutrons at energies of low 10 keV/tens of meV; fourth component is presented by epithermal neutrons are responsible for the shape of the spectrum between the thermal and the evaporation peak. According to “Summary of Recommended Radiation Weighting Factors and Q–L Relationships” (IAEA, Annex I, 1999) we have separated the neutron spectrum respectively to energy ranges and to weighting factors. The drastic increase of neutron fluxes relatively typical level in the range of fast and medium neutron energy with weighting factor 20 was found for fast component of GLE 45. The similar neutron spectra with drastic increase of neutron flux was observed for delayed component of GLE 43. For explanation of multiple radiation effects in cellular cultures during GLEs, the contribution of the neutron fluxes with certain energy range from fast and delayed components and, respectively, Ambient Dose Equivalent (ADE) were calculated. The total number of neutrons generated by a fast and delayed components during GLE 43 amounted to 13801,7 n/cm²/h with ADE 3,17 microSv cm²/h; during GLE 44 - 5714,10 n/cm²/h with ADE 1,32 microSv cm²/h; during GLE 45 - 19807,1 n/cm²/h with ADE 4,56 microSv cm²/h. The sum of ambient dose equivalent during three days from three cases of GLEs amounted about 217 micro SV cm²/day, that is almost half of daily doses which were measured on the board of space stations (Reitz et.al., 2005; Semkova et al,2012). The sum of calculations gives only preliminary estimations of number of particles and ambient dose equivalent during GLE’s events. Nonetheless one can see that about 40000 neutrons per hour passed the cellular monolayer of every cellular lines during three GLE events. It is mean, that in average, every second cell were passed by one or several particles. The increase of neutron fluxes during three GLEs in the range with high Linear Transfer Energy (LTE) is evidence, that charged particles, gamma rays, heavy recoils which were generated in result of neutron interactions with carbon, nitrogen, oxygen could be responsible for phenomena in cellular cultures during GLEs. These components could be generated in result of neutron interaction with matter according to neutron energy and composition of biological substances. The type and multiplicity of finding phenomena in cellular cultures during GLE’s have demonstrated that revealed effects could be arise in result of interactions of particles and recoils of the high LET with cellular substance. Presented results are the first direct and visible evidence of biological effects of cosmic rays in the ground-based experiments.

About interrelation of biochemical and physiological indicators with the cosmophysical factors, the system of data processing of Deep Data Diver revealed with use

E.S. Gorshkov, V.V. Ivanov (*St. Petersburg Branch of Institute of terrestrial magnetism, ionosphere and distribution of radio waves of the Russian Academy of Sciences, 199034 St. Petersburg, Mendelevskaya St., 1*)

Carrying out monitoring researches of the biochemical mechanism of adaptation of the person to extreme conditions of Antarctic was accompanied by simultaneous registration of a number of indicators - physiological, psychophysical, and also cosmophysical factors and meteorological data. Selection of most informative of them by the analysis of charts of dispersion of each couple of variables, their regression curves with confidential intervals of 95% and levels of correlation communication between indicators is made. As dependent variables quantities (\sum_{SH} , \sum_{ur}) and concentration (C_{SH} , C_{ur}) thiols and urochrome in urine were accepted. It is shown that practically all physiological (except for pulse rate) and cosmophysical (except components of a magnetic field of Earth) have distributions other than the normal. Correlation communications were considerably shown only in group of biochemical indicators. Possibilities of use of various methods of the mutual analysis of various parameters are investigated. Their main conceptual restriction, consisting that they allow to find only numerical dependences between variable (groups), instead of internal causal relationships lying in their basis is revealed. Use of the Data mining methods (detection of knowledge in a database) and, in particular, one of its systems realizing the new principle and technology of search of logical regularities in studied data (Deep Data Diver), allowed to solve the problem designated above. Thus the Deep Data Diver system is intended for search in diverse data of if-then of rules, at which assessment two characteristics - rule R_{ij} accuracy (a share of cases of B_j among A_i cases) and completeness (a share of cases of A_i among B_j cases) are used. The analysis of interrelations of each couple of variables is made: biochemical indicators, on the one hand, and physiological, psychophysical - with another. For a number of biochemical indicators logical laws (according to the rule Deep Data Diver), reliable and unambiguous (owing to manifestation of characteristics of each law in the only interval of the analysis) are defined. It is shown that to low levels of biochemical indicators there correspond high values of the pulse rate (PR), the breath frequency (BF), arterial pressure, etc. And to high levels - low values of physiological and psychophysical indicators. Ranges of values of the biochemical indicators characterizing norm of a functional condition of thiol-urochrome system of an organism are determined. Ranges of values of the biochemical indicators characterizing norm of a functional condition of thiol-urochrome system of an organism are determined. It appeared that to them there correspond the intervals including values of medians of indicators: $\sum_{SH} = 27.5 \pm 1.5$, $\sum_{ur} = 19.5 \pm 1.4$, $C_{SH} = 45.5 \pm 2$, $C_{ur} = 36.5 \pm 3.5$, state of emergency $PR = 63$ beats/min, $BF = 9.2$ beats/min. Thus values of state of emergency, PR , BF and their relation of $PR/BF = 6.85$ are related to the optimum organization of warm activity and to a "gold" proportion. The analysis of interrelations of each couple of variables is made: biochemical indicators, on the one hand, and cosmophysical factors and meteorological data, - with another which allowed to receive the regularities defining new elements of relationship between them. As the oxidability index of thiols I_{ok} is, some kind of, criterion of an assessment of oxidation-reduction balance in a live organism, search of reliable internal communications between it and studied indicators, cosmophysical factors and meteorological data with use of the same elements of technology of logical search of regularities (Deep Data Diver) is carried out. The interesting facts defining relationship between them are received. In particular, it appeared that optimum values of state of emergency, PR , BF and their relation are connected with a minimum level of I_{ok} and value of duration "individual minute", equal 60 with, i.e. average norm. Thus, use of new approaches to processing of a multidimensional database from a technique of the Data mining, realizing the principle and technology of search of logical regularities in studied information (Deep Data Diver), allowed to find a number of internal communications and the regularities concerning influence of cosmophysical and other factors on a condition of thiol-urochrome system of a human body and its adaptation opportunities. The received facts can be used, in some cases, for forecasting of a condition of system of antioxidant protection (the thiol status of an organism) in which mechanism the leading role is allocated for thiol connections.

Cosmophysical conditionality of fluctuations of a ratio of pulse rates and breath in the conditions of Antarctic

V.V. Ivanov, E.S. Gorshkov (*St. Petersburg Branch of Institute of terrestrial magnetism, ionosphere and distribution of radio waves of the Russian Academy of Sciences, 199034 St. Petersburg, Mendelevskaya St., 1*)

Dynamics of the relation of pulse rate to the frequency of breath of PR/BF registered at one person (on the average - 7-8 times per day) during 29.01.2001-26.01.2002 at the polar Wostok station (Antarctica) is investigated. Range of change of the relation made 5.0 - 13.5 (average value - 7.0, a standard deviation of 0.92 or 13% from an average). The law of distribution of an indicator is close to the normal. Daily distribution of an indicator has wave character. Authentically (in relation to a confidential interval of CI-95) minima (2-4, 10-12 and 16-18 hour) and maxima (0-2,

8-10 and 14-16 hour) are shown. The norm of the relation of PR/BF, by a way of comparison to the similar relation of biochemical indicators, - concentration thiols and urochrome which registration was carried out to the same time is determined. The average level of PR/BF equal 7 ± 0.5 , can be conditionally taken for individual norm. And regularity violations at PR/BF exit out of the specified limits ($PR/BF < 6.5$ or $PR/BF > 7.5$) can be (as a first approximation) a symptom of dysfunction or influence of an external factor. It is shown that changes of average daily data have oscillatory character. Spectral Fourier analysis revealed existence in a range of the relation of the main harmonicas with the periods of 56.89, 51.2, 64.0, 30.12, 39.38, 46.55, 42.67 and 34.13 days. It is possible to see that some of the periods are very close on the values to the periods: variations of indicators of a condition of solar and geomagnetic activity, fluctuations of the relation of thiols and urochrome concentration, variations of the main inequalities in the geocentric ecliptic longitude of the Moon, caused by indignations from the Sun. In particular, rhythms of 30.12 and 34.13 days evictions close to the period 31.8 days are observed. One of rhythms of solar and geomagnetic activity of 44.0 ± 1.0 days is defining in PR/BF fluctuations and is shown in a range in the form of harmonicas with the periods of 39.38 and 42.67 days. Dynamics of averages for a week of levels of the relation of PR/BF will well be coordinated with such seasonal factors, as change of polar day and polar night. On the border defining the beginning of polar night, $PR/BF \sim 6$ also has the minimum value. With the advent of the Sun over the horizon and the beginning of polar day level of the relation reaches a maximum – about 9. The analysis of correlation communications of average daily fluctuations of PR/BF with variations of cosmophysical factors of the electromagnetic (solar activity - SA, etc.) and not electromagnetic (time equation - TE, the equation of equinoxes, Moon phases, etc.) nature, and also meteorological data (temperature, humidity of air, etc.) showed the correlation (exceeding on the module 0.5, $p < 0.05$) between PR/BF, on the one hand, and SA ($r = 0.61$), TE ($r = -0.63$), temperature ($r = 0.56$) and humidity of air ($r = 0.53$), - with another. Comparison of the 1st making TE and polynomial trend of average daily data on PR/BF relation is carried out. It is shown that both curves are almost in an antiphase, however changes of a physiological indicator happen to lag on a phase approximately for a month from changes of the 1st component of TE. After comparison of the 2nd component of TE and the new polynomial trend defined for a deviation of an indicator of PR/BF from the first polynomial trend, it will appear that both curves almost coincide on a phase. However and in this case changes of a physiological indicator happen to lag on a phase approximately for a month from changes of the 2nd component of TE. Comparison of a deviation of PR/BF from the sum of polynomial trends and some cosmophysical factors is carried out. By comparison to SA ($r = 0.24$) appeared that correlation between a physiological indicator and SA increased in process of approach and approach of polar day: for an interval from the middle of polar night until the end of work the coefficient of correlation made 0.33, at a stage - the termination of polar night – the work end - 0.52. PR/BF change in bathing days (more than 40) is analysed. Dynamics of an average indicator for time of carrying out "action" with 9 to 12 and with 13 to 16 has similar character. In both cases PR/BF level increase to a maximum with 7.0 to 7.3 and 7.7 came after a capture of two tests of urine. Decrease in the PR/BF level to initial value happened approximately in 8 hours after influence "thermal" a factor. However the PR/BF level after influence of a studied factor in the second case exceeds norm (7.5). Thus, the relation of PR/BF testifies to existence of communication of an indicator with environment influence. In particular, with variations of a gravitational field, with the solar and lunar phenomena, change of seasons of year. There is a possibility of the objective and quantitative analysis of reaction of an organism on cosmophysical factors.

The interrelationship of the physiological parameters and effects of heliogeophysical agents

A.A. Martynova, N.K. Belisheva, S.V. Pryanichnikov, V.V. Pozharskaya (*Kola Science Centre RAS, Apatity, Russia*)

The task of the study was to assess the interrelationship of psychophysiological indicators of the body state and the revealing of correlations between the dynamics of psychophysiological state and variations of heliogeophysical agents. The study was conducted on a group of volunteers (12 men) aged 19-37 years. Psychophysiological parameters of the body state were daily registered for 25 days (24.09.2012 – 10.18.2012). The special indices of Heart Rate Variability (HRV) measured with using of a non-invasive analyzer "OMEGA-M" were selected in the research. In these indices were included such indicators as magnitudes of Adaptation (A), Arterial Blood Pressure (systolic - ABPs and diastolic - ABPd), Heart Rate (HR). ABPs, ABPd, and HR were recorded in the supine and sitting. In addition, the duration of the individual minute (DIM) were evaluated. DIM is usually considered as a psychophysiological indicator which reflects the integral functional state of human body, as well as exogenous and endogenous influences and the direction of adaptation. Along with this, the indices of the situational and personal anxiety (SA and PA, respectively) were calculated (by the Spielberger-Khanin) and indicators of self-sensation of self health (S), Activity (Act) and Mood (M) were estimated by using "SAM" method. The indices of geomagnetic activity (GMA) (<http://www.sgo.fi/>), neutron count rate (neutron monitor station in Apatity, PGI KSC RAS), indices

Heliosphere

of the Solar activity and the phases of the Moon were used for correlations with psychophysiological parameters. The results shown that magnitudes of DIM varied widely in the fairly homogeneous sample of healthy mans in the range of individual values from 52.4 ± 5.7 to 135.7 ± 4.2 at average value for a sample of 75.1 ± 2.0 (229 measurements). Such variability of the DIM, probably, could reflect different levels of adaptation and different psychophysiological state of the separate persons. Shown that the value of the DIM in healthy adult persons is stable indicator which proportional to the degree of emotional stress, while the DIM is significantly decreased under low adaptation. This is explained that the DIM correlates with changes of the somatic and vegetative indicators of the body state and therefore, it reflects to some extent, the adaptation of the body (N. Moiseeva, 1989). In this study it was revealed that the DIM significantly correlates with ABPs in the sitting position ($r = -0.57$, $p < 0.05$), with ABPd in supine and sitting ($r = -0.50$, $r = -0.63$, respectively, $p < 0.05$), with HR as in supine and sitting ($r = 0.73$, $r = 0.43$, respectively, $p < 0.05$), with the level of SA and PA ($r = -0.59$, $r = -0.49$, respectively, $p < 0.05$), with indices of S, Act and M ($r = 0.46$, $r = 0.74$, $r = 0.48$, respectively, $p < 0.05$), as well as with the heliogeophysical indices: with the increase of Moon's disk ($r = 0.47$, $p < 0.05$), with the flux of the solar X-rays (1-8 Å) and with the Wolf numbers ($r = -0.51$, $r = -0.56$, respectively, $p < 0.05$). Significant correlations were found between the ABPs in supine and sitting ($r = 0.54$, $r = 0.41$, respectively, $p < 0.05$), the PA ($r = -0.46$, $p < 0.05$), the M ($r = 0.48$, $p < 0.05$) and GMA indices. Indicator of adaptation (A), was associated with ABPd and HR in a sitting position ($r = 0.40$, $r = -0.41$, respectively, $p < 0.05$), as well as with X-rays of the Sun and the Wolf numbers ($r = 0.41$, $r = 0.45$, respectively, $p < 0.05$). Thus we have shown: 1) the psycho-physiological state of the body in a large extent is determined by hemodynamics, in particular, by the blood pressure and by the heart rate, that was manifested in the DIM: decrease of the systolic and diastolic blood pressure leads to an increase of the DIM, 2) DIM positively correlates with self-sensation of self health (S), Activity (Act) and Mood (M) and negatively, as SAN, with personal anxiety. That is, the increase of S, Act, M, leads to an increase of DIM and decrease of anxiety 3) Such indices as blood pressure, heart rate, SAN, DIM, situational and personal anxiety, to some extent, are controlled by the heliogeophysical agents which can modulate the functional state of the body. What is the contribution of internal and external agents in adaptation, stability and vulnerability of the human body should be determined in the further studies.

Frequency distribution of deaths in psychoneurological boarding by phases of the solar cycle and the relationship of mortality with variations of geophysical agents

R.E. Mikhailov¹, H.K. Belisheva¹, R.G. Novoseltsev², S.D. Chernej²

¹*FGBUN Kola Scientific Center*

²*State regional stationary establishment of social service of system of social protection of the population, the Apatity Psychoneurological Internat*

In this study we investigated the frequency distribution of deaths by phase cycle of solar activity (SA) and the relation of mortality with variations of geophysical agents. Was used the health-statistics on the dates of birth and death in patients of psychoneurological boarding from November 1984 to December 2009., and some indicators characterize SA: Wolf numbers (W), the mean value of the GMP nT ($|B|$), Magnitude of Average Field vector GMP (B), the variability of intensity and vector GMP (sigma $|B|$ and sigma B, respectively), the indices of the GMA: Kp, AE, ap, PC (N), solar radio emission with a wavelength of 10.7 cm (f10.7). In the analyzed period at the boarding occurred 967 deaths, of which 70% are related to cardiovascular disease (CVD). In work results of the correlation analysis ($p < 0.05$) showing a significant association of average mortality from CVD with some indicators SA and GMP. Also, a comparative analysis of two samples of subjects born in the years with varying levels of SA, it was shown that people born in years with high SA are more vulnerable to the effects of variations in geophysical agents than those born in years with low SA. It has been shown that men are more sensitive to variations of geophysical agents than women.

Evaluation of the natural ionizing radiation genotoxicity on the meristematic cells of the *Vigna radiata*

D.A. Petrashova, N.K. Belisheva, N.A. Melnik (*Department of Medical and Biological Problems of human adaptation in the Arctic, KSC of the Russian Academy of Sciences, e-mail: petrashova@admksc.apatity.ru*)

Underground mining of ores containing natural radionuclides such as uranium, thorium, radium, is dangerous to the health of workers. The aim of our study was to determine the genotoxic effects of the natural ionizing radiation sources formed during underground mining for the extraction of ore loparite (Murmansk region). For indication of

genotoxic effect of natural radiation the ana-telophase method for cytogenetic analysis of meristematic cells (*Vigna radiata* (L.) R.Wilczek) was used.

Seeds (in triplicate) were placed on 50 pcs. in Petri dishes with moist filter paper, where they were held for 5 days under the mine conditions at to $t = 7$ °C. Control samples were held at the same temperature for the same time in the laboratory in Apatity. Sprouting was carried out in the dark to avoid the effect of the light on the rhythm of mitotic activity. Procedure of root fixing and preparing of sample for analysis were conducted according to Butorina and al (2008). Microscopic analysis was performed using light microscope AXIOSTAR PLUS (Karl Zeiss, 15x40). Eight slides were prepared from each Petri dish and 1000 cells were evaluated per slide to determine mitotic index (MI) and cytogenetic pathologies. Measurement of natural radionuclides (232Th и 238U, 40K) on the ore body surface and in different compartments in the Lovozero district mine shaft (Revda) have shown that exposure dose at the ore body exit surface was 1.9 mSv/h while the gamma-ray background and the exposure rate throughout the mine were in the range of 0.5-1.5 mSv/h in the absence of tehnogenic radionuclides (137Cs, 90Sr et al). The daughter products of 226Ra, 228Ra, 224Ra such as radon, thoron, RaA, RaV and RaS were found in the airspace of all mine sections. The maximum concentrations of radon (20,000 Bq/m³) were found at the working surface and in poorly ventilated areas (Петрашова и др., 2011). The Petri dishes with seeds of *V. radiata* were incubated on the working surface with maximum concentrations of radon inside of mine. The results are presented in the table. The cytotoxic effects in the *V. radiata* meristem are manifested in mitotic index reducing, lagging chromosomes, bridges in telophase, chromosomes fragmentation and chromosomes stickiness, multiple and multi mitosis.

Table. Mitotic index and cytogenetic pathologies

Data	Control 1	Exposure 2	Exposure 3	Exposure 4
MI, %	4,6±1,27	3,2±0,71	2,3±0,56	1,2±0,27
Percentage mitosis abnormalities, %	9,3±0,29	4,1±2,08	21,7±6,20	39,9±12,54

It was found that the mitotic indices and the number of violations of mitosis were different in the seed from different Petri dishes despite the fact that dishes with seed were located on the same place of the mine. Such differences are likely due to the fact that the samples received the different radiation doses in the result of exposure to the mixed and heterogenic kind of radiation.

According to published data, the increase of the number of pathological mitoses is observed under radiation damage and viral infections. In the cases of the exposure of ionizing radiation on human body, a dramatic reduction in mitotic activity with its subsequent recovery could be observed. In such situation the increase of the number of the abnormal mitosis can be revealed during proliferation recovery.

The results presented consistent with the received data on the cytogenetic abnormalities in buccal epithelium of miners working in the same conditions of mixed ionizing radiation.

Psychophysiological effects of heliogeophysical agent

S.V. Pryanichnikov, N.K. Belisheva, A.A. Martynova, V.V. Pozharskaya (*Kola Science Centre RAS, Apatity*)

The study of the influence of heliogeophysical agents on the human body took on a mass character. However, "individual characteristics, the nature and expression of the heliomagnetic reactions and their role in the psychosomatic state, in the dynamics of adaptation...as well as the neurophysiological mechanisms of individual adaptation to high latitudes ... still not well understood" , (Soroko, 1985; Shepovalnikov, Soroko, 1992). Despite on the fact that the geomagnetic field (GMF) disturbances is considered as a hazard factor (Breus et al., 2002), It was be shown that the prevalence of the paradoxical reactions, confusion (Belisheva et.al., 1995), as well as the psychopathic reactions (Belisheva, Kachanova, 2002) increases in the lack of geomagnetic activity (GMA). In order to understand the mechanisms by which heliogeophysical agents affect on an individual level, and thus to predict the consequences of these impacts for a particular person, the prolonged multidimensional study need to conduct. The analysis of the link between the psychophysiological dynamics and the variations of the cosmophysical environment characteristics should be included in such study. The aim of this study was to reveal the link between the psychophysiological dynamics of the individual body state and variations of the heliogeophysical agents. The study was performed on male volunteers (12 men, mean age 25 years), for 25 days (09.24.2012 – 10.18.2012). In the course of the daily research of the psychophysiological parameters of the examinees, the indices of situational and personal anxiety (SA and PA, respectively) were estimated by the Spielberger-Hanin method; the self-sensation of self health (S), Activity (Act) and Mood (M) (SAM method) were also calculated. In addition, magnitudes of the rate of adaptation (A), of the psycho-emotional state (PS), of the integral health index (IH), of the mean cardiac interval (RR), of the regulatory system stress index (IS), of the high-frequency (HF), low frequency (LF), of the ratio of the

Heliosphere

frequency bands (LF / HF) and the total frequency range (Total) in the heart rhythm were estimated by using of the "OMEGA-M" analyzer. To find the correlation between the psychophysiological parameter dynamics and the indices of the heliogeophysical agents, the data of the local GMA (<http://www.sgo.fi/>), of the neutron count rate (Apatity, PGI KSC RAS), the solar activity, of atmospheric pressure and temperature were used. The results shown that the magnitude of the cardiac interval (RR) is a main indicator of the body functional state, which determines the psychophysiological state. In particular, it was found that magnitudes of the A, IH, HF increase with increase of duration of the R-R interval. However, increase of R-R interval is accompanied by increase of the anxiety, (SA and PA) and by the decrease of the health level (S) and the activity (Act). Can be assume, that the magnitude of the RR interval has threshold at which the signs of correlations with some physiological parameters could be reversed. The negative correlations with GMA (Ak-average index for day of GMA) and the positive correlations with the Wolf numbers were also found for the RR interval ($r = -0.42$ and $r = 0.45$, respectively, $p < 0.05$). The need to study the individual reactions on the GMA was confirmed by the detail analysis of the correlations between anxiety and GMF variations for every person. It turned out that 16.7% persons had no significant correlations between the anxiety and GMA; 41.6% persons had negative correlations ($p < 0.05$) between the situational anxiety (SA) and GMA, that is when the GMA increases, the SA decreases. The personal anxiety (PA) of 25% persons also decreases with increasing of GMA. And the anxiety of 16.7% persons increases with increasing of GMA. Thus, the prediction of personal psycho-physiological reactions to the act of the heliogeophysical agents requires a detailed study of individual neurophysiological mechanisms which mediates the impact of environment on the body..

Impact of solar and volcanic activity on the growth of pine trees at Kola Peninsula over the last 560 years

O.I. Shumilov, E.A. Kasatkina and A.G. Kanatjev (*Institute of North Industrial Ecology Problems, Kola Science Center RAS, Apatity, Russia*)

In the paper we analyzed the external factor (solar activity, volcanic eruptions) influence on tree growth at the Kola Peninsula, northwestern Russia. *Pinus sylvestris* L. (Scots pine) tree-ring chronologies collected nearby the northern timberline (68.63N, 33.25E) include the oldest (1445-2005 AD) living pine tree found up to date in the Kola Peninsula. A total of 18 living trees *Pinus sylvestris* were sampled taking two cores. Tree rings measured with a precision of 0.01 mm by using an image analysis system (scanner and relevant software). The samples were cross-dated using standard dendrochronological practices and the COFECHA program. A negative exponential curve was used to remove the age trend from individual annual ring series prior to construction of the chronology using the ARSTAN modeling. It was shown that the past climatic variations in the Kola Peninsula were fairly strongly connected to solar variability and volcanic activity. A superposed epoch analysis of 18 large (Volcanic Explosivity Index, $VEI > 5$) volcanic events revealed a significant suppression of tree growth for up to 8 years following volcanic eruptions. The data analysis enabled us to get some conclusions on the past climate variations and to demonstrate the relation of global and regional climatic variations in the European North.

Space weather and injury rates among people living and working behind the Polar Circle

O.I. Shumilov¹, E.A. Kasatkina¹, T.B. Novikova² and A.V. Chramov³

¹*Institute of North Industrial Ecology Problems, Kola Science Center RAS, Apatity, Russia*

²*Main Hospital, Kola Science Center RAS, Apatity, Russia*

³*Baltic State Technical University, S.-Petersburg, Russia*

In the work we considered the traumatism level of employers working at the joint stock company Apatit, the largest mining and concentrating enterprise in Europe and Russia, for the period 2000-2010 years. The enterprise is located in twin towns Kirovsk and Apatity (67.58 N; 33.31 E) right at auroral zone of geomagnetic activity. It was shown that the injury rate resembles that of suicides for peoples living in Kirovsk (not only miners). In a seasonal distribution one can select several clear occurrence maxima: in March-April, June-Jule, September-October and December-January. The first three maxima coincide with that in the seasonal distribution of the most intensive geomagnetic ($Ap > 150$ nT) storms for the period considered. The forth winter maximum coincides to the maximum in the seasonal distribution of cardiovascular diseases in Kirovsk and seems not to be connected to geophysical distribution and takes place during the hardest life period of people living far in the North (dark and cold Polar Nights). Analysis of some concrete geomagnetic storms and trauma appearance behind the polar circle supports above mentioned connection between geomagnetic disturbances and extreme situation events. The conclusion may be used in preventive measures of traumatism taking into account the world wide tendency of spreading economic activity to the Arctic (and possibly Antarctic) region of the Earth.

Influence heliogeophysical agent on the functional state of human peripheral blood conditions of the Arctic

T.S. Zavadskaya¹, N.K. Belisheva¹, I.V. Kalashnikova²

¹*FGBUN Kola Scientific Center*

²*FGBUN Polar Alpine Botanical Garden-Institute KSC RAS*

The study was conducted on a group of healthy male volunteers (7 men, mean age 33 years) during the period from 20 to 30 December 2010. Data on the dynamics of the functional state of the peripheral blood were obtained on the basis of the daily clinical analysis obtained by using automatic hematology analyzer ABACUS. Data characterizing heliogeophysical agents include parameters of the interplanetary magnetic field, solar wind plasma, the solar activity (SA) and geomagnetic field activity (GMA) indices (http://omniweb.gsfc.nasa.gov/html/ow_data.html # 1). In addition, the geophysical agent indices near the Earth's surface were selected at the latitude of site, where studies were carried out (Apatity, 67.57 ° N, 33.4 ° E). These indices included: variations of the geomagnetic field (GMF), the neutron count rate (station of neutron monitor, PGI KSC RAS, Apatity) corrected and uncorrected on atmosphere pressure. Statistical analysis was performed by using of the software package Statistica 6.0. By analysis of peripheral blood dynamics, the significant functional changes of the system of platelets were revealed. The mean of platelets (PLT) exceed to the upper boundary of norm ($360.7 \pm 11.7 * 10^9 / L$), where normal range is $180-320 \times 10^9 / L$. Moreover, this index can reaches up to $416.0 \times 10^9 / L$ in some persons. Generally, during the study of the peripheral blood, the content of the plates were typical for thrombocytosis. At the same time, the average volume of the platelets (MPV) were increased by factor 2.3 in comparing with the normal ($21.5 \pm 0.8 \text{ mkm}^3$ and $8.9-9.5 \text{ mkm}^3$, correspondingly). In the same time, the plateletcrit (PCT) ($0.8 \pm 0.04\%$) and platelet distribution width (PDWc) ($41.8 \pm 3.8\%$) were by factor 2 higher than the normal values ($0.15-0.4\%$ and $1-20\%$, respectively). It was revealed that homeostasis shifts are manifested by a moderate erythrocytosis, by increase of hemoglobin with a decrease of hemoglobin concentration in erythrocyte, by increasing heterogeneity of red blood cells, by increasing of the number, size, heterogeneity of platelets and by increasing of platelet crit. To determine the variations heliogeophysical agents dependence of the blood functional state correlation coefficients between the daily average values of indices of peripheral blood and averaged per day heliogeophysical indices were calculated. The obtained data manifested the modulation of the peripheral blood functional state by the heliogeophysical agent variations in the Arctic. Adaptation to their effects could be leads to a shift of homeostasis associated with the increased risk of cardiovascular events in the healthy young adults.

AUTHOR INDEX

A

Akhmetov O.I. 49, 53
Alexeyev V.N. 15
Amosova M. 14
Angelopoulos V. 13, 17
Antonenko O. 46
Artamonova I.V. 61
Astafieva N.M. 63
Astafjev A.M. 51

B

Balabin Yu.V. 37, 38, 39, 65, 66
Barkhatov N.A. 40
Barkhatova O.M. 54
Belakhovsky V.B. 29, 31
Belisheva N.K. 69, 71, 72, 73, 75
Beloglazov M.I. 62
Beloshkurskaya M.M. 13
Beloushko K.E. 61
Bessarab F.S. 45, 48
Bondareva T.V. 29
Botova M.G. 45
Brandstrom B.U.E. 48

C

Chechetkin V.M. 63
Chernej S.D. 72
Cherniak Ju. 18
Chernous P.A. 61
Chernouss S.A. 45, 46, 48
Chernyaev I.A. 13
Chkhetiani O.G. 57
Chramov A.V. 74

D

Danilova O.A. 58
Demekhov A.G. 30, 31, 32
Demin V.I. 61
Despirak I.V. 13, 19
Dmitrieva N.P. 13, 23
Dremukhina L.A. 16, 20

E

Efishev I.I. 18, 45
Ermakova E.N. 32, 55

F

Fedorenko Yu.V. 46, 49, 53
Fedotova E.A. 66
Feldstein Y.I. 14, 55
Filatov M. 46
Frank-Kamenetsky A.V. 56
Frolov V.L. 62

G

Galakhov A.A. 62
Germanenko A.V. 37, 38, 39, 65, 66
Golovchanskaya I.V. 30
Gordeev E. 14
Gorshkov E.S. 70
Gromov S.V. 16, 20
Gromova L.I. 16, 20
Gvozdevsky B.B. 37, 38, 39, 65, 66

I

Ievenko I.B. 15, 23
Ismagilov V.S. 20, 24, 33
Ivanov V.V. 70

K

Kalashnikova I.V. 75
Kanatjev A.G. 74
Kangas J. 57
Karavaev Yu.A. 17
Kargapolov D.A. 47
Karpachev A.T. 47
Karpov M.I. 47
Kasatkina E.A. 74
Katkalov Ju. 15, 18
Kireev A.P. 56
Kirillov V.I. 62
Kleimenova N.G. 30, 38, 56
Klimenko M.V. 45, 47, 48
Klimenko V.V. 45, 47, 48
Klimushkin D.Yu. 29
Koleva R. 13
Kopytenko Yu.A. 20, 24, 33
Koren'kov Yu.N. 45, 48
Kornilov I.A. 13, 15, 16, 23
Kornilova T.A. 13, 15, 16, 23
Korobeynikov A.G. 33
Kosolapova N.V. 25, 41, 54
Kotik D.S. 55
Kotikov A.L. 20, 33, 50, 56
Kotova D.S. 48
Kozelov B.V. 16, 25, 32, 48
Kozelova T.V. 16
Kozlovsky A.E. 31
Kozyreva O.V. 30, 38, 56
Kruglov A.A. 56
Krushinsky V.V. 64
Krymsky A.M. 56
Kubitski M. 56
Kubyshkina M.V. 13
Kulikov Y.Y. 62
Kuznetsova I.N. 64

L

Larchenko A.V. 46, 49
Lebed O.M. 49, 53
Levitin A.E. 16, 20, 40
Lubchich A.A. 13, 33, 41
Lubchich V.A. 30
Lunyushkin S.B. 17

M

Makarova L.N. 47, 50
Manninen J. 30, 31
Martynova A.A. 71, 73
Maslov I.A. 53
Maurchev E.A. 39, 69
Melnik N.A. 72
Meshalkina N.S. 40
Mikhailov R.E. 72
Mingalev I.V. 50, 53, 63, 66
Mingalev O.V. 53, 63
Mingalev V.S. 49, 50, 53, 63
Mingaleva G.I. 49, 50
Mishin V.M. 17
Mishin V.V. 17
Mochalov A.A. 32, 51
Mogilevskiy M.M. 32
Moroz V.N. 61
Murr D. 31

N

Namgaladze A.A. 45, 47
Nikitenko A. 46
Nikolaev A.V. 17
Nikolaeva V.D. 50
Novikova T.B. 74
Novoseltsev R.G. 72

O

Odzimek A. 56
Orlov K.G. 63

P

Parnikov S.G. 15
Panyutin A.A. 55
Pashin A.B. 32, 51
Pasmanik D.L. 31
Pchelkin V.V. 62, 64
Petlenko A.V. 20, 33
Petrashova D.A. 72
Petrishev M.S. 20, 33
Pilgaev S.V. 18, 46, 49, 52
Pilipenko V.A. 29, 31
Pirjola R. 18
Podgorny A.I. 39, 40
Podgorny I.M. 39, 40
Ponyavin D.I. 40
Popov G.M. 24, 33
Popova T.A. 26
Pozharskaya V.V. 71, 73

Prokhorov B.E. 45
Pryanichnikov S.V. 71, 73
Punanova A.F. 64

R

Raita T. 50
Ratovsky K.G. 47
Remenets G.F. 51
Revunov S.E. 25, 41
Revunova E.A. 40
Roldugin A.V. 18, 48, 52
Roldugin V.C. 18, 52, 53
Ryabov A.V. 55

S

Sakharov Ya. 18
Samsonov S.N. 29
Sarychev D.Yu. 20, 33
Semenov V.S. 23
Semenova N.V. 52
Serebryakova R.I. 54
Sergeev V.A. 13, 14, 17, 19
Shadrukov D.V. 25, 41
Shagimuratov I.I. 18, 45
Shalimov S.L. 57
Shirochkov A.V. 47, 50
Shkarbalyuk M.E. 46, 52
Shumilov O.I. 58, 74
Shvec M. 46
Sigernes F. 16, 23, 48
Singer H. 17
Slivka K.Yu. 23
Smirnova N.A. 29
Soraas F. 32

T

Tereshchenko P.E. 20, 33
Tereshchenko V.D. 57
Terramoto M. 31
Timofeev E.E. 57
Timofeeva S.A. 19
Titova E.E. 31, 32
Tsyganenko N.A. 17

U

Ugolnikov O.S. 53, 64
Ul'ev V.A. 58

V

Vallinkoski M.K. 57
Vashenyuk E.V. 37, 38, 39, 65, 66, 69
Veretenenko S.V. 61
Viljanen A. 15, 18
Volkov M.A. 24
Vorobjev V.G. 14, 53, 55, 58

W

Wik M. 15
Wintoft P. 18

Y

Yagodkina O.I. 19, 53, 58
Yahnin A.G. 24, 26, 32, 52
Yahnina T.A. 24, 26, 32

Z

Zakharenkova I. 18
Zakharov V.E. 48
Zavadskaya T.S. 75
Zaytsev D.B. 20, 33
Zolotova N.V. 40
Zverev V.L. 55
Zvyagintsev A.M. 64